THE EFFECT OF MECHANICAL VIBRATION ON THE NEGATIVE PRESSURE OF PURE LIQUIDS

By

GEORGE PATRICK MULHOLLAND
Bachelor of Science in Mechanical Engineering
New Mexico State University
University Park, New Mexico
1961

Master of Science in Mechanical Engineering
New Mexico State University
University Park, New Mexico
1962

Submitted to the Faculty of the Graduate School of
the Oklahoma State University
in partial fulfillment of the requirements
for the degree of
DOCTOR OF PHILOSOPHY
May, 1967

THE EFFECT OF MECHANICAL VIBRATIONS ON THE

NEGATIVE PRESSURE OF PURE LIQUIDS

Thesis Approved:

Jerald D. Parker

Thesis Adviser

Ladislaus J Fila

Allen Rowe

Robert L. Robinson, Jr.

O. D. Durham

Dean of the Graduate College

PREFACE

This thesis is concerned with the ability of fluids to withstand negative pressures while being subjected to vibratory forces. The analysis is concerned with motions of small amplitude and frequency but can be extended to include motions of large amplitude and frequency.

I would like to express my appreciation to my adviser, Dr. Jerald Parker, for his comments and the interest he has shown in this study. The comments and criticisms expressed by the members of the author's committee, Professor Ladislaus Fila, Dr. Robert Robinson and Dr. Allan Rowe are also greatly appreciated.

I would also like to express my appreciation to Mr. Ronald Goggia for his invaluable assistance with the computer programs and I would like to thank Miss Sharon Meyers and Mrs. Sharon Stewart for typing the thesis.

It is impossible to express my appreciation to my family for the daily encouragement which they offered during this study. I hope this work in some way justifies their sacrifices.

TABLE OF CONTENTS

LIST OF TABLES

LIST OF FIGURES

LIST OF FIGURES

(Continued)

LIST OF SYMBOLS

Symbol	
a	Tube amplitude
c	Speed of sound in fluid
g	Acceleration due to gravity
h	Height of liquid column
I_0	Modified Bessel function of the first kind of zeroth order
I_1	Modified Bessel function of the first kind of first order
J_0	Bessel function of the first kind of zeroth order
J_1	Bessel function of the first kind of first order
P	Pressure
S	Laplace variable
v_r	Radial velocity
v_z	Azimuthal velocity
μ	Absolute viscosity
ν	Kinematic viscosity
ρ	Fluid density
ω	Angular frequency of vibration
G	Input acceleration amplitude

CHAPTER I

INTRODUCTION

Since the end of the last World War, a large part of engineering work, either directly or indirectly, has been associated with the development of vehicles that are suitable for space travel. Although there are many problems associated with rockets and space travel, it is generally agreed that the damaging effects due to vibration is one of the more serious problems. Vibration inputs, either during launch conditions or during transonic conditions, can cause structural damage and, indirectly, can cause damage which is directly connected with the cavitation of either the fluid or the oxidizer. In this analysis, the term "cavitation" shall denote the formation of vapor or gas-filled voids within a liquid under the influence of local pressure reductions due to dynamic action. The eroding effects due to the collapsing cavitation voids will be referred to as "cavitation damage."

The onset of cavitation can cause damage to the space vehicle in two ways: The first way is due to cavitation damage while the second way is due to the effect of a changing mass rate of flow on the rocket engine. This latter effect is a result of cavitation. Thus it can be seen that vibration is a problem not only to the structural engineer, but also to the engineer concerned with the fluid inside the space vehicle.

For the engineer to obtain a better understanding of this phenomena of cavitation, it is necessary to investigate the physics of the problem more closely. For example, it is assumed by most hydraulic engineers that a fluid will cavitate as soon as it reaches its vapor pressure; this would imply that a fluid is unable to exist in a state of tension. Now it is a known fact that liquids do have a tensile strength, but it is generally believed that this state can only be reached when the fluid is stressed in a static manner. If it can be shown that a fluid, by some pre-conceived operation, can exist in a state of tension while under the influence of a vibratory force, the advantage to the engineer will be great in that he will not be hindered by the fluid's vapor pressure, but by a pressure which is lower than the vapor pressure and which can be controlled by the engineer. In fact, this pre-flight operation on the fluid could be specified so as to enable the fluid to not only withstand any vibratory effects, but also to give the engineer a greater design latitude in that he would be able to specify flow-rates that could lower the fluid pressure below the vapor pressure; this greater latitude could very well manifest itself in a greater utilization of all fluids that are aboard the spacecraft or lower the gross fluid weight which is definitely a very important parameter in space flight.

The purpose of this study is to determine whether liquids can exist in a state of tension while subjected to vibratory forces and to develop a general, straightforward, analytical method which will accurately describe this phenomena in the fluid. The fluids that are used for this test will be confined in a cylindrical

container and will have values for viscosity which vary from one to thirty-two centipoise and values for surface tension which vary from forty-eight to seventy-two dynes per cm. This spread in the values for viscosity and surface tension is desirable since they are the two principle variables which affect the tensile strength of a fluid.

Although the major part of this work is directed toward the solution of problems where the fluid is confined within a cylinder of small radius and where the cylinder is subject to vibrations of small amplitude and frequency, a set of equations has been obtained which are completely general and can be used in obtaining solutions for any problem that satisfies the prescribed boundary conditions and is subject to the governing equations.

The equations for the pressure field and the velocity field inside the cylindrical tube have been programmed for use on an IBM 1620 digital computer. The method is simple and straightforward and is given in Appendix B.

Graphical representations of the pressure field and the velocity field are given so that a convenient pictorial representation of how these variables behave can be easily seen for any value of the frequency, viscosity, or azimuthal coordinate.

CHAPTER II

REVIEW OF PREVIOUS INVESTIGATIONS

Before starting the discussion, a clear distinction between the terms "liquid tensile strength" and "negative pressure" should be obtained. In this study the term "negative pressure" will be used to denote a pressure within the fluid that is below the vapor pressure, while "liquid tensile strength" will be used to denote the maximum negative pressure that the fluid can sustain.

The first recorded work on the measurement of liquid tension was that of F. M. Donny (38)* in 1843. Donny found that a column of sulphuric acid 1.255 meters long would hang in a vertical glass tube which was sealed at the upper end when the pressure at the lower end was below atmospheric.

In 1850 Berthelot (7) introduced his method for measuring tension in liquids. A strong capillary tube sealed at one end and drawn to a fine point at the other end was nearly filled with water. The small residual space that remained in the tube was occupied by water vapor. The tube was then heated until the air in the tube dissolved. Next the tube was cooled until the water column broke. The break occurred at a lower temperature than the temperature at which the water had first filled the tube. Berthelot found that the water had increased in volume

*Numbers in parentheses refer to references in the Bibliography.

by one part in 420 and, by assuming that the extensibility and compressibility of water are equal, he was able to calculate a tension of about 50 atmospheres by measuring the extension of the liquid.

Since the method described above due to Berthelot has been used by many investigators in determining the tensile strengths of various liquids, it would be advantageous to discuss some of the assumptions in his method (35, 38, 39, 41). The assumption that the extensibility and compressibility of water are equal does not seem to be too much in error since Temperley (36) measured the tensile stress of water as being between 30 and 50 atmospheres by a method which did not assume this equality. An assumption by Dixon (38) that the pressure in the tube is nearly zero at the moment when it fills with liquid is seriously in error. It actually takes high liquid pressures in the tube to force the final gas bubble to dissolve (36). This point will be discussed in detail later.

Osborne Reynolds (38) in 1878 used a centrifugal method to stress a liquid column. His method consisted of a sealed U-tube containing air-free liquid, ABC, and vapor, CD, being rotated on a lathe about an axis O as shown in Figure 1. If EC is the arc of a circle about point O, then during rotation the liquid between E and A will be in a state of tension. The minimum tension will occur at E and it will increase to a maximum at A. Reynolds calculated a tensile stress of approximately 5 atmospheres for water and Worthington (41) using the same method reported tensile stresses of 7.9 atmospheres for ethyl alcohol and 11.8 atmospheres for strong sulphuric acid. Temperley and Chambers (35) point out that in this method water does not move as a rigid body. This has no effect on the pressure distribution, but it does imply a considerable

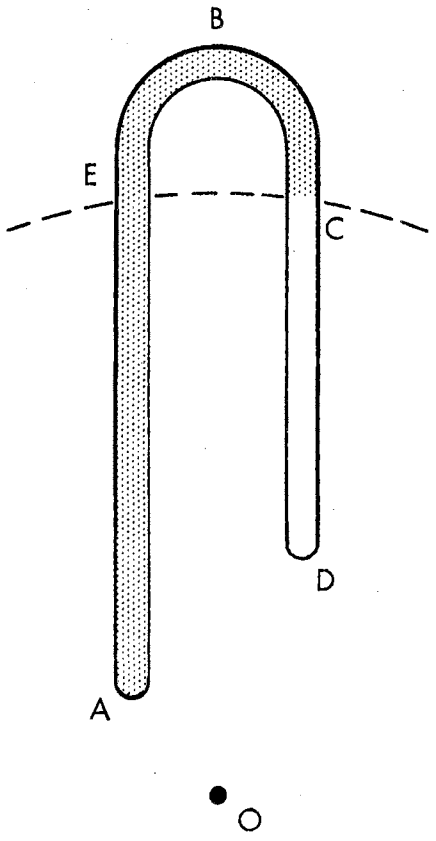

FIGURE 1. Reynolds U-Tube

amount of stirring. Thus any small bubbles would be brought near the region of greatest tension in a time that was comparable with the time of the experiment. This migration of the bubbles would tend to give low values for the tensile stress.

In 1892 Worthington (41) using the Berthelot method measured the tension of ethyl alcohol as 17 atmospheres. His method differed from Berthelot in that he actually measured the tension instead of calculating it from the temperature difference. Worthington's measuring apparatus, which he called a tonometer, consisted of an ellipsoidal bulb containing mercury. This bulb enclosed within the glass had a capillary tube in which the top of the mercury column indicated changes of volume of the bulb. The bulb and capillary tube had been calibrated with positive pressure and the scales extended in the negative direction by extrapolation.

In 1895 Dixon and Joly (38) using Berthelot's method obtained a value of 7.5 atmospheres for water at room temperature. Their method differed from Berthelot's original work in that they calculated the volume of the cavity formed by contraction of the liquid after failure by measuring its geometric dimensions rather than by the temperature difference.

Later Dixon (38) using Berthelot's method estimated tensions up to 200 atmospheres by assuming values for compressibility and extensibility at zero pressure. These high estimations as explained later by Vincent and Simmonds (40) and Temperley (36) were due to the erroneous assumption that the pressure in the tube was zero when the last vapor bubble disappeared. Actually the pressure in the tube was very large thereby leading to this error.

Askenasey (38) in 1895 and Hulett (38) in 1903 performed experiments illustrating the theory of transpiration in plants. Askenasey was able to obtain a tension corresponding to 13 cm of mercury for a gypsum solution while Hulett obtained a tension corresponding to 37.7 cm of mercury for water.

Julius Meyer (35) in 1911 measured tensions of 34 atmospheres for water at 24°C, 39 atmospheres for ethyl alcohol at 22°C and 72 atmospheres for ether at 18°C. Meyer's method was similar in principle to that used by Worthington. The only difference between the two methods was in the tension-measuring device. Worthington's device, as explained previously, measured the tension by the volume change of an ellipsoidal bulb, while Meyer's device consisted of a helical glass tube upon which a mirror was mounted. A slight rotation of the end of the glass helix, which was observed by means of the attached mirror, gave a measure of the internal tension. Meyer's method, like Worthington's, had to be previously calibrated by means of a positive pressure and then the scale extrapolated to include negative pressures.

In 1912 Budgett (38) measured the force necessary to rupture a film of liquid between two flat steel surfaces. He obtained a value of 4 atmospheres for the critical tension of water using the assumption that the liquid film was continuous over the surface. Upon examination of the surfaces after separation, he found that the effective area of the water was only about 7% that of the steel. This would indicate that the critical tension of water is about 60 atmospheres.

The reader has probably already noticed the wide variations in values obtained for similar fluids by different experimenters. This

variation can be partially explained by considering some of the underlying assumptions in each method and by noting that not all of the experimenters were measuring the same thing. An example of the latter is the work of Worthington in which the liquid failed by tearing away from the supporting surface of the glass vessel. Since the liquid failed in this manner, the properties of the glass are important and most certainly would vary from vessel to vessel. This could explain the variation even in Worthington's results. Some of the assumptions which could have led to errors in reported values are the following:

(a) Certain physical properties of liquids under tension have the same values when measured at zero or positive pressures (7, 35, 38, 41).

(b) In the Berthelot method the assumption that the pressure in the tube is nearly zero when it fills with liquid.

These assumptions, along with the fact that the quantity of undissolved gases present in each liquid was not even considered, would lead to a wide variation in the results. It must be remembered that these results were quite amazing in that they did show that fluids were capable of passing to a state of tension without any breach of continuity when the contrary was being asserted by many eminent physicists and hydrodynamicists (41).

The next work of importance was due to Vincent (38) in 1941. He applied tension to a liquid by enclosing the liquid within a metal bellows and then applied tension to the bellows. Vincent obtained a value of 2.38 atmospheres for ethyl alcohol, 2.94 atmospheres for mineral oil and 2.21 atmospheres for ether.

Vincent (39) in 1943 introduced his viscosity tonometer which, as the name implies, depends on the fluid's viscosity for measuring tensions. His method consisted of cooling the liquid in a vessel thereby sucking it backwards through a capillary tube. By comparing the rates of flow just before and just after the fracture of the fluid Vincent was able to calculate the critical tension from the ratio of these rates of flow. This was accomplished by assuming that the pressure within the bubble was equal to the vapor pressure and by also assuming that the viscosity is unaffected by tension. This method is suitable only for fluids with fairly large values of viscosity. Vincent obtained a value of 7.8 atmospheres for mineral oil using this method. As pointed out by Temperley and Chambers (35, the tonometer has a gradient of tension which tends to drive any nuclei towards the region of greatest tension, and this gradient may be the reason for the low values.

In 1943 Vincent and Simmonds (40) used a modified Berthelot method in which the pressure in the tube at the moment of sealing was known, and they were able to obtain a value of 25 atmospheres for mineral oil. This was the first time that anyone showed that the pressure within the tube at sealing is not approximately zero but is very large. In fact Vincent obtained a value of 119 atmospheres for mineral oil using the Berthelot method. This value is approximately 5 times larger than the one obtained using the modified method. The value obtained by this modified method is still much larger than the value obtained from Vincent's tonometer. However it should be remembered that for both cases it was assumed that tension does not affect the physical properties of liquids. This assumption could be the cause of the discrepancy.

In 1944 Harvey (21) found that by precompressing a fluid the tensile strength could be increased. He estimated values between 100 and 1000 atmospheres for water but gave no definite values. In a later paper Harvey (22) gave an explanation for this phenomena; he stated that the reason fluids fracture or cavitate is due to the presence of nuclei within the fluid. These nuclei consist of a solid hydrophobic particle having a re-entrant crack in their surface which is filled with undissolved gas as shown by Figure 2. This gas is the active part of the nucleus or the weak spot in the liquid. From the figure it is seen that the surface tension will tend to keep the gas pressure low since the surface of the liquid is convex toward the gas; therefore, the gas will not dissolve. Harvey reasoned that if a high enough hydrostatic pressure would force the liquid up into the crack against the surface tension force and cause the gas to dissolve, the weak spot would be eliminated. As noted by Knapp (24), the existence of these nuclei is still inferential, but Harvey's model does enable one to get a better feeling for what is taking place within the fluid.

Temperley and Chambers (35) in 1945 studied the Berthelot and Reynolds method. They found that the low values of tension obtained from the Reynolds method was due to the mixing in the tube. They obtained a value of 2 atmospheres for water using this method. For the Berthelot method, the above mentioned authors found that a pressure on the order of 50 to 100 atmospheres is needed to force the last vapor bubble into solution. These high pressures were predicted by Vincent and Simmonds (40,) but this was the first time that anyone actually measured these values. The authors reasoned that these high pressures were

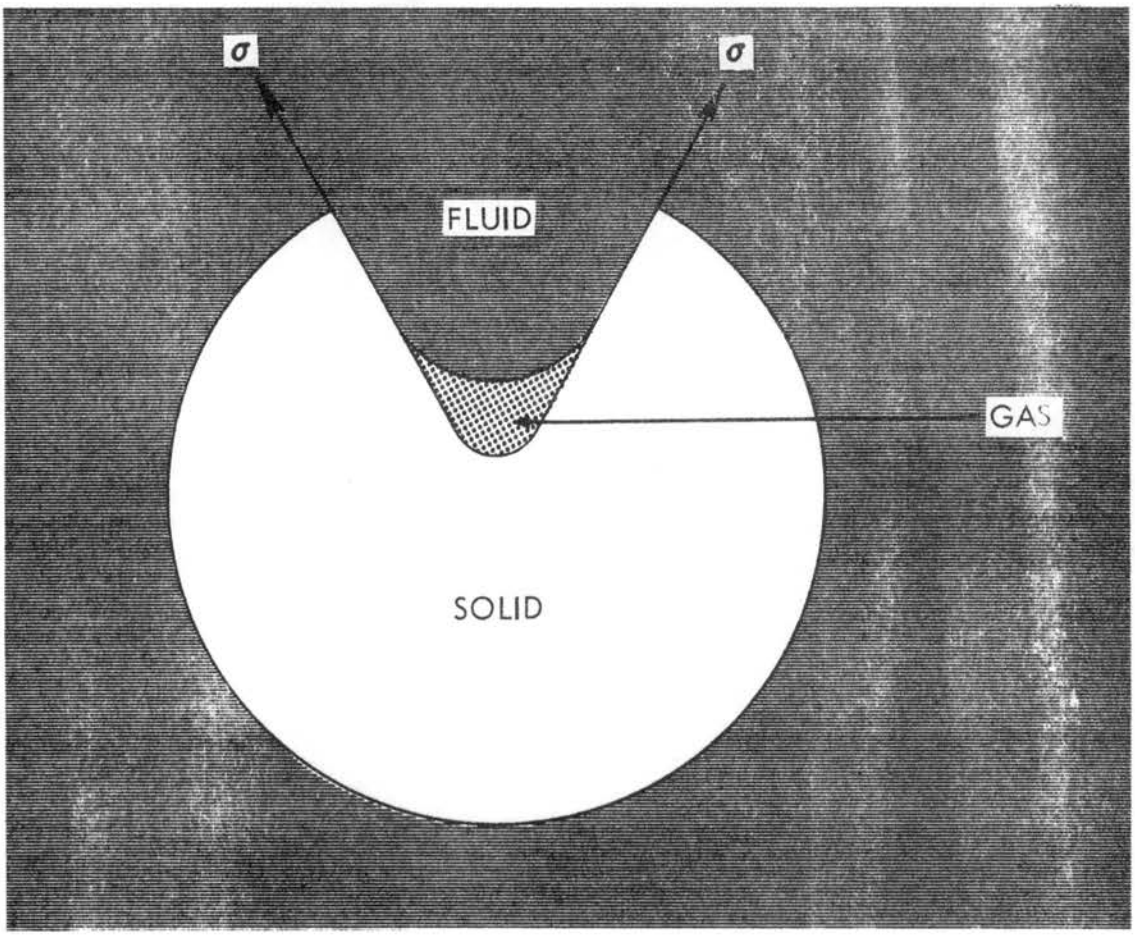

FIGURE 2. Harvey's Model of Nucleus

probably caused by the trapped gases being forced into fissures in the glass. From Harvey's model, it can be seen that these values are not unreasonable in that the external pressure not only has to overcome the force due to the pressure of the gas but also the force due to the surface tension. Temperley and Chambers obtained a tensile stress of 32 atmospheres for water using the Berthelot method.

Later Temperley (36) in 1946 again reached the conclusion that it was necessary to develop pressures on the order of 50 to 100 atmospheres inside the Berthelot tubes in order to force the last gas bubble into solution. He also concluded that the tensile strength of water in the presence of glass is of the order of 30 to 50 atmospheres. These measurements were performed by a method which did not assume that the extensibility and compressibility of water are equal. Lewis (26) in a similar type of experiment verified the equality between the extensibility and the compressibility of water. Temperley's values for the tensile strength agree favorably with the values obtained by Meyer (35). This is to be expected since Lewis had shown that the extensibility and compressibility are equal.

Scott (33) in 1948 and Lewis (26) in 1961 performed some further work on the Berthelot method for stressing a liquid. Both investigators obtained values around 30 atmospheres for water which agree favorably with Temperley's and Meyer's values. Lewis stated that any pre-compression of the liquid had no detectable effect on the critical tension. This is true if the fluid is free of all undissolved gases as it was in Lewis's case, but if the fluid has undissolved gases present, then any pre-compression will have a marked effect. This relative

independence between the fluid's tensile strength and the amount of dissolved gases present in the fluid was pointed out by Kuper and Trevena (25) when they found that dissolved gases reduce the tensile strength of water by less than 0.5%.

Briggs (9) in 1949 used a centrifugal method in which a capillary tube was rotated in a horizontal plane by means of a high speed three-phase induction motor. He was able to calibrate the maximum tensile stress of water as 277 atmospheres. This value is greatly in excess of any values obtained using a method similar to Reynolds, but still it is only about 20% of the theoretical value as calculated from nucleation theory. As pointed out by Briggs these results should only be applied to boiled water (no dissolved gases) in a Pyrex glass capillary tube with an internal diameter of 0.6 to 0.8 millimeters. Thus the same predicament is still present in that the results are only able to be duplicated when the fluid is enclosed in a similar container and when the process used to stress the fluid is similar to the original procedure. For example, the tensile stress of water in the presence of steel is about one-third the value of water in the presence of glass when the Berthelot method is used in each case. Of course this is easily explained since there are many more crevices for undissolved gases on a steel surface than on glass surface, but the fact remains that the only way a tensile stress can be quoted which has any meaning is to also quote both the container in which the fluid was enclosed during the test and the method used to stress the fluid.

Later Briggs (10), using the same centrifugal method, calculated the tensile stress of acetic acid as 288 atmospheres, benzene as 150 atmos-

pheres, aniline as 300 atmospheres, carbon tetrachloride as 276 atmospheres and chloroform as 317 atmospheres. Briggs made the observation that a polarized derivate (aniline) of a fluid (benzene) has a higher tensile stress. This must be due to the fact that the dipoles increase the cohesion of the liquid.

Bull (12), using his electrical pressure bar, measured tensile stresses for water of 17 atmospheres and for glycerol of 63 atmospheres. These fluids were tested in steel containers and the results for water agree fairly well with those obtained using the Berthelot method with a steel container. Later Bull (13) used olive oil and syrup and obtained values for tension of 29 atmospheres for the former and 130 atmospheres for the latter. He obtained an empirical relationship between the critical pressure and the viscosity for viscosities in the range of 0.01 poise to 400 poise:

$$P_c = k \mu^{0.2}.$$

Bull reasoned that since the surface tensions, compressibilities and densities of all the fluids used in his work were of the same order of magnitude, the factor which will influence cavitation is the viscosity. It must be remembered, though, that Bull's equation is valid only for fluids with values for surface tension, compressibility and density of the same order of magnitude as olive oil and syrup, and the fluid viscosity must be in the range of 0.01 to 400 poise.

There has been very little work on the measurement of the tensile strength of cryogenic liquids. One paper of note is that of Beams (4) in which he measured the tensile strengths of liquid Argon, liquid Helium, liquid Nitrogen and liquid Oxygen. Beams' method is to

accelerate an inverted U tube completely filled with fluid and then to quickly decelerate it to a zero velocity; while the U tube is being stopped, the liquid will tend to continue its downward motion and will create a tensile stress in the liquid in the upper part of the U tube. By this method Beams was able to obtain values of 12 atmospheres for Argon, 10 atmospheres for Nitrogen, 15 atmospheres for Oxygen and 0.16 atmospheres for Helium. It should be mentioned that the U tube was made of flamed Pyrex glass. Previous to this work, Misener and Herbert (29) used a bellows method and obtained a value of 3.5 atmospheres for liquid Nitrogen and a value less than 0.3 atmospheres for liquid Helium.

The principle points of this literature review can be summed up by the following three statements:

(1) Fluids, like solids, are able to withstand large tensile stresses but, unlike solids, no definite values can be set for them.

(2) For a pure (no solid particles) fluid, the weak spots that cause fracture or cavitation are the undissolved gases present in the fluid. Dissolved gases will change the tensile strength by less than 0.5%.

(3) For a value of the tensile strength of a fluid to have any meaning, it must be accompanied by both the method by which it was tested and the type of container in which it was tested.

The above statements should point to the need for some sort of standardization of liquid tensile strengths. An important step in this direction would be the development of a container whose interior

surface was such that the adhesive force between it and the fluid was greater than the cohesive force within the fluid. This would enable a fluid to be tested until it fractured from within and not by tearing it away from the wall. This cohesive force will be discussed in the following chapter.

CHAPTER III

THEORETICAL ANALYSIS OF LIQUID TENSILE STRENGTH

The principle theoretical work on the tensile strength of liquids has been due to Langmuir (17), Temperley (37), Benson (5), Fisher (15) and Furth (18). Langmuir using the assumption of a pure, gas-free, homogeneous liquid obtained a value of 10,000 atmospheres for the tensile strength of water. This so-called intrinsic pressure has been shown to be many orders of magnitude higher than any tensile strength that has been measured (35, 37, 38). This discrepancy can be more easily accepted by reminding the reader of a similar discrepancy between the theoretical and the actual tensile strength of a solid. An example of this is rock crystal (38); the theoretical tensile strength of this solid is many hundreds of times greater than any value that has been measured. For solids this discrepancy can be partially explained by the presence of surface cracks which lead to non-uniform stressing (23). For fluids these weakening mechanisms are the undissolved gases and the hydrophobic nuclei that are present within any fluid. These weak spots were not taken into account by Langmuir.

Temperley (37) and Benson (5) used the Van der Waals and the Berthelot equations of state to obtain values for the tensile strength of liquids. Benson used these equations to calculate values for the reduced volume, energy of vaporization, coefficient of thermal expansion and the coefficient of compressibility at the boiling

points of various fluids. He then compared these values with the observed values and found that the observed values fell between the values calculated from the Van der Waals equation and the values calculated from the Berthelot equation. He then deduced that the actual tensile strength of a fluid should fall somewhere between the values obtained from the respective equations of state. Benson (6) later introduced another equation of state which he claimed was a marked improvement over the Van der Waals and the Berthelot equations for the fluids considered. Temperley and Benson placed the value for the theoretical tensile strength of water at room temperature as being between 1000 atmospheres and 5000 atmospheres.

Fisher (15) used nucleation theory and Furth (18) used the Theory of Holes to obtain values of 1320 atmospheres and 500 atmospheres respectively for the tensile strength of water at room temperature.

In the remaining paragraphs of this chapter, the methods used by the above mentioned authors will be reviewed. All the assumptions used will be discussed and the final results will be summarized for comparison purposes. Water at a temperature of 80°F (26°C) will be used as the working fluid.

Tensile Strength of an Ideal Liquid

Langmuir imagined the liquid to be a prismatic rod with a cross section A. He then imagined the rod to be divided in half thereby producing a new free surface 2A and an additional surface energy 2Aw. The surface energy, w, is defined as the additional potential energy per unit surface due to the fact that the particles of the surface layer lack neighbors on the external side (17). This sub-

division of the liquid is then continued until the fluid is separated into single molecules. The surface energy will be increased by Nqw where N is the number of molecules and q is the area of the surface of each molecule. Langmuir postulated that each molecule was similar to a sphere with a surface area of $4 \pi r^2$ and a volume equal to $4/3 \pi r^3$. The volume of a molecule is also equal to the volume of the liquid per number of molecules present in the liquid:

$$4/3 \pi r^3 = \frac{V}{N} = \frac{1}{n} \qquad \text{(III-1)}$$

By manipulating Equation (111-1), an equation for the radius of the molecule is obtained:

$$r = \left(\frac{3}{4 \pi n}\right)^{1/3} . \qquad \text{(III-2)}$$

The value for the radius as calculated from the above equation is

$$r \quad 2 \times 10^{-8} \text{ cm},$$

where

$$n = 3.34 \times 10^{21} \text{ molecules/cm}^3$$

for water.

The energy which is required to fracture the liquid over an area A is made up of two parts; the first part is the work, $2A \sigma$, which must be done if the temperature is to remain constant, and the second part is the quantity of heat which must be transferred to the region of fracture to ensure this constant temperature. Since a fracture will occur if the gap between corresponding surface layers is increased by an amount on the order of the molecular radius, the minimum value of the work of fracture per unit area, 2σ, must be equal to the product of r and the breaking strength which the liquid can bear without fracturing.

This gives the following expression for the pressure:

$$p = \frac{2\sigma}{r} \qquad \text{(III-3)}$$

Eq. (111-3) gives a value of 10,000 atmospheres for the theoretical tensile strength of water.

Tensile Strengths from the Van der Waals Equation

The Van der Waals equation is a semi-empirical equation which is derived by assuming a microscopically random and uniform molecular distribution function for the liquid and complete communality of its free volume.

The method used here to obtain values for the tensile strength is basically that due to Temperley (37) and Benson (5).

The Van der Waals equation,

$$\left(P + \frac{a}{v^2}\right)(V - b) = RT, \qquad \text{(III-4)}$$

can be put in the reduced form,

$$\pi = \frac{8\theta}{3\phi - 1} - \frac{3}{\phi^2}, \qquad \text{(III-5)}$$

by the substitution of the appropriate values of the constants a,b, and R into Eq. (111-4) where

$$\pi = \frac{P}{P_c},$$
$$\theta = \frac{T}{T_c},$$
$$\phi = \frac{V}{V_c}. \qquad \text{(III-6)}$$

The liquid tensile strength is defined as the maximum tension that a liquid can maintain at constant temperature. It has physical significance if there is a unique tension above which the liquid will become mechanically unstable. This is expressed analytically as

$$\left(\frac{\partial \pi}{\partial \phi}\right)_{\theta} = 0, \qquad \text{(III-7)}$$

or in terms of the coefficient of extensibility,

$$\beta = -\frac{1}{P_c \phi}\left(\frac{\partial \phi}{\partial \pi}\right)_{\theta} = \infty \quad .$$

The coefficient of extensibility can be expressed in this way since an infinitesimal increase in tension will produce an infinite increase in volume.

When the condition of instability, Eq. (111-7), is applied to Eq. (111-5) the following equation is obtained:

$$\left(\frac{\partial \pi}{\partial \phi}\right)_{\theta} = -\frac{24\,\theta}{(3\phi-1)^2} + \frac{6}{\phi^3} = 0 \qquad \text{(III-8)}$$

When the above expression is expanded, the following third order equation is obtained:

$$\phi^3 - \frac{9}{4\theta}\,\phi^2 + \frac{3}{2\theta}\,\phi - \frac{1}{4\theta} = 0 \qquad \text{(III-9)}$$

Simple relations for θ and π_{min} in terms of ϕ_{min} can be obtained from Eq. (111-5) and Eq. (111-8):

$$\theta = \frac{1}{4}\left(\frac{(3\phi-1)^2}{\phi^3}\right) \qquad \text{(III-10)}$$

and

$$\pi_{min} = \frac{3}{\phi^2} - \frac{2}{\phi^3} \quad . \qquad \text{(III-11)}$$

When $\phi = 2/3$ in Eq. (111-11), π_{min} equals zero, and θ equals 27/32. This point is the maximum temperature above which a liquid is incapable of existing at zero pressure. Temperley called it the maximum temperature of superheating.

From Eq. (111-9), it is seen that this equation may have three positive roots. One of the roots is between zero and 1/3. This root belongs to the physically meaningless portion of the Van der Waals isotherm since π is always negative in this region. The behavior of π corresponding to this root can easily be seen by examining Eq. (111-5). The largest root of Eq. (111-9) corresponds to a maximum in the isotherm for which π is positive. This root is usually associated with the minimum volume of the supercooled vapor. The third root which is the one that is of interest corresponds to a minimum in the isotherm and yields negative values of π for values of θ below 27/32. For this range of θ, ϕ lies between 1/3 and 2/3 and can easily be calculated by synthetic division. Fig. 3 is a plot of the isotherms from Eq. (111-5).

The variation of tensile strength with temperature can be calculated from Eq. (111-10) and Eq. (111-11). Since Eq. (111-11) gives π_{min} as a function of ϕ, the variation of the tensile strength with the temperature can be written as

$$\frac{\partial \pi_{min}}{\partial \theta} = \frac{\partial \pi_{min}}{\partial \phi} \frac{\partial \phi}{\partial \theta} = \frac{8}{3\phi - 1} , \qquad \text{(III-12)}$$

Eq. (111-12) can also be written in terms of the normal variables,

$$\left(\frac{\partial P_{min}}{\partial T} \right)_V = \left(\frac{1}{3\phi - 1} \right) \frac{3R}{V_c} , \qquad \text{(III-13)}$$

since

$$P_{min} = P_c \pi_{min} ,$$

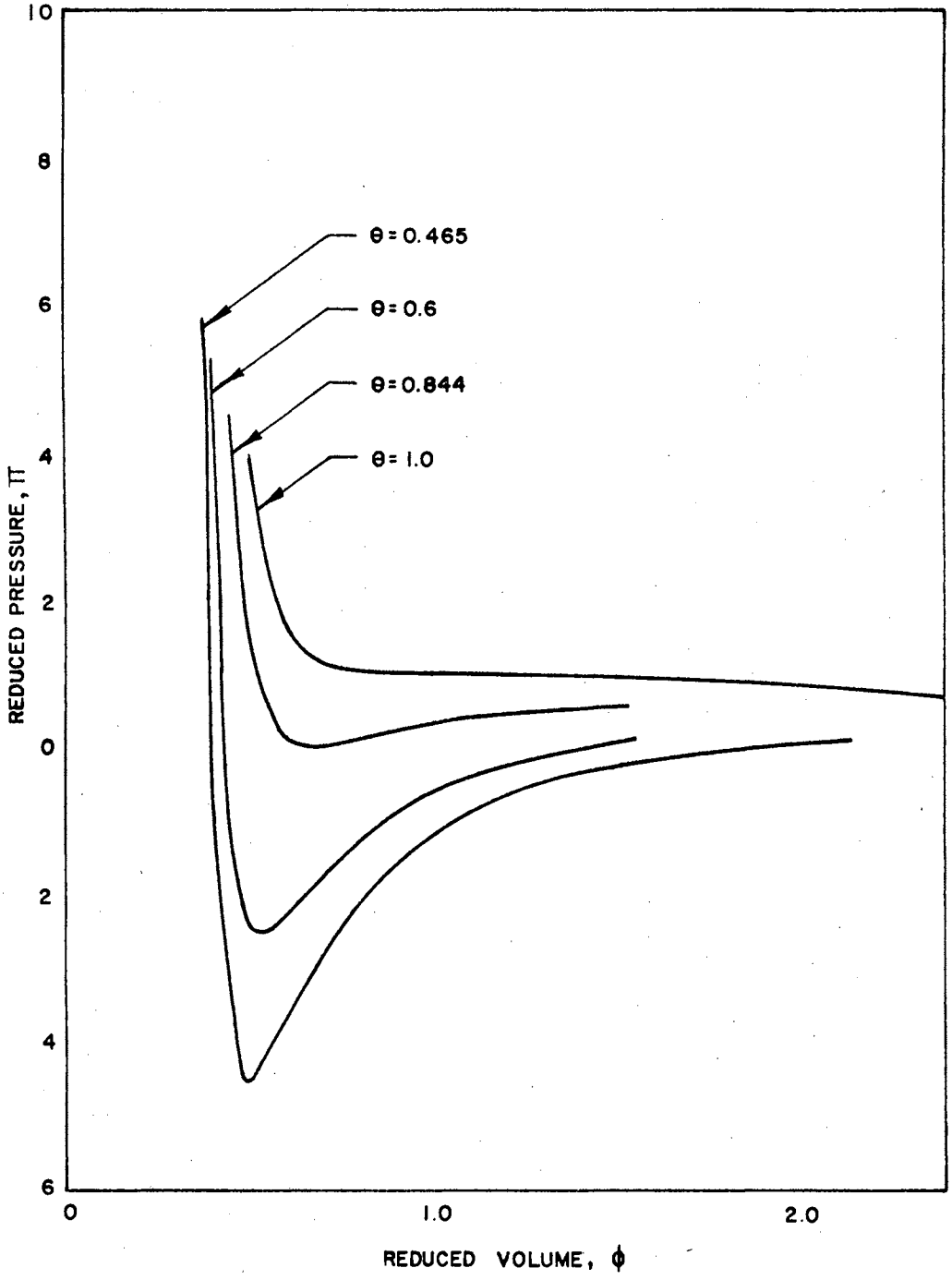

FIGURE 3. Isotherms From Van der Waals Equation

and

$$T = T_c \theta ,$$

$$\frac{P_c}{T_c} = \frac{3R}{8V_c} .$$

The ratio between the critical pressure and the critical temperature is obtained from the Van der Waals critical isotherm. The value $\frac{3R}{V_c}$ in Eq. (111-13) is equal to 2.7 atm/°C for water. For $\phi = 0.48$, which is a root of Eq. (111-9), Eq. (111-13) is approximately equal to 6 atm/°C. When this value is compared to the results of Briggs (9), it appears to be good considering the assumptions that were used. This discrepancy can very probably be attributed to the fact that the Van der Waals constants, a and b, have been assumed to be temperature-independent when in reality they are temperature-dependent. Eq. (111-13) does predict that the tensile strength is temperature-dependent and that it decreases with increasing temperature. This trend is physically accurate down to a temperature around 10°C (9). At this point, the tensile strength reaches a maximum and starts to decrease as the temperature is decreased. Figure 4 which is the results of Briggs' work shows this phenomena. Fisher (16) explained this strange behavior between 0°C and 10°C in terms of the nucleation of ice under reduced pressure. He assumed that ice nuclei form readily and grow when the solid phase is stable and that ice will nucleate the vapor phase. Near 0°C the limiting tension that water will withstand is that required to raise the freezing point to the testing temperature. For water a negative pressure of 300 atmospheres will raise the freezing point 2.7°C. This is in fairly good agreement with Briggs' work when it is remembered that nucleation theory predicts values that are 5 times greater than Briggs' values.

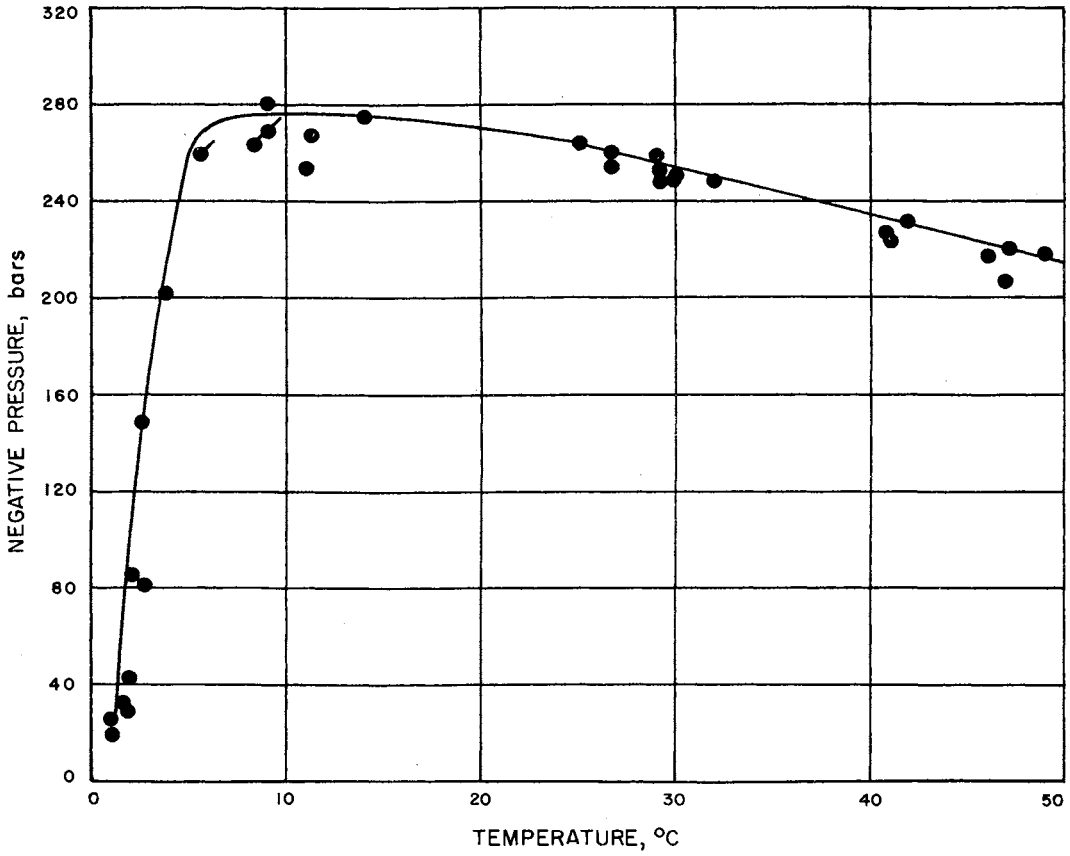

FIGURE 4. Tensile Strength as a Function of Temperature

The relations derived so far, Eq. (111-11) for the maximum value of tensile strength and Eq. (111-12) for the change of tensile strength with temperature, have assumed that the constants a and b are independent of termperature. Since the theoretical tensile strength is sensitive to the value of b, as well as to that of a, it seems advantageous to consider the following two questions. First, what effect is there on the theoretical tensile strength if the quantities a and b are dependent on temperature, and secondly, what can be predicted theoretically about the behavior of a and b as functions of temperature?

The effect of possible changes of b with temperature will be considered first. Since b is a measure of the excluded volume, it will decrease as the temperature rises due to the collisions being more energetic and conversely it will increase as the temperature decreases. The previous statement will be valid except in the limiting case of rigid molecules. For this case b will remain constant.

To get a better feeling for how this variation of b affects the tensile strength, Eq. (111-5) and Eq. (111-11) should be written in terms of their normal variables:

$$\left(P + \frac{a}{V^2}\right)\ (V - b)\ = RT \qquad \text{(III-14)}$$

and

$$P_{min} = \frac{a}{V^2} - \frac{2ab}{V^3}\ . \qquad \text{(III-15)}$$

Now it is clear from the above two equations that any increase in b above the value $V_c/3$ for a given temperature will give a smaller value for the tensile strength. As mentioned before, for a decreasing temperature, b will increase so that the theoretical tensile strength

should be less than the value predicted by Eq. (III-11).

It is obvious from Eq. (III-14) and Eq. (III-15) that any increase in a will increase the value of the tensile strength. The point which is not so obvious is whether a will increase or decrease with increasing temperature. Temperley (37) considered this problem by assuming that the mutual potential energy of two molecules can be expressed by means of an attraction and a repulsion of power-law type. Temperley did show that the constant a was an increasing function of the temperature for values of temperature less than 27/32 T_c-100. This corresponds to a temperature less than 170°C for water. But Temperley was unable to say definitely whether for a given temperature a would have an effective value greater or less than that at its critical temperature. In summing up, it can be said that it is impossible to make any numerical prediction about the variation of the constant a with temperature, but it is possible to predict the variation of b with temperature.

As mentioned before, Benson (5) calculated values for the reduced volume, ϕ, the coefficient of thermal expansion, α, and the coefficient of compressibility, β, so that he could compare the results thus obtained with the observed values. He reasoned that if the values thus obtained agreed fairly well with the observed values then any value of tensile strength obtained from the equation would be fairly close to an actual theoretical tensile strength.

The equation for the reduced volume is obtained from Eq. (III-5) where the reduced vapor pressure, π, is neglected since it is much smaller than either ϕ or θ. For this case the reduced volume is

$$\phi = \left(\frac{9}{16\theta} \quad 1-(1-\frac{32}{27}) \right)^{1/2} . \qquad \text{(III-16)}$$

The coefficient of thermal expansion,

$$\alpha = \frac{1}{V} \left(\frac{\partial V}{\partial T}\right)_P ,$$

is obtained from Eq. (111-5):

$$\alpha = \frac{1}{T} \left(\frac{8\theta\phi}{9-16\theta\phi}\right) . \qquad \text{(III-17)}$$

The coefficient of compressibility,

$$\beta = -\frac{1}{V} \left(\frac{\partial V}{\partial P}\right)_T ,$$

is also obtained from Eq. (111-5):

$$\beta = \frac{8\theta\phi^3}{27P_c} \left(1 - \frac{48}{27}\theta\phi\right)^{-1} \qquad \text{(III-18)}$$

The results for the above three equations, Eq. (111-11) and Eq. (111-13) are given in Table 1 along with similar calculations for the Berthelot and the Benson equations of state.

Tensile Strengths from the Berthelot and Benson Equations

In reduced form the Berthelot equation is given by

$$\pi = \frac{8\theta}{3\phi-1} - \frac{3}{\theta\phi^2} \qquad \text{(III-19)}$$

and the Benson equation is given by

$$\pi = 3.624 \left(\frac{\theta}{\phi-0.1567\phi}^{-1/2} - \frac{0.9099}{\phi^{5/3}\theta^{2/3}}\right) \qquad \text{(III-20)}$$

If the same method that was used for the Van der Waals equation is used for the Berthelot equation, the following equations can be written:

$$\left(\frac{\partial \pi}{\partial \phi}\right)_\theta = -\frac{24\theta}{(3\phi-1)^2} + \frac{6}{\theta\phi^2} = 0 , \qquad \text{(III-21)}$$

$$\pi_{min} = \frac{2}{\phi^{3/2}} \left(\frac{3\phi-2}{3\phi-1}\right) , \qquad \text{(III-22)}$$

and

$$\left(\frac{\partial \pi_{min}}{\partial \theta}\right)_{\phi} = \frac{8}{3\phi-1} + \frac{3}{\theta^2\phi^2} \quad . \qquad \text{(III-23)}$$

$$\phi^3 - \frac{9}{4\theta^2}\phi^2 + \frac{3}{2\theta^2}\phi - \frac{1}{4\theta^2} = 0 \quad . \qquad \text{(III-24)}$$

The root of Eq. (111-24) which corresponds to θ at T = 80°F for water is $\phi = 0.415$. For Benson's equation, the minimum pressure equations can be written as

$$\left(\frac{\partial \pi}{\partial \phi}\right)_{\theta} = 3.624\theta \left(\frac{1.5165}{\phi^{7/3}\theta^{5/3}} - \frac{1 + 0.0784\,\phi^{-3/2}}{(\phi - 0.1567\phi^{-1/2})^2} \right) = 0 \quad , \qquad \text{(III-25)}$$

$$\pi_{min} = 3.624 \left(\frac{(\phi - 0.1567\phi^{-1/2})^{-4/5}}{(0.66\phi^{7/3} + 0.0516\phi^{5/6})^{3/5}} - \frac{0.9099(0.66\phi^{7/3} + 0.0516\phi^{5/6})^{2/5}}{\phi^{5/3}(\phi - 0.1567\phi^{-1/2})^{4/5}} \right) \qquad \text{(III-26)}$$

and

$$\frac{\partial \pi_{min}}{\partial \theta} = 3.624 \left(\frac{1}{\phi - 0.1567\phi^{-1/2}} + \frac{0.6066}{(\phi\theta)^{5/3}} \right) \quad . \qquad \text{(III-27)}$$

The reduced volume, coefficient of thermal expansion and the compressibility coefficient for both the Berthelot and the Benson equations are obtained in exactly the same manner as for the Van der Waals equation. For the Berthelot equation

$$\phi = \frac{9}{16\theta^2}\left(1 - \left(1 - \frac{32}{27}\theta^2\right)^{1/2}\right) \quad , \qquad \text{(III-28)}$$

$$\alpha = \frac{1}{T}\left(\frac{16\phi\theta^2}{9 - 16\phi\theta^2}\right) \quad , \qquad \text{(III-29)}$$

and

$$\beta = \frac{8\theta^3\phi^3}{27\,P_c}\left(1 - \frac{48}{27}\theta^2\phi\right)^{-1} \qquad \text{(III-30)}$$

For Benson's equation the relation between ϕ and θ must be solved by numerical methods:

$$\frac{\phi^{3/2} - 0.1567}{\phi^{13/6}} = 1.1\theta^{5/3} \quad . \qquad \text{(III-31)}$$

The equations for α and β are

$$\alpha = \frac{5}{3T_c} \left(\frac{(\theta\phi)^{2/3}}{1.365 - 2.167\theta^{5/3}\phi^{2/3}} \right) \qquad \text{(III-32)}$$

and

$$\beta = \frac{\theta^{2/3}\phi^{5/3}}{3.297P_c} \left(\frac{1.365}{\phi^{2/3} - \theta^{5/3}} - 2.167 \right) - 1 \quad . \qquad \text{(III-33)}$$

The values for ϕ, α, β, maximum tensile strength and change of tensile strength with temperature as calculated from the Van der Waals, Berthelot and Benson equations are given in Table 1 along with the actual values for ϕ, α, and β.

When the calculated and the observed values are compared in Table 1, the expected wide variation in results is noticed. Thus, the only information that can be garnered from this analysis is that the theoretical tensile strength of water at room temperature is between 1000 and 5000 atmospheres.

Tensile Strength as Calculated From the Theory of Holes

The general method for obtaining the thermodynamic properties of a system of particles is to calculate the partition function of the system as a function of the volume and the temperature. This calculation can be performed if the law of force between the particles is known. Obviously this method can only be applied if the configurations of the system which contribute to the partition function are such that it can be handled mathematically.

TABLE I

VALUES OF REDUCED VOLUME, COEFFICIENT OF THERMAL EXPANSION, COMPRESSIBILITY COEFFICIENT, TENSILE STRENGTH AND CHANGE OF TENSILE STRENGTH WITH RESPECT TO TEMPERATURE FOR WATER AT ROOM TEMPERATURE AS CALCULATED FROM THE VAN DER WAALS, BERTHELOT AND BENSON EQUATIONS OF STATE

	Φ: Obs. Value:	% Deviation from	$\alpha \times 10^4$: Obs. Value:	% Deviation from	$\beta \times 10^5$: Obs. Value:	% Deviation from	P(atm):	$\frac{dP}{dT}$ (atm/°C)
Van der Waals	0.346	+ 24	10.7	+ 365	5.74	+ 26	- 996	5.8
Berthelot	0.355	+ 11	7.34	+ 315	0.655	- 85	-4800	38
Benson	0.322	+ 0.6	6.65	+ 190	14.9	+226	-3200	24
Observed	0.32		2.3		4.57			2.0

There are two general cases where this method can be applied; the case of a gas and the case of a crystallized solid. Due to a large amount of work on the scattering of X-rays by liquids, it is generally concluded that the structure of a liquid is similar to that of a solid crystal rather than to that of a gas as was assumed by Van der Waals.

The simplest model, proposed by Furth (18), is suggested by the fact that a certain number of sites in a crystal lattice are unoccupied and the atoms can change their positions by jumping from one place to a neighboring unoccupied place or hole. Furth's theory uses a model which makes it possible to use a statistical treatment of the liquid which is analogous to that used in the statistical theory of gases. He does not use a model which is an exact analogy between a liquid and a crystal because the statistical theory of gases is much easier to handle than that of the solid state.

In his theory Furth considers the holes as the equivalent of clusters in a dense gas or vapor. They are formed by the action of the irregular thermal movement and are destroyed again by the same process. They interact with each other and perform a kind of Brownian motion. The hole sizes obey a certain distribution law in which the frequency of the larger holes increase as the temperature is increased or as the pressure is decreased. Evaporation is the complete destruction of the system by the holes so that it consists of pieces which are not connected with one another. It is further assumed that the matter outside the holes is a continuum with the normal surface tension of the liquid, and the holes are filled with saturated vapor corresponding to the given temperature. Using the above assumptions, Furth's equation

for liquid tensile strength can be obtained.

The energy, Eq, required for the formation of a spherical hole of radius r is equal to the sum of the work to be done against the surface tension and the work to be done against the pressure. In equation form this is expressed as

$$Eq = 4/3\ \pi\ r^3\ (P-P_o) + 4\ \pi\ r^2\ \sigma\ , \qquad \text{(III-34)}$$

where P is the external pressure, P_o is the pressure of the saturated vapor and σ is the surface tension of the liquid. The probability that the radius r of a hole formed by statistical fluctuations has a value between r and r + dr is

$$W(r)dr = Cdr \int_{-\infty}^{\infty} Exp. \left(-\frac{E_T}{kT}\right) dxdydzdP_x dP_y dP_z dP_r \qquad \text{(III-35)}$$

where x, y and z are the coordinates of the center of the hole, P_x, P_y and P_z are the corresponding moments, P_r is the momenta corresponding to the variable r and E is the total energy. The constant C is a normalizing function and is such that

$$\int_o^{\infty} W(r)dr = 1. \qquad \text{(III-36)}$$

The total energy, E_T, is equal to the sum of the energy required to form the hole and the energy due to the momentum of the hole:

$$E_T = Eq + \frac{P_x^2 + P_y^2 + P_z^2}{2m_1} + \frac{P_r^2}{2m_2} \quad . \qquad \text{(III-37)}$$

In the above equation m_1 is the apparent mass of the hole for a translation,

$$m_1 = 2/3\ \rho\ \pi\ r^3 \qquad \text{(III-38)}$$

and m_2 is the apparent mass for the expansion of the hole,

$$m_2 = 4 \rho \pi r^3 . \qquad \text{(III-39)}$$

The variable ρ is the density of the liquid.

Since Eq. (111-37) is independent of the space variable, the integration with respect to these variables in Eq. (111-35) gives a factor V which is equal to the volume of the liquid. Eq. (111-35) can now be written as

$$W(r)dr = Cdr \int_{-\infty}^{\infty} \text{Exp} \quad - \frac{E_T}{kT} dP_x dP_y dP_z dP_r \quad , \qquad \text{(III-40)}$$

where the constant C now contains the factor V.

If Eq. (111-40) is integrated over all momenta, the probability function takes the form

$$W(r)dr = Cdr(2\pi kT)^2 m_1^{3/2} m_2^{1/2} \text{Exp} \left(- \frac{Eq}{kT}\right), \qquad \text{(III-41)}$$

where use has been made of the well-known integral

$$\int_{-\infty}^{\infty} \text{Exp} \left(-x^2\right) \quad d\,x = \sqrt{\pi} \qquad \text{(III-42)}$$

Eq. (111-40) can be put in the more convenient form

$$W(r)dr = C \text{ Exp} \left(- \frac{Eq}{kT}\right) \quad r^6 \, dr \quad , \qquad \text{(III-43)}$$

where all the quantities in Eq. (111-41) that do not depend on r are incorporated into the constant C.

The integral

$$\int_0^{\infty} \text{Exp} \left(- \frac{Eq}{kT}\right) r^6 dr = \int_0^{\infty} \text{Exp} \left(-4/3\pi r^3 \frac{(P-P_o)}{kT} - \frac{4\pi r^2 \sigma}{kT}\right) r^6 dr \qquad \text{(III-44)}$$

can be put in the following form

$$\frac{3(P-P_o)}{7kT} \int_0^{\infty} 4/3\pi r^3 \text{Exp} \left(- \frac{Eq}{kT}\right) r^6 dr + \frac{2\sigma}{7kT} \int_0^{\infty} 4\pi r^2 \text{Exp} \left(- \frac{Eq}{kT}\right) r^6 \, dr \qquad \text{(III-45)}$$

by an integration by parts. If the average volume, v, of a hole,

$$v = \int_0^\infty 4/3\pi r^3 W(r)dr \qquad \text{(III-46)}$$

and the average surface, f, of a hole,

$$f = \int_0^\infty 4\pi r^2 W(r)dr \qquad \text{(III-47)}$$

is substituted into Eq. (111-45), it can be put in a much simpler form:

$$\int_0^\infty \text{Exp}\left(-\frac{Eq}{kT}\right) r^6 dr = \frac{3(P-P_o)}{7kT} v + \frac{2\sigma}{7kT} f \quad . \qquad \text{(III-48)}$$

When Eq. (111-36) is substituted into Eq. (111-48), the following equation results:

$$1 = \frac{3(P-P_o)}{7kT} v + \frac{2\sigma}{7kT} f \qquad \text{(III-49)}$$

where the constant C is set equal to unity. If it is further assumed that the ratio $v/f^{3/2}$ is approximately equal to the value obtained when P is equal to P_o, the ratio of Eq. (111-46) to Eq. (111-47) raised to the 3/2 power can be written as

$$\frac{v_o}{f_o^{3/2}} = \frac{v}{f^{3/2}} = \frac{1}{9.64} \quad . \qquad \text{(III-50)}$$

This ratio has been shown by Furth (18) to be a very good approximation.

When Eq. (111-50) is substituted into Eq. (111-49), the following equation results:

$$7kT = 3(P-P_o)\, v + 9.06\, \sigma\, v^{2/3} \quad . \qquad \text{(III-51)}$$

If P_o is substituted for P in Eq. (111-34) and if this value for W(r) is used in Eq. (111-46), the following equation for v_o is obtained:

$$v_o = 0.68 \left(\frac{kT}{\sigma}\right)^{3/2} \qquad \text{(III-52)}$$

When Eq. (111-52) is used in Eq. (111-51) to eliminate σ, the following equation can be written:

$$\frac{3(P-P_o)}{7kT} = \left(1 - \left(\frac{v}{v_o}\right)^{2/3}\right)\frac{1}{v} \quad . \qquad \text{(III-53)}$$

Furth (18) plotted Eq. (111-53) with $\frac{P-P_o}{kT}$ as one coordinate and v as the other coordinate. It is represented graphically by Figure 5. For $P > P_o$ the holes will increase in size as the external pressure P is reduced at constant temperature. The part of the curve below the v axis does not correspond to any real statistical equilibrium since the integral

$$\int_o^\infty \mathrm{Exp}\left(-\frac{Eq}{kT}\right) r^n \, dr$$

will not converge for $P-P_o < 0$. The non-convergence of the above integral does have physical significance in that it predicts the probability for the formation of holes of large size is infinite. This corresponds to the phenomena of boiling. Normally this phenomena starts with P equal to P_o; since there is no discontinuity at v equal to v_o, it is assumed that the states represented by that portion of the curve below the v axis can exist in a kind of metastable equilibrium. The minimum value of P in this range is given by

$$\left(\frac{\partial P}{\partial}\right)_T = 0 \qquad \text{(III-54)}$$

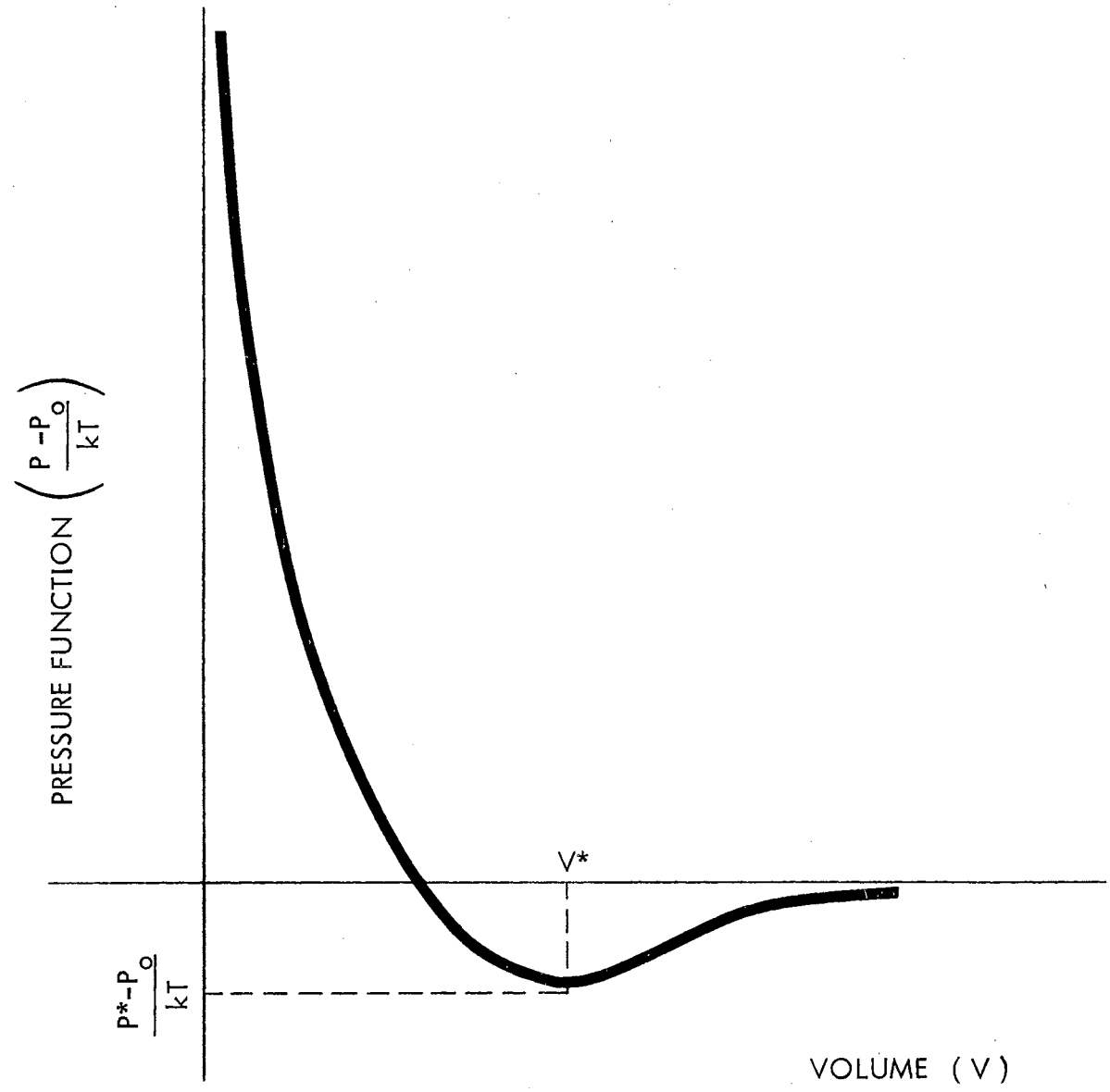

FIGURE 5. Graphical Representation of Eq. (III-53)

which by means of Eq. (III-53) becomes

$$\left(\frac{\partial P}{\partial v}\right)_T = \frac{7kT}{3v^2}\left(1 - \frac{1}{3}\left(\frac{v}{v_o}\right)^{2/3}\right) = 0 \quad . \qquad \text{(III-55)}$$

The value for v which satisfies Eq. (III-55) is

$$v^* = 5.2\ v_o \quad . \qquad \text{(III-56)}$$

The compressibility, which is the reciprocal of Eq. (III-54) multiplied by 1/v, of a hole in this state is infinitely great. This implies that for any state below that corresponding to $v = v^*$ the liquid will become completely unstable. This state will therefore correspond to the maximum tensile strength that the liquid can stand. From Eq. (III-52), Eq. (III-53) and Eq. (III-56) the value for the maximum tensile strength is obtained:

$$P^* - P_o = -1.3\ \sigma^{3/2}\ (kT)^{-1/2} \quad . \qquad \text{(III-57)}$$

The above equation gives a value of 3900 atmospheres for water at 25°C.

An equation similar to Eq. (III-57) can be obtained without using the assumption of Eq. (III-50). To do this the shape of the distribution function when $P > P_o$ and when $P < P_o$ must be considered. The distribution function for the region $P > P_o$ will be similar to the first curve of Figure 6 (18). For the metastable region, $P^* < P < P_o$, the curve will be altered to one similar to the second curve of Figure 5. As P approaches P* the values for r_{max} and r_{min} come closer together and finally take the shape of the third curve of Figure 6.

The value for r corresponding to the inflection point in the third curve of Figure 6 is given by

$$\frac{dW}{dr} = 0 \quad ,$$

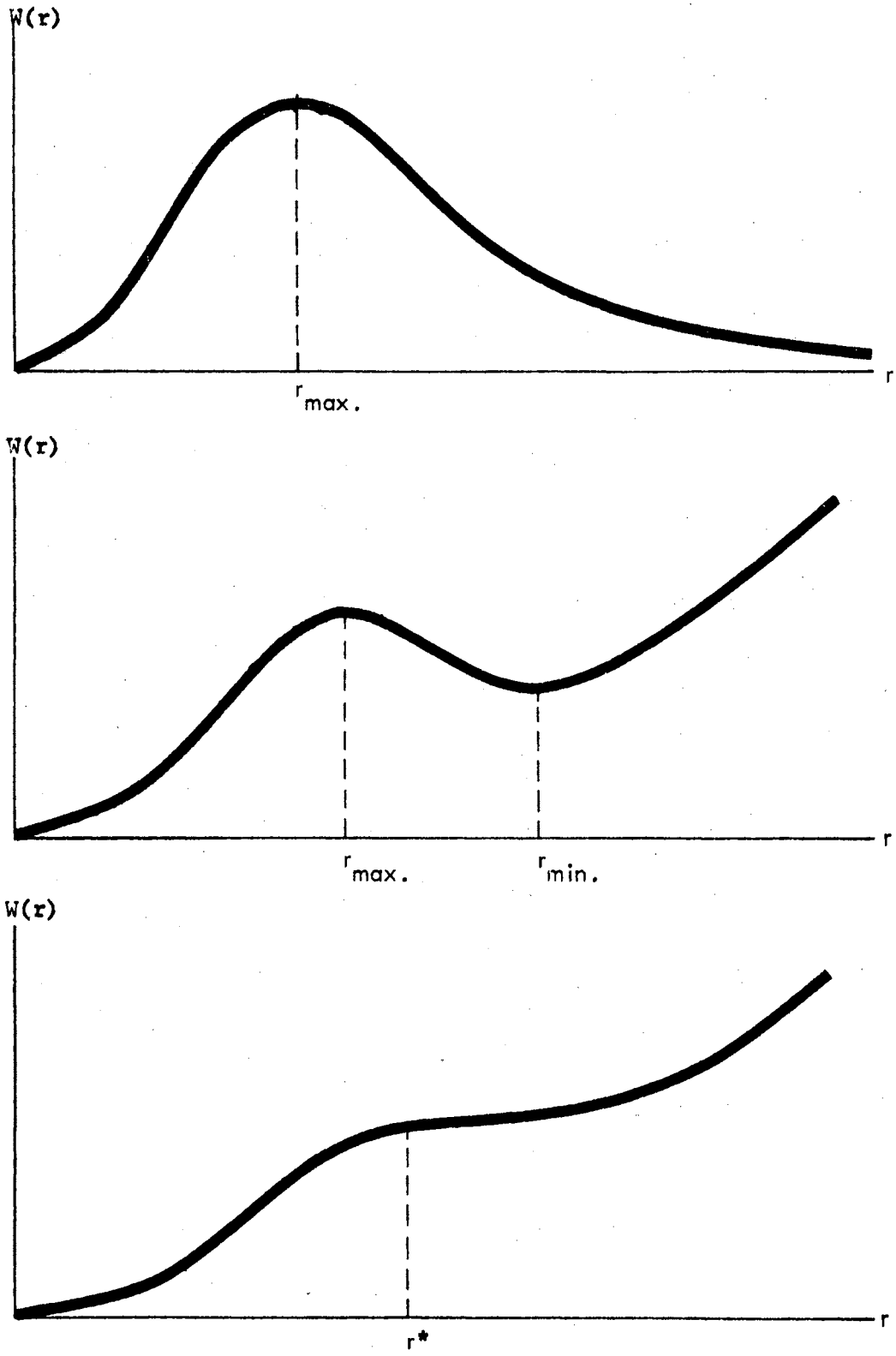

FIGURE 6. Distribution Functions

and

$$\frac{d^2W}{dr^2} = 0 \quad .$$

When the above conditions are applied to Eq. (111-43), the values for r, v and P at the inflection point are obtained:

$$r^* = \frac{3}{2\sqrt{\pi}} \left(\frac{kT}{\sigma}\right), \tag{III-58}$$

$$v^* = \frac{9}{2\sqrt{\pi}} \left(\frac{kT}{\sigma}\right)^{3/2} = 3.73\ v_o \tag{III-59}$$

and

$$P^*-P_o = -\frac{8\sqrt{\pi}}{9}\ \sigma^{3/2}(kT)^{-1/2} = -1.57\ \sigma^{3/2}(kT)^{-1/2} \quad . \tag{III-60}$$

Eq. (111-60) gives a value of 4730 atmospheres for the tensile strength of water at 25°C. When the assumption of Eq. (111-50) is used, a value of 3900 atmospheres is obtained. This is a difference of 17% from the above value. When the assumptions that are implicit in all of the above calculations are considered, the assumption of Eq. (111-50) cannot be considered as being too much in error.

Tensile Strength as Calculated From the Theory of Nucleation

The theory of nucleation states that the rate of bubble formation is proportional to $\text{Exp}\left(-\frac{E_{max}}{kT}\right)$ where E_{max} is the maximum energy for the reversible formation of a spherical vapor bubble of radius r. The proportionality factor can be estimated from the theory of absolute reaction rates to be

$$\frac{nkT}{h}\text{Exp}\left(-\frac{\Delta f_o^*}{kT}\right) \tag{III-61}$$

where n is the number of molecules per gram-mole in the liquid, Δf_o^* is the free energy of activation for the motion of an individual molecule of liquid past its neighbors into or away from the bubble surface, k is Boltzman's constant, h is Planck's constant and T is the temperature (15).

The energy required for the formation of a spherical vapor bubble or radius r is

$$E = 4\pi r^2\sigma + 4/3\pi r^3(P-P_o) \quad , \tag{III-62}$$

where the variables are the same as for Eq. (111-34). To find the value of r corresponding to E_{max}, the derivative with respect to r of Eq. (111-61) is set equal to zero and then solved for r. This operation yields

$$r = \frac{2\sigma}{P-P_o} \quad , \tag{III-63}$$

and

$$E_{max} = \frac{16\pi\sigma^3}{3(P-P_o)^2} \quad . \tag{III-64}$$

The equation for the rate of formation of vapor bubbles in a gram-mole of liquid subjected to a negative pressure, P, can now be written:

$$\frac{dn}{dt} = \frac{nkT}{h}\mathrm{Exp}\left(-\frac{\Delta f_o^*}{kT} + \frac{16\pi\sigma^3}{3kT(P-P_o)}\right) . \tag{III-65}$$

Eq. (111-65) assumes that the pressure is kept at P even after the first bubbles have begun to grow.

The value of Δf_o^* for the motion of a molecule into or away from the bubble surface can be estimated from the free energy of activation for viscosity, Δf_{vis}, since the two free energies should be approximately equal. Roseveare (15) states that Δf_{vis}^* is between 0 and 5000

cal/mole for most liquids that are fluid at room temperature. Fisher (15) found that by putting Δf_o^* equal to 0 a value of P is obtained which is generally less than 5 percent too small for room temperature liquids.

When the above simplification is utilized, Eq. (111-65) can be rewritten as

$$\frac{dn}{dt} = \frac{nkT}{h} \text{ Exp } \left(\frac{-16\pi \sigma^3}{3kT(P-P_o)^2} \right) . \qquad \text{(III-66)}$$

Since the first bubble that forms in a liquid will fracture the liquid, the fracture pressure, or tensile strength, will be the negative pressure that gives one bubble in t seconds. Then dn/dt is equal to 1/t and Eq. (111-66) yields

$$(P-P_o) = - \left(\frac{16\pi}{3} \quad \frac{1}{kT \ln \frac{nkTt}{h}} \right)^{1/2} . \qquad \text{(III-67)}$$

Fisher (15) calculated values for the fracture pressure corresponding to a number of waiting times for water at 27°C. He covered time values from 10^{-15} sec, which is less than the time required for sound to travel one atomic distance, to a time period of 10^{18} sec, which is longer than the estimated age of the universe. The ratio of the maximum to the minimum fracture pressure was only 1.58 while the corresponding time ratio was 10^{33}. Thus, Fisher concluded that one cannot be seriously in error by taking the fracture pressure corresponding to one vapor bubble per gram-mole per second as the theoretical tensile strength of the liquid. With this assumption, Eq. (111-67) becomes

$$(P-P_o) = - \frac{16\pi}{3} \left(\frac{\sigma^3}{kT \ln \frac{nkT}{h}} \right)^{1/2} . \qquad \text{(III-68)}$$

For water at 25°C Eq. (111-68) gives a value of 1320 atmospheres for the tensile strength.

Table 2 is a summary of the theoretical tensile strengths that have been reviewed in this chapter.

TABLE II

LIQUID TENSILE STRENGTH OF WATER

	Langmuir	Van der Waals	Berthelot	Benson	Hole Theory	Nucleation Theory
P(atm)	-10,000	-1000	-4800	-3200	-4700	-1300

It can be seen from the above table that there is quite a wide variation in the calculated theoretical tensile strengths for water. This is not something that is peculiar to water but would be the same for any fluid considered due to the limitations of the theories considered. The remaining portion of this chapter will be used to discuss the various theories and their shortcomings.

The theory of a homogeneous liquid as given by Langmuir gives results which are too high because of the basic assumption that the liquid has no microscopic impurities or vapor bubbles. Though one might argue that this condition is not impossible, it would certainly have to be agreed that it is very improbable.

The Van der Waals, Berthelot and Benson equations of state were then considered. Aside from the fact that these equations are not supposed to be applicable to associated liquids, such as water, the constants that are used in them are definitely temperature-dependent and have an effect on the results.

The Theory of Holes was considered next. As pointed out by Furth, this theory will be in error since Furth used concepts such as surface tension and hydrodynamic virtual mass which are essentially macroscopic in connection with cavities of molecular dimensions. This theory predicts values for the tensile strength which are only one-half the value obtained by Langmuir. To obtain an idea of the enormousness of this figure, it should be remembered that the largest void or hole that would be possible in water would be on the order of 10^{-8} cm radius. This is approximately equivalent to a molecular distance.

The Nucleation Theory has essentially the same discrepancy as the Theory of Holes in that a measured value of surface tension is used for the effective surface tension on the interface between a very small bubble and the liquid. These measured values of surface tension may be considerably different from the effective surface tension, but this theory does give values which are more reasonable than Furth's values (4).

So it is seen that all of the theories discussed in this chapter have basic assumptions that cast doubt on the validity of the results, but at least they have given a better understanding of the actual structure of the liquid. Thus the only statement that can be made about the liquid tensile strength of water is that it should fall somewhere between 1000 atmospheres and 3000 atmospheres and very probably closer to the lower value. When this is compared to the highest value obtained experimentally (which is 300 atmospheres), it is noticed that the theory and the experimentally observed values are getting closer together; that is, they are at least within an order of magnitude.

The maximum radius of a vapor bubble that can exist in a fluid that is stressed to 300 atmospheres is on the order of 0.5×10^{-6} cm and that corresponding to 1000 atmospheres is on the order of 0.1×10^{-6} cm. These two radii are on the order of the minimum radius of a stable gas bubble that can exist in a liquid according to Frenkel (17). Any bubble that is smaller than this should be unstable and would be compressed out of existence if it existed in the body of the liquid. This might be a solution to the problem of liquid standardization. That is, if any bubble smaller than the critical radius would be compressed out of existence due to instability and if any bubbles larger than this critical radius could be eliminated by a precompression of the fluid, then a fluid with a tensile strength that is indicative of the actual strength of the fluid and not on a number of other factors would be obtained. Though this is simplifying a very complicated phenomena, it is a step in the right direction and certainly deserves some consideration.

CHAPTER IV

THEORETICAL ANALYSIS

Much of the theoretical and experimental work on axially-excited tanks performed to date has been concerned with the sloshing phenomena for both rigid and elastic tanks.

A very good theoretical analysis of the liquid response in annular cylindrical tanks and circular quarter-tanks has been given by Bauer (3). Bauer derived an equivalent mechanical model consisting of masses, springs, dampers and a massless disc with a moment of inertia so chosen that it exerts the same forces and moments and has the same natural frequencies as the fluid in the container. This mechanical analog method has been tried by other authors but Bauer's analog differs from the others in that he used a velocity proportional damping force in his system (2, 19, 20, 27, 30). In this way he was able to obtain results even for frequencies which were close to the natural frequencies of the fluid. Abramson (2) discusses some of the liquid dynamic behavior which occurs in tanks. These include normal sloshing, vortexing, liquid impact, bubble formations, spray formations and low gravity phenomena. He also discusses some of the equivalent mechanical models that are used to describe the dynamics of the tank.

A complete review of the literature on liquid dynamic behavior in moving containers has been written by Cooper (14) and Abramson (1).

They cover rigid and elastic containers of various geometries that are excited in the vertical and horizontal directions. A few authors are mentioned who have considered the liquid motion due to pitch about a horizontal axis and roll about a vertical axis for rectangular and cylindrical tanks.

In the papers mentioned above, the governing equation for the fluid motion was Laplace's equation which is a combination of the continuity equation and the equation of motion for a non-viscous incompressible fluid. Viscous effects were taken into account in the mechanical analogs by the introduction of damping forces.

The analysis presented in this chapter is unique in that it takes the basic linear Navier-Stokes equation and the continuity equation for compressible fluid flow, and by assuming only that the density is a function of the time t, it develops a set of equations for the radial velocity, azimuthal velocity and the pressure field anywhere within the cylinder. These general equations are then applied to a specific problem at the end of the chapter.

Mathematical Equations and Boundary Conditions

This analysis is concerned with the behavior of a fluid which is confined within a closed circular cylinder and is subject to a sinusoidal varying force along its longitudinal axis, Figure 7. Initially the cylinder has displacement equal to the amplitude of the input displacement, a, and a zero velocity. The boundary conditions on the cylinder for all time greater than or equal to zero are that the pressure at the free surface is zero, the radial velocity at the wall is zero, and the azimuthal velocity at the wall and at the tube bottom is

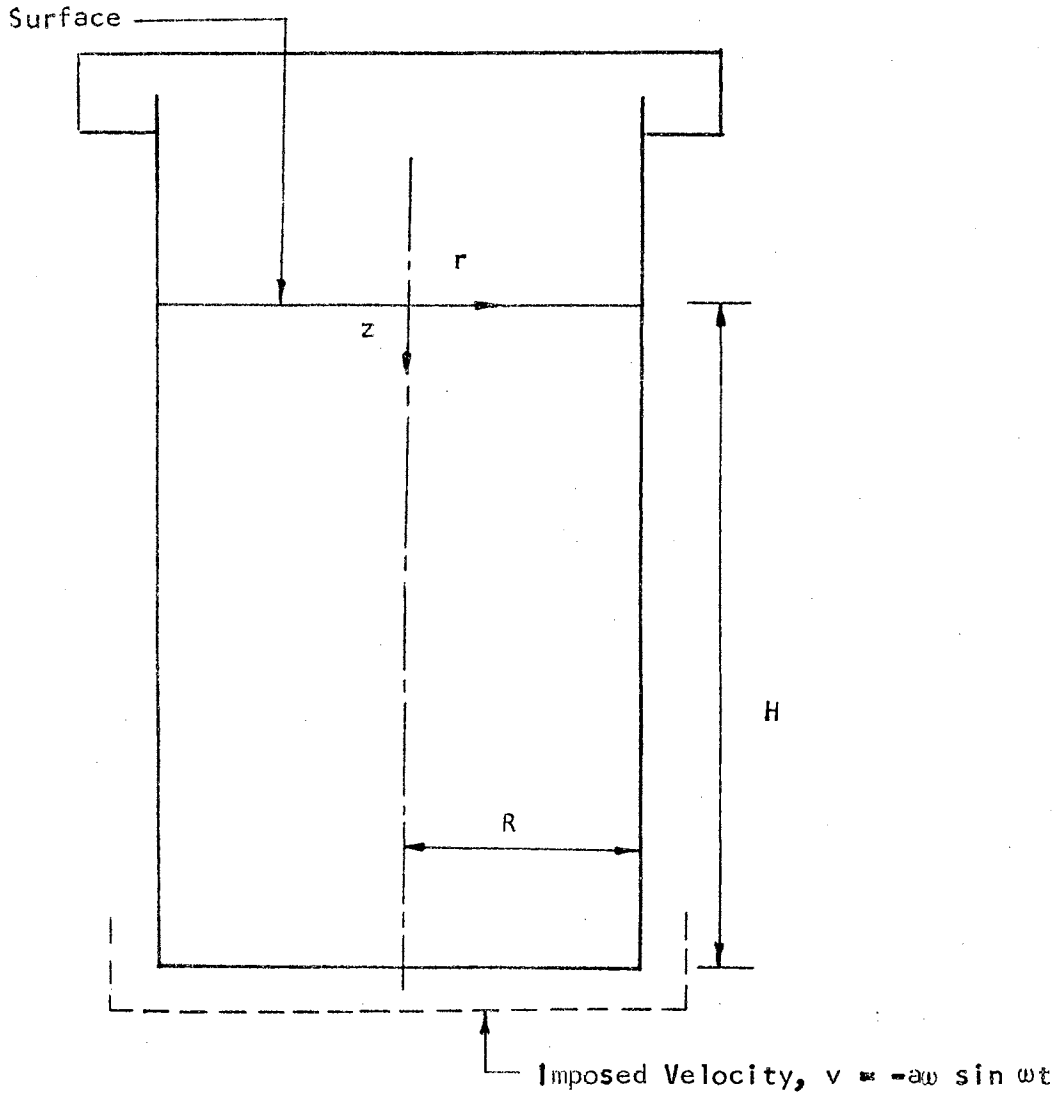

FIGURE 7. Physical Model for Eq. (IV-6)

equal to $-a\omega \sin \omega t$; that is

$$\text{(a)}\quad P = 0 \text{ at } z = 0,$$

$$\text{(b)}\quad v_r = 0 \text{ at } r = R,$$

$$\text{(c)}\quad v_z = -a\omega \sin \omega t \text{ at } r = R$$

and

$$\text{(d)}\quad v_z = -a\omega \sin \omega t \text{ at } z = h. \qquad \text{(IV-1)}$$

The general linear equations of hydrodynamics will be used to describe the system. The nonlinear convective terms have been ignored because they are negligible when compared with the time derivatives of the dependent variables. The dependent variables v_r and v_z are assumed to be functions of the radius r, the height z and the time t while the density, ρ, is assumed to be only a function of the pressure P which is a function of r, z and t.

The continuity equation for a compressible fluid can be written in the form:

$$\frac{\partial \rho}{\partial t} + \rho \left(\nabla \cdot V \right) = 0, \qquad \text{(IV-2)}$$

where V is the velocity. Eq. (1V-2) can be put in the more convenient form

$$\frac{\partial P}{\partial t} = -\frac{1}{\beta_T} \nabla \cdot V, \qquad \text{(IV-3)}$$

where the isothermal compressibility coefficient, β_T, is defined as

$$\beta_T = \frac{1}{\rho} \left(\frac{\partial \rho}{\partial P} \right)_T . \qquad \text{(IV-4)}$$

The general Navier-Stokes equation for a viscous compressible fluid is

$$\rho \frac{\partial V}{\partial t} = -\nabla P + \mu \nabla^2 V + \frac{\mu}{3} \nabla (\nabla \cdot V). \qquad \text{(IV-5)}$$

The two partial differential equations, Eq. (IV-3) and Eq. (IV-5), subject to the boundary conditions, Eq. (IV-1), can most easily be solved by the superposition principle. That is, the partial differential equations subject to the boundary conditions

$$\text{(a)}\quad P = 0 \text{ at } z = 0,$$

$$\text{(b)}\quad v_r = 0 \text{ at } r = R,$$

$$\text{(c)}\quad v_z = 0 \text{ at } r = R,$$

and

$$\text{(d)}\quad v_z = -\alpha\omega \sin \omega t \text{ at } z = h, \qquad \text{(IV-6)}$$

are first solved and the same partial differential equations subject to the boundary conditions

$$\text{(a)}\quad P = 0 \text{ at } z = 0$$

$$\text{(b)}\quad v_r = 0 \text{ at } r = R,$$

$$\text{(c)}\quad v_z = -\alpha\omega \sin \omega t \text{ at } r = R,$$

and

$$\text{(d)}\quad v_z = 0 \text{ at } z = h \qquad \text{(IV-7)}$$

are then solved. The two solutions thus obtained can be added together and this final solution will be a solution of Eq. (IV-3) and Eq. (IV-5) and will converge to the boundary conditions, Eq. (IV-1), at the boundary. This principle of superposition is valid only for linear boundary value problems and can be used here since Eq. (IV-3) and Eq. (IV-5) are linear equations.

Cylinder with Oscillating End and Stationary Walls

The physical problem corresponding to Eq. (IV-3) and Eq. (IV-5) and satisfying the boundary conditions of Eq. (IV-6) is that of an oscillating piston in a cylinder, Figure 8. It has been shown that for a velocity much less than the speed of sound there will be only a velocity component in the longitudinal direction (8). With this

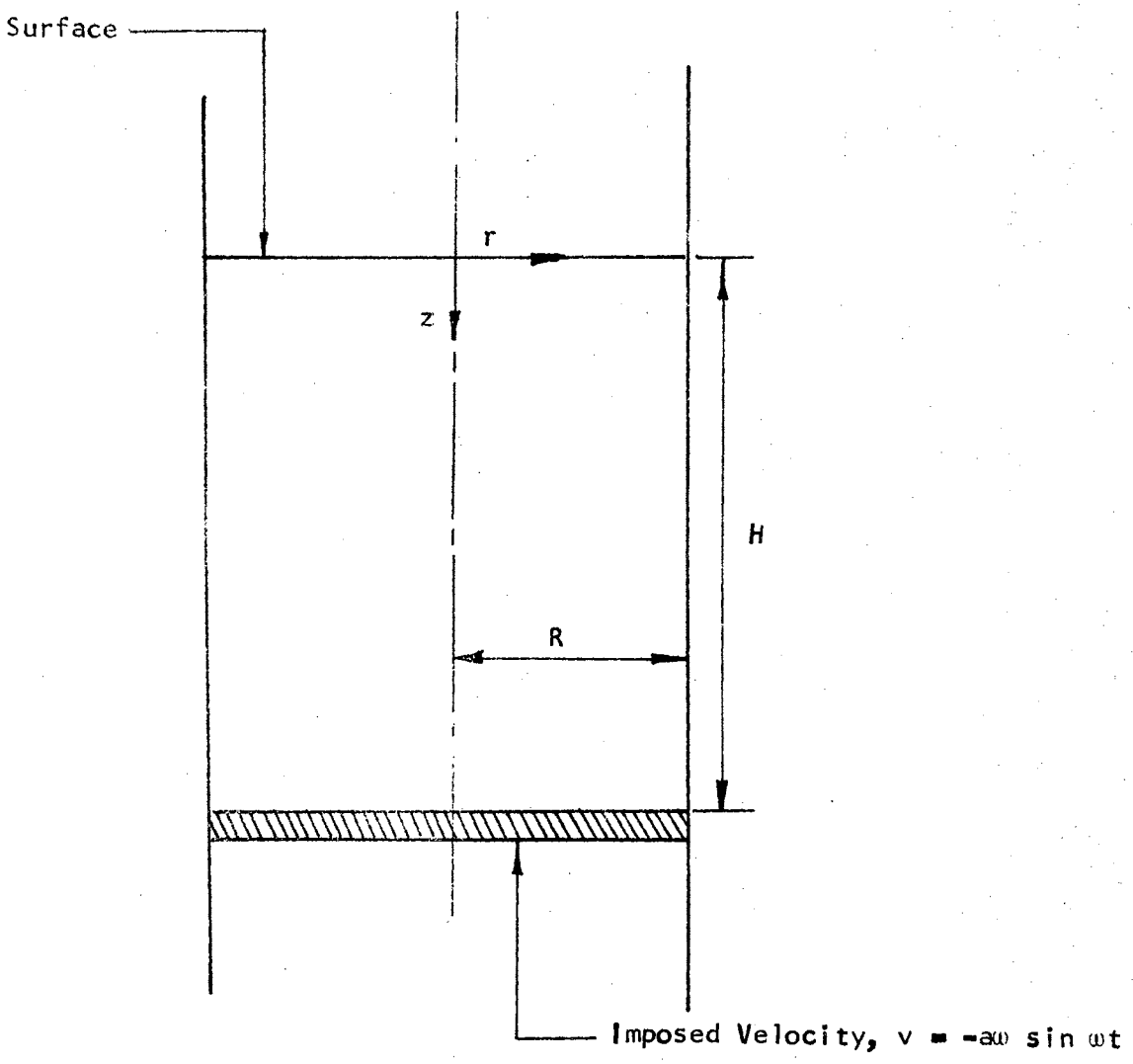

FIGURE 8. Physical Model for Eq. (IV-7)

assumption, Eq. (IV-3) and Eq. (IV-5) reduce to

$$\frac{\partial P}{\partial t} = -\frac{1}{\beta_T} \frac{\partial v_z}{\partial z} \qquad \text{(IV-8)}$$

and

$$\frac{\partial v_z}{\partial t} = -\frac{1}{\rho}\frac{\partial P}{\partial z} + \nu \frac{\partial^2 v_z}{\partial r^2} + \frac{\nu}{r}\frac{\partial v_z}{\partial r} + 4/3\nu \frac{\partial^2 v_z}{\partial z^2} \quad . \qquad \text{(IV-9)}$$

The above equations can most easily be solved by utilizing the Laplace Transform technique. The transformed equations corresponding to Eq. (IV-8) and Eq. (IV-9) are

$$S\bar{P} - P(o) = \frac{1}{\beta_T}\frac{\partial \bar{v}_z}{\partial z} \quad , \qquad \text{(IV-10)}$$

and

$$S\bar{v}_z = -\frac{1}{\rho}\frac{\partial \bar{P}}{\partial z} + \nu\left(\frac{\partial^2 \bar{v}_z}{\partial r^2} + \frac{1}{r}\frac{\partial \bar{v}_z}{\partial r} + 4/3\frac{\partial^2 \bar{v}_z}{\partial z^2}\right) \quad , \qquad \text{(IV-11)}$$

where the bars denote the dependent variables in the Laplace domain. When Eq. (IV-10) is differentiated with respect to z, the following equation is obtained:

$$\frac{\partial \bar{P}}{\partial z} = -\frac{1}{\beta_T S}\frac{\partial^2 \bar{v}_z}{\partial z^2} \quad , \qquad \text{(IV-12)}$$

where it has been assumed that the derivative of P(o) with respect to z is equal to zero.

When Eq. (IV-12) is substituted into Eq. (IV-11), the following equation for v_z results:

$$\frac{\partial^2 \bar{v}_z}{\partial r^2} + \frac{1}{r}\frac{\partial \bar{v}_z}{\partial r} + \left(4/3 + \frac{1}{\rho\beta_T S\nu}\right)\frac{\partial^2 \bar{v}_z}{\partial z^2} - \frac{S}{\nu}\bar{v}_z = 0 \quad . \qquad \text{(IV-13)}$$

This equation can be solved by assuming a solution of the form

$$\bar{v}_z = R(r)\, Z(z) \qquad \text{(IV-14)}$$

which is the commonly used Separation of Variables technique. Eq. (IV-13) now takes the form

$$-\frac{1}{R}\frac{d^2F}{dr^2}-\frac{1}{r}\frac{1}{R}\frac{dR}{dr}+\frac{S}{\nu}=l^2\frac{1}{Z}\frac{d^2Z}{dz^2} \qquad \text{(IV-15)}$$

where

$$l^2=4/3\,\frac{1}{\rho\beta_T S\nu} \quad .$$

Since the left-hand side of Eq. (IV-15) is a function of R and the right-hand side is only a function of Z, both sides of the equation must be equal to some constant, say γ^2. When the right-hand side of Eq. (IV-15) is set equal to γ^2 the following equation results:

$$\frac{d^2Z}{dZ^2}-\frac{\gamma^2}{l^2}Z=0 \quad . \qquad \text{(IV-16)}$$

A solution of the above equation is

$$Z=\cosh\frac{\gamma}{l}Z \quad . \qquad \text{(IV-17)}$$

The hyperbolic sine term has been omitted since the pressure at $z=0$ must always equal zero. The left-hand side of Eq. (IV-15) takes the form

$$\frac{d^2R}{dr^2}+\frac{1}{r}\cdot\frac{dR}{dr}+\left(\gamma^2-\frac{S}{\nu}\right)R=0 \quad . \qquad \text{(IV-18)}$$

A solution of the above equation is

$$R=J_o\left(\sqrt{\gamma^2-\frac{S}{\nu}}\;\right)r \quad . \qquad \text{(IV-19)}$$

When Eq. (IV-17) and Eq. (IV-19) are substituted into Eq. (IV-14) the solution for v_z is obtained

$$\bar{v}_z=\sum_{n=0}^{\infty}A_n J_o\left(\sqrt{\gamma_n^2-\frac{S}{\nu}}\;r\right)\cosh\frac{\gamma_n}{l}Z \quad , \qquad \text{(IV-20)}$$

where A is a constant dependent on the boundary conditions.

The constants A and γ are determined by equating Eq. (IV-20) to the transformed boundary conditions:

$$\bar{v}_z = 0 \text{ at } r = R;$$

$$\bar{v}_z = -\frac{a\omega^2}{s^2+\omega^2} \text{ at } Z = h \quad . \tag{IV-21}$$

The homogeneous boundary condition yields the following infinite sum:

$$\sum_{n=0}^{\infty} A_n J_o\left(\sqrt{\gamma_n^2 - \frac{s}{\nu}}\, R\right) \cosh \frac{\gamma_n}{l} Z = 0 \tag{IV-22}$$

where the γ_n are the roots of

$$J_o \sqrt{\gamma_n^2 - \frac{s}{\nu}}\, R = 0 \quad . \tag{IV-23}$$

The second boundary condition yields the following equality:

$$-\frac{a\omega^2}{s^2+\omega^2} = \sum_{n=0}^{\infty} A_n J_o\left(\sqrt{\gamma_n^2 - \frac{s}{\nu}}\, r\right) \cosh \frac{\gamma_n}{l} h. \tag{IV-24}$$

Since the sequence $J_o(\alpha R)$ is orthogonal on the interval (0,R), the constant A_n can be determined by multiplying both sides of Eq. (IV-24) by $r J_o(\alpha r)$. The resulting equation is then integrated between zero and R. When this method is applied to Eq. (IV-24), the following equality results:

$$A_n \int_0^R r J_o(\alpha r) J_o\left(\sqrt{\gamma_n^2 - \frac{s}{\nu}}\, r\right) \cosh \frac{\gamma_n}{l} h \, d r = -\frac{a\omega^2}{s^2+\omega^2} \int_0^R r J_o(\alpha r) \, d r \quad . \tag{IV-25}$$

The constant A_n is

$$A_n = \frac{-2a\omega^2}{s^2+\omega^2} \frac{1}{R\sqrt{\gamma_n^2 - \frac{s}{\nu}}} \frac{1}{J_1\left(\sqrt{\gamma_n^2 - \frac{s}{\nu}}\, R\right)} \frac{1}{\cosh \frac{\gamma_n}{l} h} \quad . \tag{IV-26}$$

The complete solution for the transformed velocity can be written as

$$\bar{v}_z = -\frac{2a\omega^2}{R(S^2+\omega^2)} \sum_{n=0}^{\infty} \frac{J_o\left(\sqrt{\gamma_n^2 - \frac{S}{\nu}}\, r\right)}{\sqrt{\gamma_n^2 - \frac{S}{\nu}}\; J_1\left(\sqrt{\gamma_n^2 - \frac{S}{\nu}}\, R\right)} \frac{\cosh \frac{\gamma_n}{l} Z}{\cosh \frac{\gamma_n}{l} h} \quad . \text{(IV-27)}$$

The velocity in the time domain is easily obtained as

$$v_z = \frac{a\omega}{R} \sum_{n=0}^{\infty} \frac{J_o\left(\sqrt{\gamma_n^2 - i\frac{\omega}{\nu}}\, r\right)}{\sqrt{\gamma_n^2 - i\frac{\omega}{\nu}}\; J_1\left(\sqrt{\gamma_n^2 - i\frac{\omega}{\nu}}\, R\right)} \frac{\cosh \frac{\gamma_n}{l} Z}{\cosh \frac{\gamma_n}{l} h} \frac{\text{Exp}(i\omega t)}{i} +$$

$$+(-)\ \frac{a\omega}{R} \sum_{n=0}^{\infty} \frac{J_o\left(\sqrt{\gamma_n^2 + i\frac{\omega}{\nu}}\, r\right)}{\sqrt{\gamma_n^2 + i\frac{\omega}{\nu}}\; J_1\left(\sqrt{\gamma_n^2 + i\frac{\omega}{\nu}}\, R\right)} \frac{\cosh \frac{\gamma_n}{l} Z}{\cosh \frac{\gamma_n}{l} h} \frac{\text{Exp}(-i\omega t)}{-i} \quad . \text{(IV-28)}$$

Since the real part of v_z is all that is of interest, Eq. (IV-28) can be written in the form

$$v_z = -\frac{a\omega}{R} \sum_{n=0}^{\infty} \frac{J_o(\alpha_n r)}{\alpha_n J_1(\alpha_n R)} \frac{\cosh (N_1 Z)}{\cosh (N_1 h)} \sin \omega t +$$

$$+(-)\ \frac{a\omega}{R} \sum_{n=0}^{\infty} \frac{J_o(\alpha_n r)}{\alpha_n J_1(\alpha_n R)} \frac{\cosh (N_2 Z)}{\cosh (N_2 h)} \sin \omega t \qquad \text{(IV-29)}$$

where the α_n are the roots of $J_o(\alpha_n R)$, N_1 equals

$$N_1 = \frac{\gamma_n + i\frac{\omega}{\nu}}{l}$$

and N_2 equals

$$N_2 = \frac{\gamma_n - i\frac{\omega}{\nu}}{l} \quad .$$

Eq. (IV-29) is still complex with respect to the space coordinates but in order to reduce the cumbersomeness of this equation, it will be written in this manner until a particular problem is solved.

The time rate of change of pressure is obtained from Eq. (IV-8) and Eq. (IV-29):

$$\frac{\partial P}{\partial t} = \frac{a\omega}{R\beta_T}\left(\sum_{n=0}^{\infty} \frac{J_o(\alpha_n r)}{\alpha_n J_1(\alpha_n R)} N_1 \frac{\sinh (N_1 Z)}{\cosh (N_1 h)} + \frac{J_o(\alpha_n r)}{\alpha_n J_1(\alpha_n R)} N_2 \frac{\sinh (N_2 Z)}{\cosh (N_2 h)}\right) \sin \omega t \quad . \tag{IV-30}$$

An equation for the pressure field in the interior of the cylinder is obtained by integrating Eq. (IV-30):

$$P = -\frac{a}{\beta_T}\left(\sum_{n=0}^{\infty} \frac{J_o(\alpha_n r)}{\alpha_n J_1(\alpha_n R)} N_1 \frac{\sinh (N_1 Z)}{\cosh (N_1 h)} + \frac{J_o(\alpha_n r)}{\alpha_n J_1(\alpha_n R)} N_2 \frac{\sinh (N_2 Z)}{\cosh (N_2 h)}\right) \cos \omega t + P_o \quad . \tag{IV-31}$$

Cylinder with Stationary End and Oscillating Walls

The problem corresponding to Eq. (IV-3) and Eq. (IV-5) and satisfying the boundary conditions of Eq. (IV-7) will now be solved. Physically, this problem is that of a cylinder with stationary ends and an oscillating wall.

The solution is most easily obtained by utilizing the principle that every vector field can be uniquely separated into a part which is the gradient of a scalar potential and a part which is the curl of a vector potential (29). Thus, the velocity can be written as

$$V = \nabla\phi + \nabla x\psi \tag{IV-32}$$

where ϕ is the scalar potential and ψ is the vector potential.

When Eq. (IV-32) is substituted into Eq. (IV-3) the following equation relating the pressure and the scalar potential is obtained:

$$\frac{\partial P}{\partial t} = -\frac{1}{\beta_T} \nabla^2 \phi \quad , \tag{IV-33}$$

where ∇^2 is the Laplacian operator. If Eq. (IV-33) is transformed from the time domain to the Laplace domain by means of the Laplace transformation, it will take the form

$$SP - \overline{P}(o) = -\frac{1}{\beta_T} \nabla^2 \overline{\phi} \quad . \tag{IV-34}$$

Eq. (IV-5) will take the following forms under the transformation:

$$\rho S\overline{v}_r = -\frac{\partial \overline{P}}{\partial r} + \mu \left(\nabla^2 \overline{v}_r - \frac{\overline{v}_r}{r^2} \right) + \frac{\mu}{3} \frac{\partial}{\partial r} \left(\frac{\partial \overline{v}_r}{\partial r} + \frac{\overline{v}_r}{r} + \frac{\partial \overline{v}_z}{\partial Z} \right) \quad , \tag{IV-35}$$

and

$$\rho S \overline{v}_z = -\frac{\partial \overline{P}}{\partial Z} + \mu \nabla^2 \overline{v}_z + \frac{\mu}{3} \left(\frac{\partial \overline{v}_r}{\partial Z} + \frac{\overline{v}_r}{r} + \frac{\partial \overline{v}_z}{\partial Z} \right) , \tag{IV-36}$$

where the bars over the dependent variables indicate that they are in the Laplace domain. Eq. (IV-32) can be put in the more convenient forms

$$\overline{v}_r = \frac{\partial \overline{\phi}}{\partial r} - \frac{\partial \overline{\psi}}{\partial Z} \quad ,$$

and

$$\overline{v}_z = \frac{\partial \overline{\phi}}{\partial Z} + \frac{\partial \overline{\psi}}{\partial r} + \frac{\overline{\psi}}{r} \quad . \tag{IV-37}$$

When Eq. (IV-34) and Eq. (IV-37) are substituted into Eq. (IV-35) and Eq. (IV-36), the desired forms for ϕ and ψ are obtained. That is,

$$\nabla^2 \overline{\phi} - k^2 \overline{\phi} = 0, \tag{IV-38}$$

and

$$\nabla_1^2 \overline{\psi} - 1^2 \overline{\psi} = 0 \quad , \tag{IV-39}$$

where

$$k^2 = \frac{S^2}{c^2 + \frac{4}{3}\nu S} \quad ,$$

$$l^2 = \frac{S}{\nu} \quad ,$$

and

$$\nabla_1^2 \bar{\psi} = \frac{\partial^2 \bar{\psi}}{\partial r^2} + \frac{1}{r}\frac{\partial \bar{\psi}}{\partial r} - \frac{\bar{\psi}}{r^2} + \frac{\partial^2 \bar{\psi}}{\partial Z^2} \quad .$$

The solution for Eq. (IV-38) is

$$\bar{\phi} = \sum_{n=0}^{\infty} A_n I_o (\beta_n r) \sin \gamma_n Z \quad , \qquad \text{(IV-40)}$$

where

$$\beta_n = \gamma_n^2 + k^2 \quad .$$

The solution for Eq. (IV-39) is

$$\bar{\psi} = \sum_{n=0}^{\infty} B_n I_1 (\tau_n r) \cos \gamma_n Z \quad , \qquad \text{(IV-41)}$$

where

$$\tau_n = \sqrt{\gamma_n^2 + l^2} \quad .$$

The constants A and B in Eq. (IV-40) and Eq. (IV-41) are arbitrary. The boundary condition of Eq. (IV-7a) has been satisfied due to the choice of $\sin \gamma_n Z$ in equation (IV-40).

The transformed boundary conditions corresponding to Eq. (IV-7) are

$$\text{(a)} \quad v_r = 0 \text{ at } r = R,$$

$$\text{(b)} \quad v_z = -\frac{a\omega^2}{S^2+\omega^2} \text{ at } r = R,$$

and

$$\text{(c)} \quad v_z = 0 \text{ at } Z = h, \qquad \text{(IV-42)}$$

where the bars over the dependent variables have been omitted for convenience, but it should be remembered that the dependent variables are still in the Laplace domain. An equation for A in terms of B can be obtained by solving for the first homogeneous boundary condition. That is,

$$A\beta l_1 (\beta R) \sin \gamma Z + B\gamma l_1 (\tau R) \sin \gamma Z = 0 \quad ,$$

from which

$$A = - B \frac{\gamma}{\beta} \frac{l_1 (\tau R)}{l_1 (\beta R)} \quad . \tag{IV-43}$$

The second homogeneous boundary condition yields

$$B \tau l_o (\tau r) \cos \gamma h - B \frac{\gamma^2}{\beta} \frac{l_1 (\tau R)}{l_1 (\beta R)} l_o(\beta r) \cos \gamma h = 0.$$

For the above relation to hold, γ_n must be equal to

$$\gamma_n = \frac{2n + 1}{2} \frac{\pi}{h} \quad . \tag{IV-44}$$

The equations for ϕ and ψ now have the following forms:

$$\phi = - B \frac{\gamma_n}{\beta} \frac{l_1 (\tau R)}{l_1 (\beta R)} l_o (\beta r) \sin \gamma_n Z \quad , \tag{IV-45}$$

and

$$\psi = B l_1 (\tau r) \cos \gamma_n Z \quad . \tag{IV-46}$$

To determine the constant B, the boundary condition of Eq. (IV-41b) must be utilized along with the fact that the sequence $\cos \gamma_n h$ is orthogonal on the interval (0,h). Thus, at the wall of the cylinder the following relationship is obtained:

$$-B \left(\frac{\gamma_n^2}{\beta} \frac{l_1 (\tau R)}{l_1 (\beta R)} l_o (\beta R) - \tau l_o (\tau R) \right) \int_o^h \cos (\gamma_n Z) \cos (\gamma_m Z) dZ =$$

$$- \frac{a\omega^2}{S^2+\omega^2} \int_0^h \cos(\gamma_m Z)\, dZ \quad .$$

An equation for B can be obtained from the above relation:

$$B_n = \frac{2a\omega^2}{S^2+\omega^2} \frac{(-1)^n}{h\,\gamma_n} \left(\frac{\beta\, 1_1 (\beta R)}{\gamma_n^2\, 1_1(\tau R)\, 1_o(\beta R) - \beta\, \tau\, 1_o(\tau R)\, 1_1(\beta R)} \right) . \quad \text{(IV-47)}$$

From Eqs. (1V-45), (1V-46) and (1V-47) the solution of Eq. (1V-38) and Eq. (1V-39), subject to the boundary conditions of Eq. (1V-42), can be written; that is

$$\phi = - \frac{2a\omega^2}{S^2+\omega^2} \sum_{n=0}^{\infty} \frac{(-1)^n}{h\,\gamma_n} \left(\frac{\gamma_n 1_1 (\tau R)}{\text{DENOM}} \right) 1_o(\beta r) \sin \gamma_n Z \quad , \quad \text{(IV-48)}$$

and

$$\psi = \frac{2a\omega^2}{S^2+\omega^2} \sum_{n=0}^{\infty} \frac{(-1)^n}{h\,\gamma_n} \left(\frac{\beta\, 1_1 (\beta R)}{\text{DENOM}} \right) 1_1(\tau r) \cos \gamma_n Z \quad . \quad \text{(IV-49)}$$

The term DENOM has been introduced for convenience and is equal to

$$\text{DENOM} = \gamma_n^2\, 1_1(\tau R)\, 1_o(\beta R) - \beta\, \tau\, 1_o(\tau R)\, 1_1(\beta R) \quad .$$

The transformation from the Laplace domain to the time domain gives

$$\phi = - a\omega \sum_{n=0}^{\infty} \frac{(-1)^n}{h\,\gamma_n} \left(\frac{\gamma_n 1_1 (\tau_1 R)}{\text{DENOM}} \right) 1_o(\beta_1 r) \sin(\gamma_n Z) \frac{\text{Exp}(i\omega t)}{i} + (-)$$

$$a\omega \sum_{n=0}^{\infty} \frac{(-1)^n}{h\,\gamma_n} \left(\frac{\gamma_n 1_1 (\tau_2 R)}{\text{DENOM}} \right) 1_o(\beta_2 r) \sin(\gamma_n Z) \frac{\text{Exp}(-i\omega t)}{-i} , \quad \text{(IV-50)}$$

and

$$\psi = - a\omega \sum_{n=0}^{\infty} \frac{(-1)^n}{h\,\gamma_n} \left(\frac{\beta_1 1_1 (\beta_1 R)}{\text{DENOM}} \right) 1_1(\tau_1 R) \cos(\gamma_n Z) \frac{\text{Exp}(i\omega t)}{i} +$$

$$a\omega \sum_{n=0}^{\infty} \frac{(-1)^n}{h\,\gamma_n} \left(\frac{\beta_2 1_1 (\beta_2 R)}{\text{DENOM}} \right) 1_1(\tau_2 R) \cos(\gamma_n Z) \frac{\text{Exp}(-i\omega t)}{-i} , \quad \text{(IV-51)}$$

where the variables with a subscripted 1 refer to $S = i\omega$ and those with a subscripted 2 refer to $S = -i\omega$. It should be noted that the unbarred dependent variables referred to from now on are in the time domain.

From Eq. (1V-33) an equation for the pressure as a function of r, z and t can be obtained; that is,

$$\frac{\partial P}{\partial t} = -\frac{1}{\beta_T} \nabla^2 \phi$$

which, after substitution and integration, becomes

$$P-P(o) = -\rho a\omega^2 \sum_{n=0}^{\infty} \frac{(-1)^n}{h \gamma_n} \left(\frac{\beta_1 1_1 (\tau_1 R)}{DENOM} \right) 1_o (\beta_1 r) \sin(\gamma_n Z) \cos(\omega t) +$$

$$+(-)\rho a\omega^2 \sum_{n=0}^{\infty} \frac{(-1)^n}{h \gamma_n} \left(\frac{\beta_2 1_1 (\tau_2 R)}{DENOM} \right) 1_o (\beta_2 r) \sin(\gamma_n Z) \cos(\omega t), \quad \text{(IV-52)}$$

where only the real time domain is used since that is all that is of interest.

By means of the superposition principle, the solution of Eq. (1V-3) and Eq. (1V-5) subject to the boundary conditions of Eq. (1V-1) can be written in the following form:

$$v_z = \text{Eq. (1V-29)} + \frac{\partial \phi}{\partial Z} + \frac{\partial \psi}{\partial r} + \frac{\psi}{r}, \quad \text{(IV-53)}$$

$$v_r = \frac{\partial \phi}{\partial r} + \frac{\partial \psi}{\partial Z}, \quad \text{(IV-54)}$$

and

$$P = \text{Eq. (1V-31)} + \text{Eq. (1V-52)}, \quad \text{(IV-55)}$$

where ϕ is given by Eq. (IV-50) and ψ is given by Eq. (IV-51). The equations are written in the above manner to avoid unnecessary writing and confusion. It should also be noted that the equations are left in complex form. Therefore, before they can be applied to a physical problem the real part of each equation must be extracted and only this part should be used to describe the problem. The remaining portion of this chapter will be devoted to just such an operation.

Illustrative Example

A true test of the worth of any mathematical theory is to see how well it applies to a practical situation. For an illustrative problem, a cylindrical rigid plexiglas tube of radius R = 1 inch and a length of 36 inches was chosen. The height of the fluid within the cylinder will be 31 inches for the first case and 23 inches for the second case. The frequency ω will vary between 50 and 400 radians per second and the oscillation amplitude will be 0.025 inches and 0.05 inches respectively.

The equation for the pressure field will be considered first. Under the above conditions, Eq. (IV-31) can be written as

$$P = -\frac{2a}{\beta_T} \sum_{n=0}^{\infty} \frac{J_o(\alpha_n r)}{n\, J_1(\alpha_n)} \frac{\gamma_n}{1} \frac{\sinh \frac{\gamma_n}{1} Z}{\cosh \frac{\gamma_n}{1} h} \cos \omega t + P_o \quad , \qquad \text{(IV-56)}$$

since the first two terms on the right hand side of Eq. (IV-31) are equivalent. The procedure used in showing the equivalence of the above mentioned terms is outlined in Appendix A. From the real part of Eq. (IV-56) an equation for the pressure field can be obtained:

$$P = 2\rho a\omega^2 \sum_{n=0}^{\infty} \frac{J_o(\alpha_n r)}{\alpha_n J_1(\alpha_n)} Z \cos \omega t + P_o \quad . \qquad \text{(IV-57)}$$

Eq. (1V-52) can be written as

$$P = -2\rho a\omega^2 \sum_{n=0}^{\infty} \frac{(-1)^n}{h\ \gamma_n} \left(\frac{\beta\ l_1(\tau)}{\text{DENOM}} \right) l_o(\beta r) \sin \gamma_r \cos \omega t \qquad \text{(IV-58)}$$

due to the equivalence of the two terms on the right-hand side of Eq. (1V-52). The real part of Eq. (1V-58) is

$$P = 2\rho a\omega^2 \sum_{n=0}^{\infty} \frac{(-1)^n}{h\ \gamma_n} \left(\frac{\text{NUM}}{\text{DEN}} \right) l_o(\gamma_n r) \sin(\gamma_n Z) \cos \omega t \qquad \text{(IV-59)}$$

where the term DEN equals

$$\text{DEN} = \gamma_n^2\, l_o^2(\gamma_n) + \frac{\omega}{\nu}\, l_1^2(\gamma_n) - 2\gamma_n \sqrt{\frac{\omega}{2\nu}}\, l_o(\gamma_n)\, l_1(\gamma_n) \quad ,$$

and the term NUM equals

$$\text{NUM} = \sqrt{\frac{\omega}{2\nu}}\, l_1(\gamma_n) - \gamma_n\, l_o(\gamma_n) \quad .$$

At time t = 0, the pressure within the cylinder will be

$$P_o = \rho g Z + \rho a\omega^2 Z \quad . \qquad \text{(IV-60)}$$

When the initial condition is substituted into the sum of Eq. (1V-57) and Eq. (1V-59), the complete pressure equation can be written as

$$P(r,Z,t) = 2\rho a\omega^2 \sum_{n=0}^{\infty} \frac{J_o(\alpha_n r)}{\alpha_n J_1(\alpha_n)} Z(\cos \omega t - 1) + \rho g Z + \rho a\omega^2 Z +$$

$$2\rho a\omega^2 \sum_{n=0}^{\infty} \frac{(-1)^n}{h\ \gamma_n} \left(\frac{\text{NUM}}{\text{DEN}} \right) l_o(\gamma_n r) \sin \gamma_n Z (\cos \omega t - 1) \quad . \qquad \text{(IV-61)}$$

Eq. (IV-61) is the equation for the pressure field within the cylinder for all $t \geq 0$ and it converges to the boundary conditions at the interior surface of the cylinder.

The azimuthal velocity of the fluid within the cylinder will be considered next. Eq. (IV-29) takes the form

$$v_z = -2a\omega \sum_{n=0}^{\infty} \frac{J_o(\alpha_n r)}{\alpha_n J_1(\alpha_n)} \sin \omega t \quad , \tag{IV-62}$$

where the ratio of the hyperbolic cosine terms has been set equal to unity since $\frac{\gamma_n}{l} << 1$. The remainder of the terms on the right-hand side of Eq. (IV-53) can be written as

$$v_z = -2a\omega \left(\sum_{n=0}^{\infty} \frac{(-1)^n}{h\ \gamma_n} \left(\frac{\gamma_n^2\, l_1(\tau R)}{\text{DENOM}} \right) l_o(\beta r) + \right.$$

$$\left. + (-) \sum_{n=0}^{\infty} \frac{(-1)^n}{h\ \gamma_n} \frac{\beta \tau\, l_1(\beta r)}{\text{DENOM}}\ l_o(\tau r) \right) \cos \gamma_n Z \sin \omega t, \tag{IV-63}$$

where use has been made of the equalities between terms containing τ_1 and τ_2 and β_1 and β_2. The real part of Eq. (IV-63) is

$$v_z = 2a\omega \left(\sum_{n=0}^{\infty} \frac{(-1)^n}{h} \left(\frac{\text{NUM}}{\text{DEN}} \right) J_o(\gamma_n r) + \right.$$

$$\sum_{n=0}^{\infty} \frac{(-1)^n}{h\ \gamma_n} \left(\frac{\text{NUM1}}{\text{DEN}} \sin\left(\sqrt{\frac{\omega}{2\nu}}\, r + \frac{3\pi}{8} \right) + \right.$$

$$\left. \left. \frac{\text{NUM2}}{\text{DEN}} \cos\left(\sqrt{\frac{\omega}{2\nu}}\, r + \frac{3\pi}{8} \right) \right) \frac{\text{Exp}\left(\sqrt{\frac{\omega}{2\nu}}\, (r-1) \right)}{\sqrt{r}} \right) \cos \gamma_n Z \sin \omega t \tag{IV-64}$$

where

$$\text{NUM1} = \sqrt{\frac{\omega}{2\nu}}\ \gamma_n\, 1_o(\gamma_n)\, 1_1(\gamma_n)\,(\sin 1_1 - \cos 1_1) - \frac{\omega}{\nu}\, 1_1^2\, \gamma_1)\sin 1_1 \ ,$$

$$\text{NUM2} = \sqrt{\frac{\omega}{2\nu}}\ \gamma_n\, 1_o(\gamma_n)\, 1_1(\gamma_n)\,(\sin 1_1 + \cos 1_1) - \frac{\omega}{\nu}\, 1_1^2(\gamma_n)\cos 1_1 \ ,$$

and

$$1_1 = \sqrt{\frac{\omega}{2\nu}} + \frac{3\pi}{8} \ .$$

The steps that are necessary to obtain Eq. (IV-64) are given in Appendix A.

The solution for the azimuthal velocity is obtained by adding Eqs. (IV-62) and (IV-64):

$$v_z = -2\varepsilon\omega \sum_{n=0}^{\infty} \frac{J_o(\alpha_n r)}{\alpha_n J_1(\alpha_n)} \sin \omega t + 2a\omega \left(\sum_{n=0}^{\infty} \frac{(-1)^n}{h} \left(\frac{\text{NUM}}{\text{DEN}}\right) 1_o(\gamma_n r) + \right.$$

$$\sum_{n=0}^{\infty} \frac{(-1)^n}{h\ \gamma_n} \left(\frac{\text{NUM1}}{\text{DEN}} \sin\left(\sqrt{\frac{\omega}{2\nu}}\, r + \frac{3\pi}{8}\right) + \right.$$

$$\left. \left. \frac{\text{NUM2}}{\text{DEN}} \cos\left(\sqrt{\frac{\omega}{2\nu}}\ r + \frac{3\pi}{8}\right) \right) \frac{\text{Exp}\left(\sqrt{\frac{\omega}{2\nu}}\,(r-1)\right)}{r} \right) \cos \gamma_n Z \sin \omega t \quad . \text{(IV-65)}$$

For the radial velocity, Eq. (IV-54) can be written in the following manner:

$$v_r = -2a\omega \sum_{n=0}^{\infty} \frac{(-1)^n}{h\ \gamma_n} \left(\frac{\beta\ \gamma_n\, 1_1(\tau R)}{\text{DENOM}} \right) 1_1(\beta r) \sin \gamma_n Z \sin \omega t +$$

$$2a\omega \sum_{n=0}^{\infty} \frac{(-1)^n}{h\ \gamma_n} \left(\frac{\beta\ \gamma_n\, 1_1(\beta R)}{\text{DENOM}} \right) 1_1(\tau r) \sin \gamma_n Z \sin \omega t \ . \qquad \text{(IV-66)}$$

Since the real part of the above equation is all that is of interest, the radial velocity equation is written as

$$v_r = 2a\omega \left(\sum_{n=0}^{\infty} \frac{(-1)^n}{h} \left(\frac{NUM}{DEN}\right) 1_1(\gamma_n r) + \right.$$

$$\sum_{n=0}^{\infty} \frac{(-1)^n}{h} \sqrt{\frac{\nu}{2\omega}} \left(\left(\frac{NUM1 + NUM2}{DEN}\right) \sin\left(\sqrt{\frac{\omega}{2\nu}}\, r + \frac{3\pi}{8}\right) + (-) \right.$$

$$\left. \left. \left(\frac{NUM1 - NUM2}{DEN}\right) \cos\left(\sqrt{\frac{\omega}{2\nu}}\, r + \frac{3\pi}{8}\right) \right) \frac{\operatorname{Exp}\left(\sqrt{\frac{\omega}{2\nu}}\,(r-1)\right)}{\sqrt{r}} \right) \sin \gamma_n Z \sin\omega t \quad . \tag{IV-67}$$

The approximations used to obtain Eq. (1V-64) and Eq. (1V-67) are valid for all values of τ r greater than 10 and therefore cannot be used to obtain the values for velocity at the center of the tube. To obtain these values, the quantity r=0 must first be substituted into Eq. (1V-53) and Eq. (1V-54). Under this substitution, the radial velocity is equal to zero since $1_1(0) = 0$. That is,

$$v_r = 0 \quad . \tag{IV-68}$$

The aximuthal velocity is

$$v_z = 2a\omega \sum_{n=0}^{\infty} \frac{(-1)^n}{h} \left(\frac{NUM}{DEN}\right) \cos(\gamma_n Z) \sin(\omega t + /-)$$

$$2a\omega \sum_{n=0}^{\infty} \left(\frac{NUM1}{DEN}\right) \frac{\left(2\pi\sqrt{\frac{\omega}{\nu}}\right)^{1/2}}{\operatorname{Exp}\sqrt{\frac{\omega}{\nu}}} \cos(\gamma_n Z) \sin(\omega t), \tag{IV-69}$$

where the procedure of Appendix A is used. When Eq. (1V-69) is added to Eq. (1V-29), with $J_o(\alpha_n r) = 1$ for all values of α_n, the equation for the azimuthal velocity at the tube centerline for all values of z

and t is obtained. This equation is written below for convenience:

$$v_z = -2a\omega \sum_{n=0}^{\infty} \frac{1}{\alpha_n J_1(\alpha_n)} \sin(\omega t) +$$

$$2a\omega \sum_{n=0}^{\infty} \frac{(-1)^n}{h} \left(\frac{NUM}{DEN}\right) \cos(\gamma_n Z)\sin(\omega t) +$$

$$2a\omega \sum_{n=0}^{\infty} \left(\frac{NUM1}{DEN}\right) \frac{\left(2\pi\sqrt{\frac{\omega}{\nu}}\right)^{1/2}}{Exp\sqrt{\frac{\omega}{2\nu}}} \cos(\gamma_n Z)\sin(\omega t) \quad . \qquad \text{(IV-70)}$$

Thus Eqs. (1V-61), (1V-65) and (1V-67) are the solutions of Eqs. (1V-3) and (1V-5) and they satisfy the boundary conditions of Eq. (1V-1). The numerical results of Eqs. (1V-61), (1V-65) and (1V-67) as applied to the above mentioned problem will be given in the following two chapters.

CHAPTER V

EXPERIMENTAL PROGRAM

As mentioned before, the true test of any mathematical theory is to see how well it applies to a practical situation. With this in mind, an experimental program was developed which would simulate the problem outlined in Chapter III.

The results obtained from the experimental program were compared directly with the results obtained from Eq. (1V-61) of Chapter 1V. Since there was no way of measuring the pressure field within the fluid without disrupting the flow field, it was assumed that if the results obtained from the experimental measurements at the wall agreed with the numerical results close to the wall, a sufficient justification of the theoretical method was obtained.

The general development of the experimental program and its comparison with the theory are the subject of this chapter.

General Considerations

The general problem outlined at the end of Chapter 1V was developed for a fluid-filled, rigid, cylindrical tube. The tube would have to be made from a material that was strong enough to withstand the stresses due to the vibration, be able to withstand the effects of a

hard vacuum, have very little or no affinity for the fluid under testing and be clear enough so that the fluid inside the tube could be seen by an observer . A material which would satisfy all of the above conditions and in addition would be easy to obtain was Plexiglas, the trade name for cast thermoplastic acrylic resin. A cylindrical Plexiglas tube 3 feet in length, 2 inches in diameter and 0.25 inches thick was chosen for the experimental model.

Next, consideration was given to the fluids that were to be tested. It was believed that under similar conditions a fluid with a high value of viscosity would have a higher value for negative pressure than a fluid with a lower value for viscosity. A number of fluids with viscosities ranging from 1 centipoise to 100 centipoise were considered. This list of fluids, which was taken from the Solvents Manual (28), was gradually reduced for a number of reasons. Among the more prevalent were health dangers due to the toxic fumes, low volatility, high fluid absorption by Plexiglas and low boiling points of the respective fluids. It was finally decided that the fluids that could most easily be handled and still have the desired characteristics were water, ethylene glycol and diethylene glycol. Two additional fluids were obtained by using a 70% by weight aqueous ethylene glycol solution and 80% by weight aqueous diethylene glycol solution. The range of viscosities were from 1 centipoise for water to 32 centipoise for diethylene glycol.

Consideration was also given to the surface tension of the liquid since the negative pressure of the fluid is related to the surface tension by

$$P = \frac{2\sigma}{r} \quad .$$

Now, if it is assumed that the fluid has no vapor bubbles that are visible to the naked eye, say 10^{-4} centimeters in diameter, then the negative pressure of all the fluids considered will be greater than 2 atmospheres. Since this value for surface tension is greater than any value that will be obtained in the test program, the equations of Chapter IV will not have to include this property of surface tension. However, if a vapor bubble greater than 10^{-4} centimeters should exist in the fluid then the fluid will fracture at a lower value than 2 atmospheres; this was experienced in the test program where the fluid fractured approximately two seconds after the test was begun. Although this was a short interval of time, it was sufficient to obtain the negative pressure of the fluid.

Experimental Apparatus

The basic test set-up is shown in Figure 9 and Figure 10. The vacuum pump is connected through a filter to a threaded pipe which is in turn screwed into a Plexiglas cap. This cap fits very snugly on top of the tube and with the aid of high vacuum grease a pressure equal to the vapor pressure of the fluid can be maintained within the tube.

The Plexiglas tube is mounted on the oscillating piston which is connected to the oscillator driver by the connecting rod. It can be kept in a vertical position by suitable manipulation of the base. Two oscillator drivers were used. One gave the tube an amplitude of 0.025 inches while the other gave it an amplitude of 0.05 inches. The

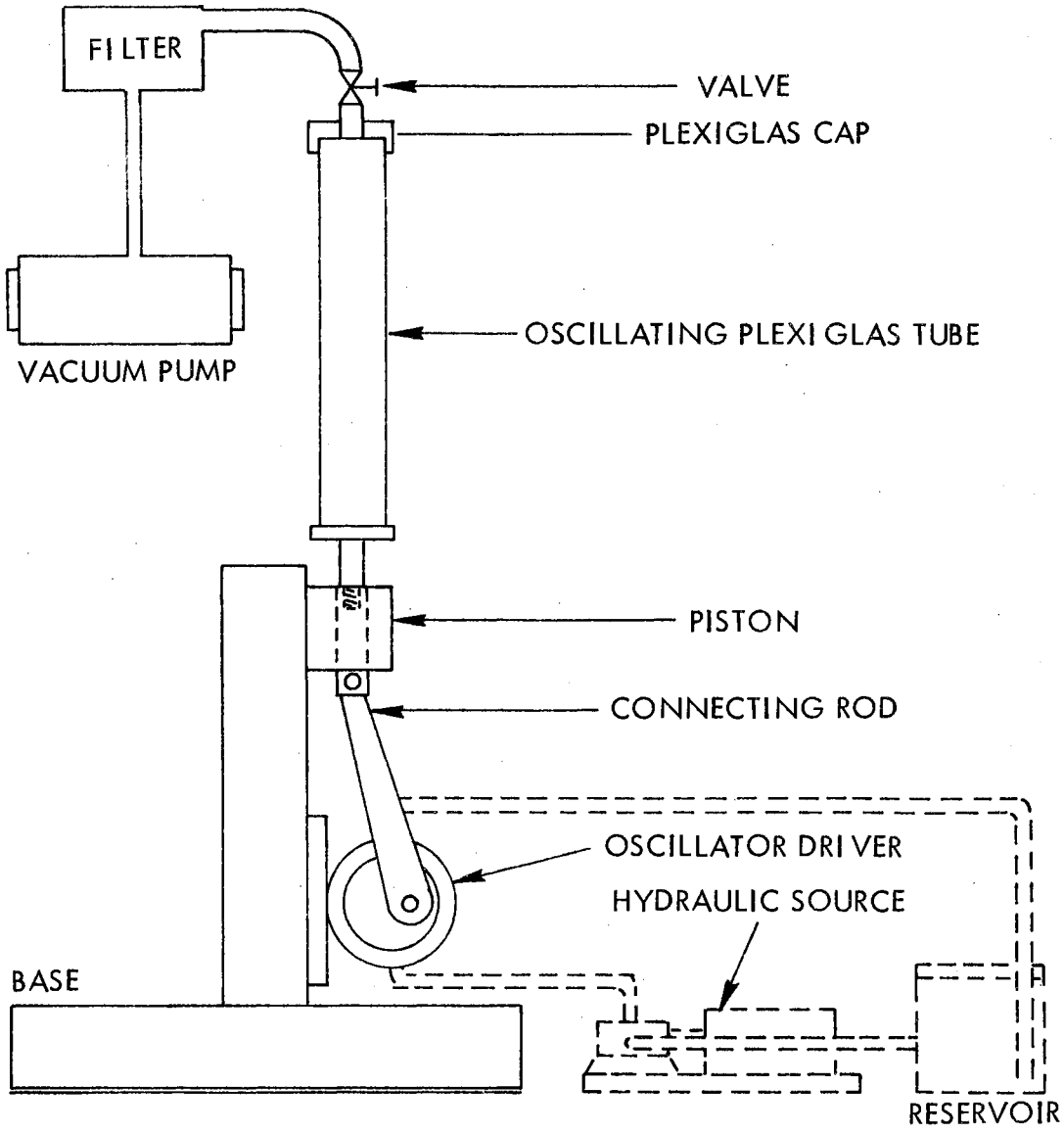

FIGURE 9. Experimental Apparatus

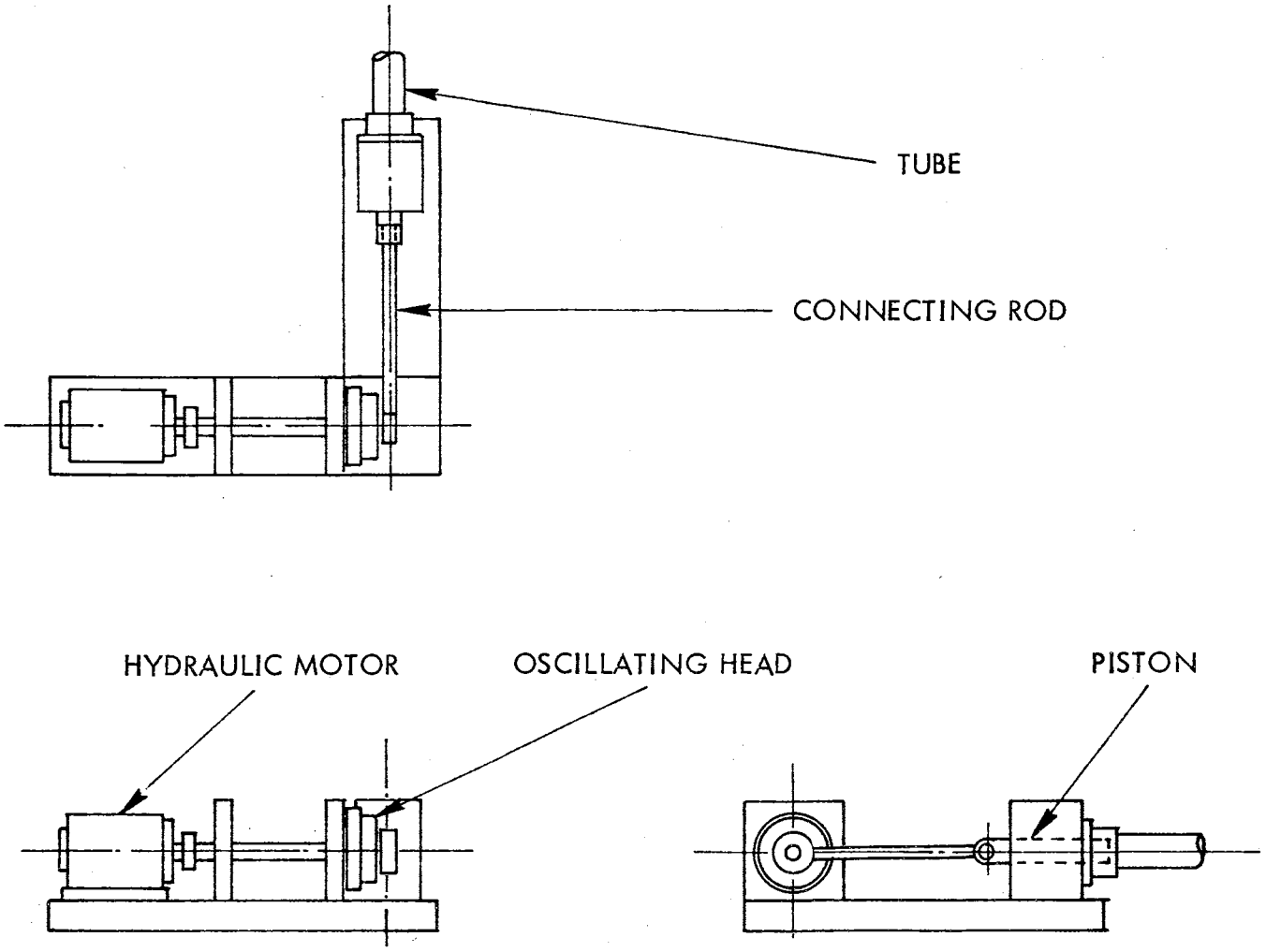

FIGURE 10. Oscillating Piston and Drive Unit

oscillator driver is driven by a hydraulic motor which has a range of speeds from nearly zero to 3500 rpm, Figure 10. The power supply for the system is an electric motor which is coupled directly to a gear pump. A flow divider valve is used for control of the oscillator speed.

The tube is instrumented as shown in Figure 11. The two Kistler quartz pressure transducers are mounted in the side of the tube with the lower transducer at the bottom of the tube and the second transducer 8 inches above. The output from the two transducers is fed through two charge amplifiers which are designed especially for the transducers and is then fed to the oscilloscope. The data were then recorded from the oscilloscope by means of a Polaroid camera. A mercury manometer graduated to read tenths of an inch was used to measure the pressure of the gas above the fluid. The oscillating frequency of the tube was obtained by measuring the rpm of the hydraulic motor. This can be seen from the Figure.

Test Procedure

Prior to any consideration for the tube or for the fluid, the control settings on the flow divider valve were set so that frequencies corresponding to 50, 100, 200, 250, 300 and 350 radians per second could be realized quickly when the power was turned on. This was done so that the control could be set to the desired frequency, the power turned on and the data corresponding to that frequency and amplitude could be read before the fluid within the tube completely fractured. This method does have the disadvantage of not being able to obtain the

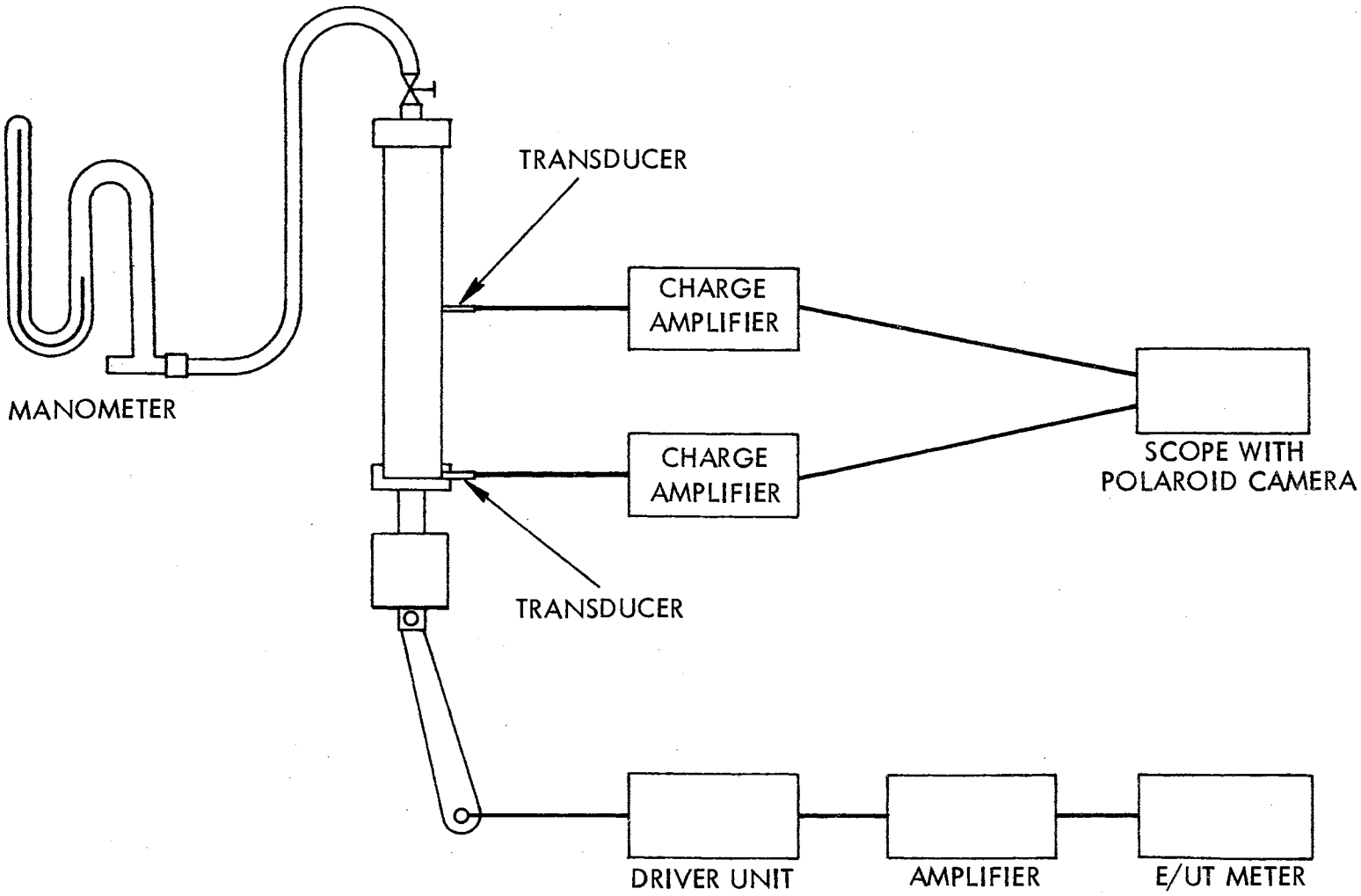

FIGURE 11. Instrumentation for Vibrating Tube

exact frequencies that are desired, but it is considered vastly superior to taking data while the fluid is fractured for obvious reasons.

After the proper settings on the control of the flow divider valve were obtained, it was necessary to clean the inside of the tube thoroughly. The cleansing agent chosen was a 30% dilute solution of nitric acid. This particular acid was chosen because of its low affinity for Plexiglas and its excellent cleansing properties.

After the inside of the tube was cleansed with the acid, it was thoroughly rinsed with distilled water and allowed to dry while care was exercised so that no foreign matter was allowed to enter the tube. The test fluid was then poured into the tube through a very fine wire screen. The screen was used to ensure that there were no solid particles of visible size in the fluid.

When the fluid reached a height of 31 inches, the cap was placed on the top of the tube and the vacuum pump was started. The pump was allowed to run for approximately two hours so that the inside of the tube would be rid of all the undissolved air that had risen to the top. The pump was then turned off and the fluid was allowed to sit overnight subject to this vacuum which was equal to the vapor pressure of the fluid. In the morning the pump was again turned on so that any air that rose to the top during the night could be eliminated. Of course one cannot be absolutely sure that all undissolved gases were eliminated just by a visual observation, but this was deemed adequate since there was no convenient way to measure just the undissolved gases in the liquid. The fluid was now ready to be tested.

After the fluid was vibrated and the pressure measurements were recorded, the vacuum pump was started and the fluid was allowed to sit until there were no visible vapor bubbles present. This usually took from 15 to 30 minutes.

When the testing was completed for both amplitudes the cap was taken off the tube and 8 inches of fluid were drained from the tube; this was done because it was desired to run a similar series of tests as before but at a different height. This series of tests was performed so that it could be determined if there were any marked changes in the pressure values obtained at this lower height other than the ones called for by the equations of Chapter IV. The cap was then placed on the tube and the vacuum pump was started. The pump was left running for approximately two hours, or until the fluid was rid of all visible bubbles. This draining process took such a short period of time that there was no need to allow the tube to sit overnight under a vacuum as was done in the original case. The same procedure was then used as was used for a height of 31 inches.

Results

Due to the number of fluids tested, the different fluid heights tested, the different amplitudes at which they were tested and the experimental values for frequency not corresponding exactly with the theoretical values, it was felt that the most realistic way to present the results would be a plot of the negative pressure amplitude as a function of the frequency. The experimental values obtained for a

fluid height of 31 inches were used in the plots. The values corresponding to a fluid height of 23 inches were similar to the 31 inch height and it would be too much of a repetition to include them. Thus, the question of the previous section is answered; that is, there is no marked change in the pressure values obtained at this lower fluid height other than the ones called for by the equations of Chapter IV.

Two values of the azimuthal coordinate, z, were used; they were for z = 23 inches and for z = 31 inches. These two values for z were chosen because they correspond to the transducer locations. A value for the radial coordinate, r, equal to 0.95 inches was used. This choice of r was necessitated because of the discontinuity of the pressure equation at the wall. This discontinuity arose because of the boundary condition that the azimuthal velocity at the wall equals zero in the first part of the solution. That boundary condition gives rise to the term

$$J_o (\alpha_n R) = 0 \quad ,$$

which is present in the pressure equation. However, from a physical standpoint it is difficult to envision a significant difference of pressure at a value of r which is very close to the wall, and the actual pressure at the wall. With this assumption, the theoretical and the experimental values for pressure can be compared.

Figures (12 - 16) are the plots of the pressure fields for all the fluids tested. From the figures, the agreement between the experimental and the theoretical results is noticed. It can therefore be stated that a close correlation exists between the experimental values for pressure at the wall and the theoretical values for pressure near the

wall and there is no reason to assume that this correlation will not hold in the interior of the fluid. The graphical results, not only for pressure but also for velocity, will be discussed more fully in the next chapter.

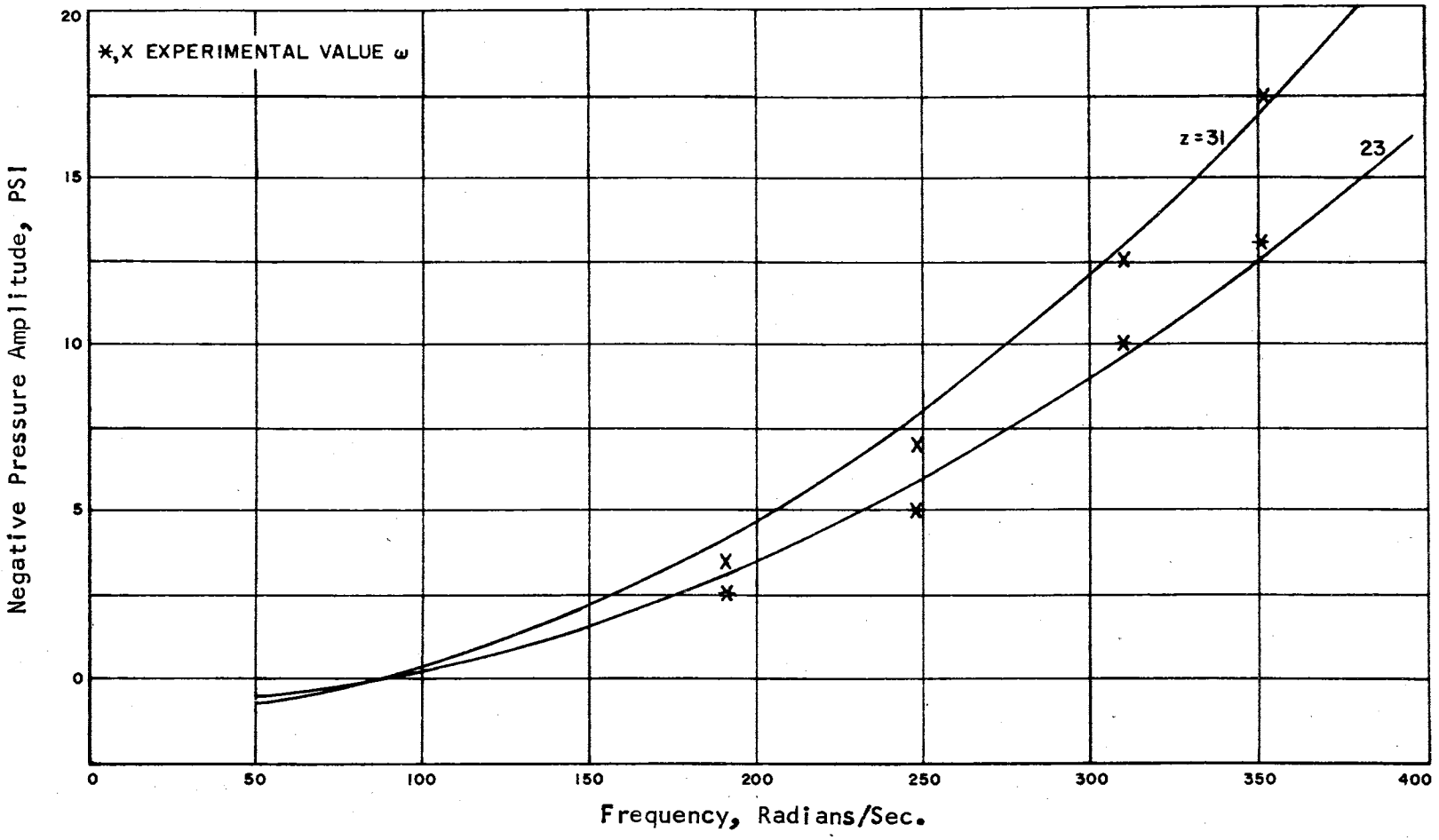

FIGURE 12. Comparison Between Experimental and Numerical Results for Water With $r = 0.95$.

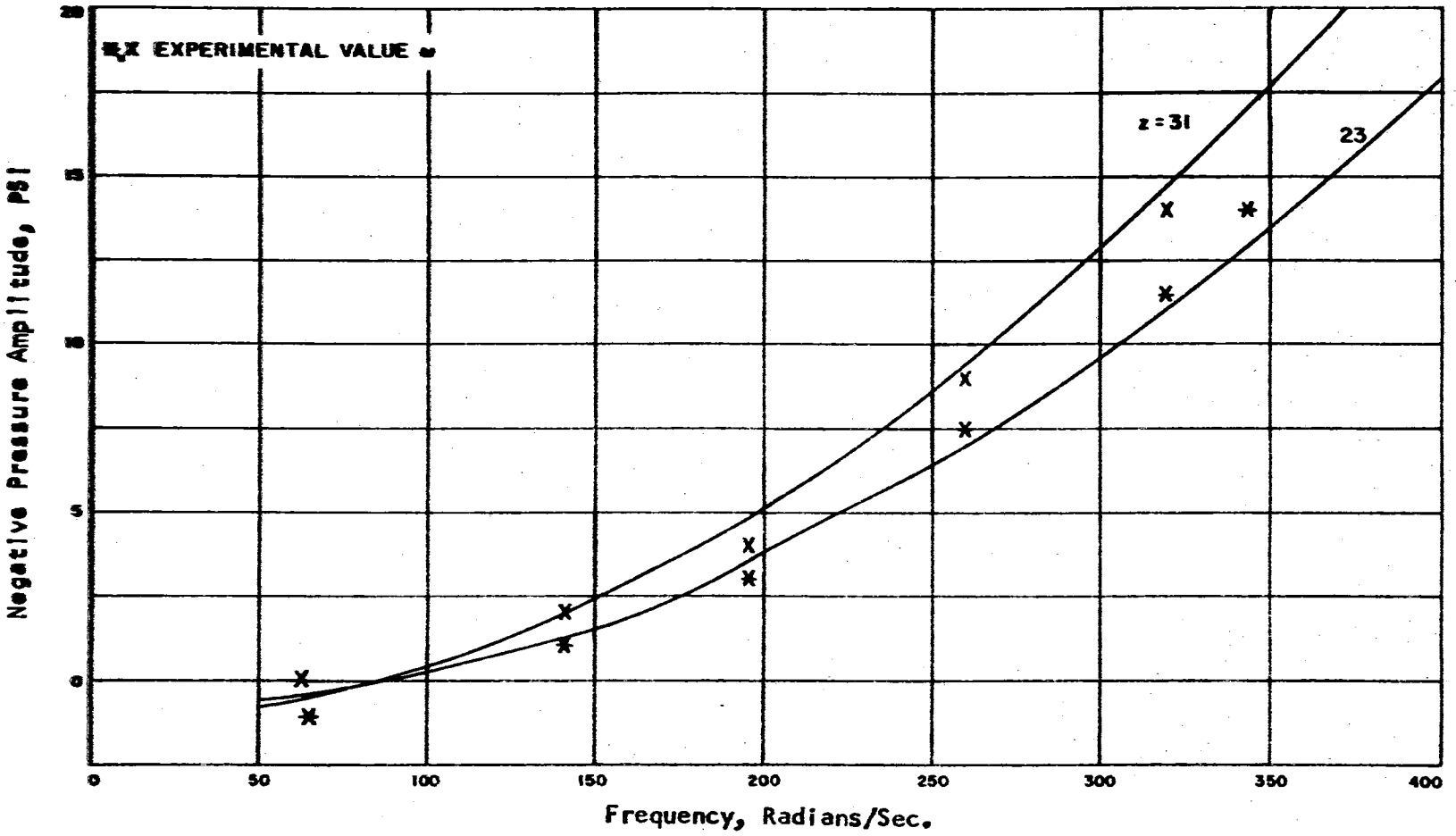

FIGURE 13. Comparison Between Experimental and Numerical Results for 70% Ethylene Glycol With r = 0.95 .

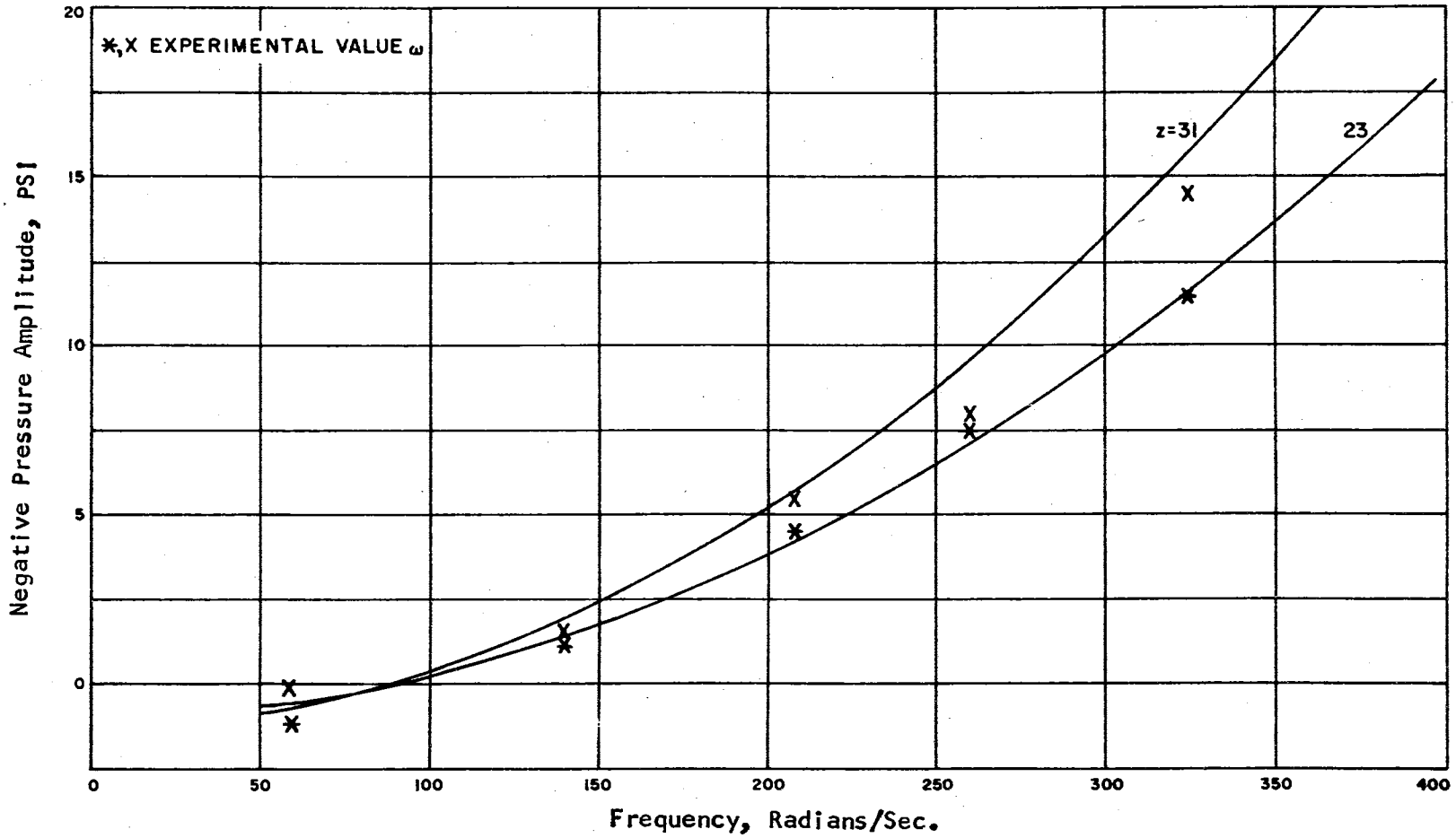

FIGURE 14. Comparison Between Experimental and Numerical Results for 80% Diethylene Glycol With $r = 0.95$.

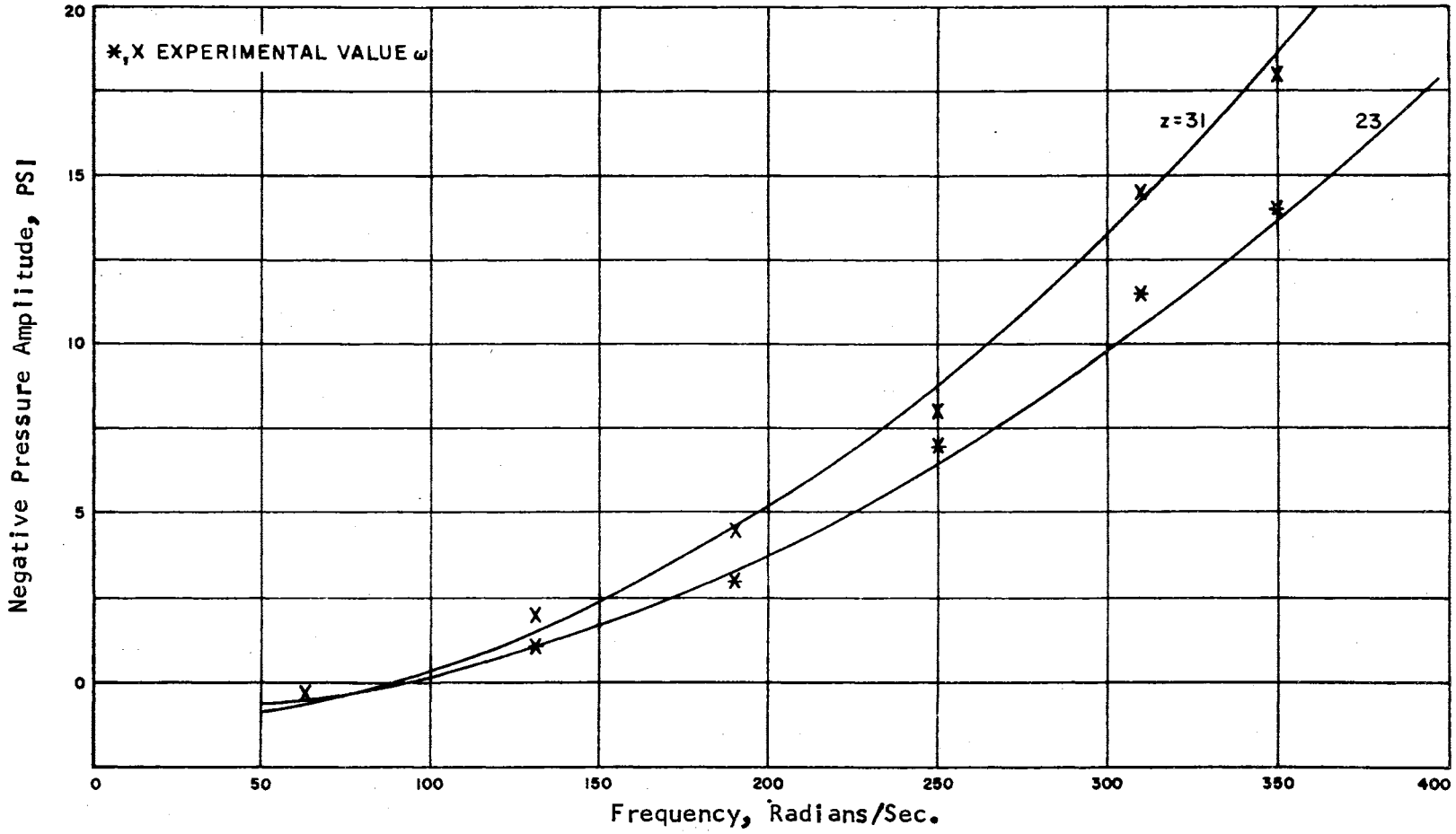

FIGURE 15. Comparison Between Experimental and Numerical Results for Ethylene Glycol With $r = 0.95$.

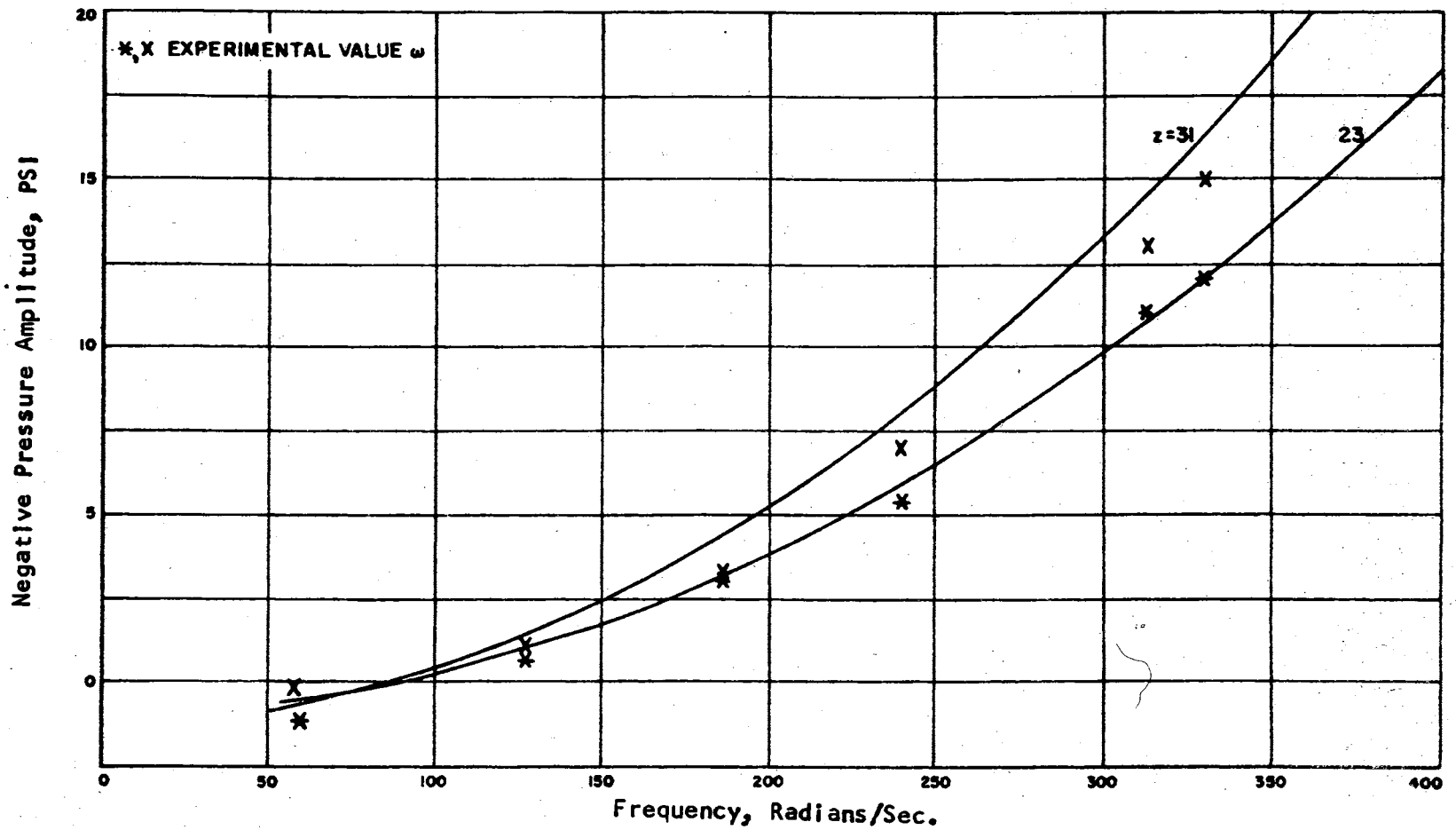

FIGURE 16. Comparison Between Experimental and Numerical Results for Diethylene Glycol With $r = 0.95$.

CHAPTER VI

GRAPHICAL RESULTS

To present a complete graphical presentation of all the results in this chapter would be quite impractical. However, as was done in the previous chapter, the results for one fluid height, h = 31 inches, and one fluid amplitude, a = 0.05 inches, will be considered and from these results observations and conclusions will be made which will be applicable to all fluid heights and amplitudes since the results are similar.

Since the principle topic of interest is the negative pressure of the respective fluids, these results will be considered first. The pressure equation has a time dependent term (cos ωt - 1) which varies between 0 and -2. This is, when the term (cos ωt - 1) is equal to -2, or when the coefficient ωt is equal to π, 3π, etc., the maximum value for negative pressure is obtained. It is this maximum value of negative pressure which is represented in the following figures and which will be denoted as the negative pressure amplitude. As for the pressure variation with time, it can be seen that the pressure will decrease from a maximum positive pressure when ωt is equal to 0, 2π, etc., to a maximum negative value when ωt is equal to π, 3π, etc. The curve will be proportional to (cos ωt - 1) with the amplitude being dependent on the values of r, ω and z that are used. This can be seen be inspecting Eq. (IV-61).

The curves of the negative pressure amplitude as a function of the frequency have been given in the previous chapter. From these curves an immediate evaluation of the negative pressure amplitude can be obtained for values of frequency up to 400 radians per second. Though only two values for z are given on the charts, negative pressure amplitudes corresponding to different a values can be easily obtained by

interpolation or extrapolation since the negative pressure amplitudes are linear with respect to z.

By utalizing the results of Schoenhals and Overcamp (31) the charts for the negative pressure amplitude can be put in a very convenient form by non-dimensionalizing the negative pressure amplitude and the azimuthal coordinate. In this way, the results for all five fluids can be condensed on one chart.

Following the work of Schoenhals and Overcamp, the chart on Figure (17) presents the dimensionless negative pressure amplitude,

$$\frac{P}{\rho a \omega^2 h}$$

as a function of the dimensionless distance, z/h, for various values of the input acceleration amplitude,

$$G = a\omega^2$$

Figure (18) is a plot of the negative pressure amplitude as a function of the viscosity. The values for negative pressure were taken at a height of 31 inches, and for a frequency of 400 radians per second. The values corresponding to the other values for ω will have the same general shape but are not included in the figure so that an enlarged ordinate could be used. From the figure, it can be seen that for fluids with low viscosities, any change in the fluid viscosity will mean a marked difference in the negative pressure amplitude while for fluids with high viscosities any change in the fluid viscosity will have a negligible effect on the negative pressure amplitude.

Though there were no actual measurements of the liquid velocity within the tube, it was decided that the derived velocity equations

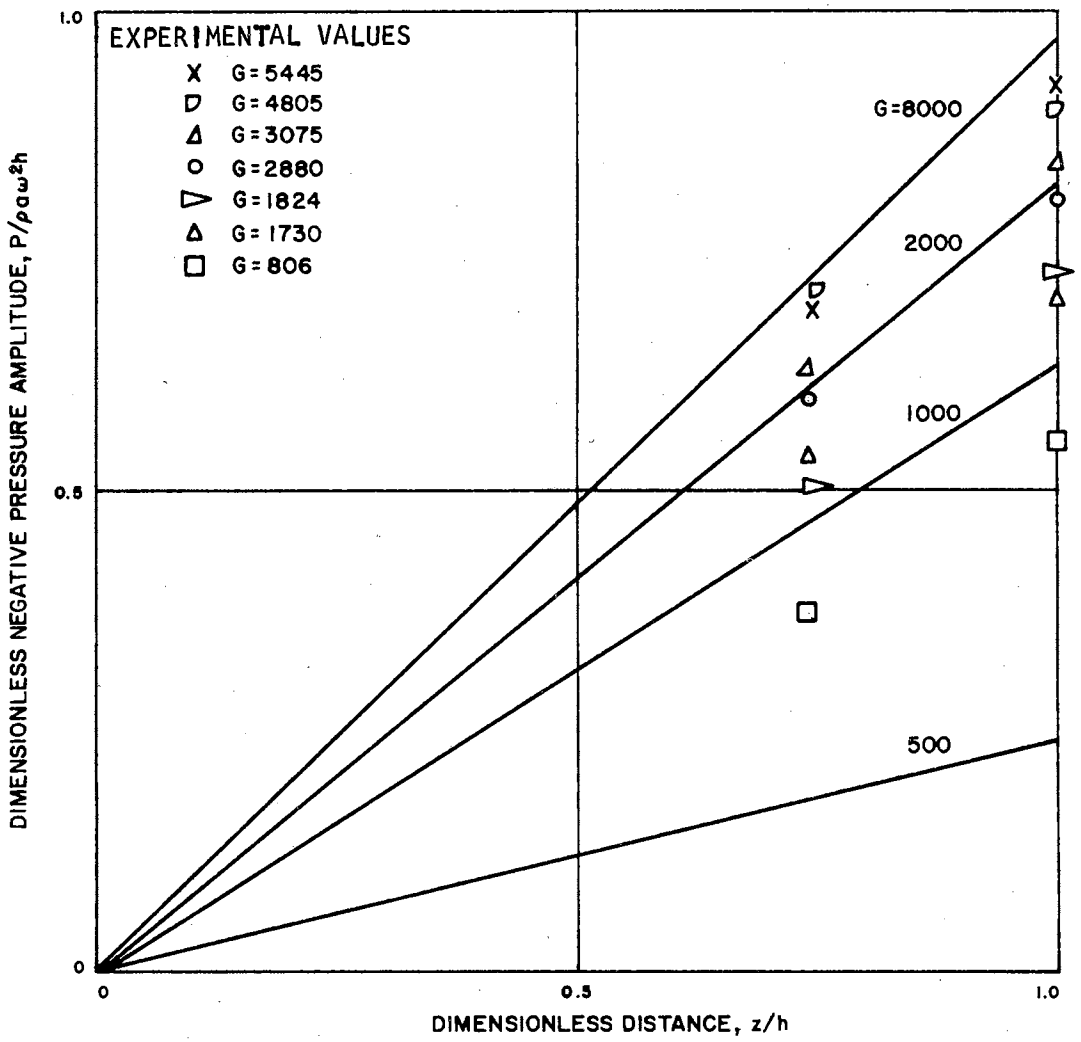

FIGURE 17. Dimensionless Negative Pressure Amplitude vs. Height.

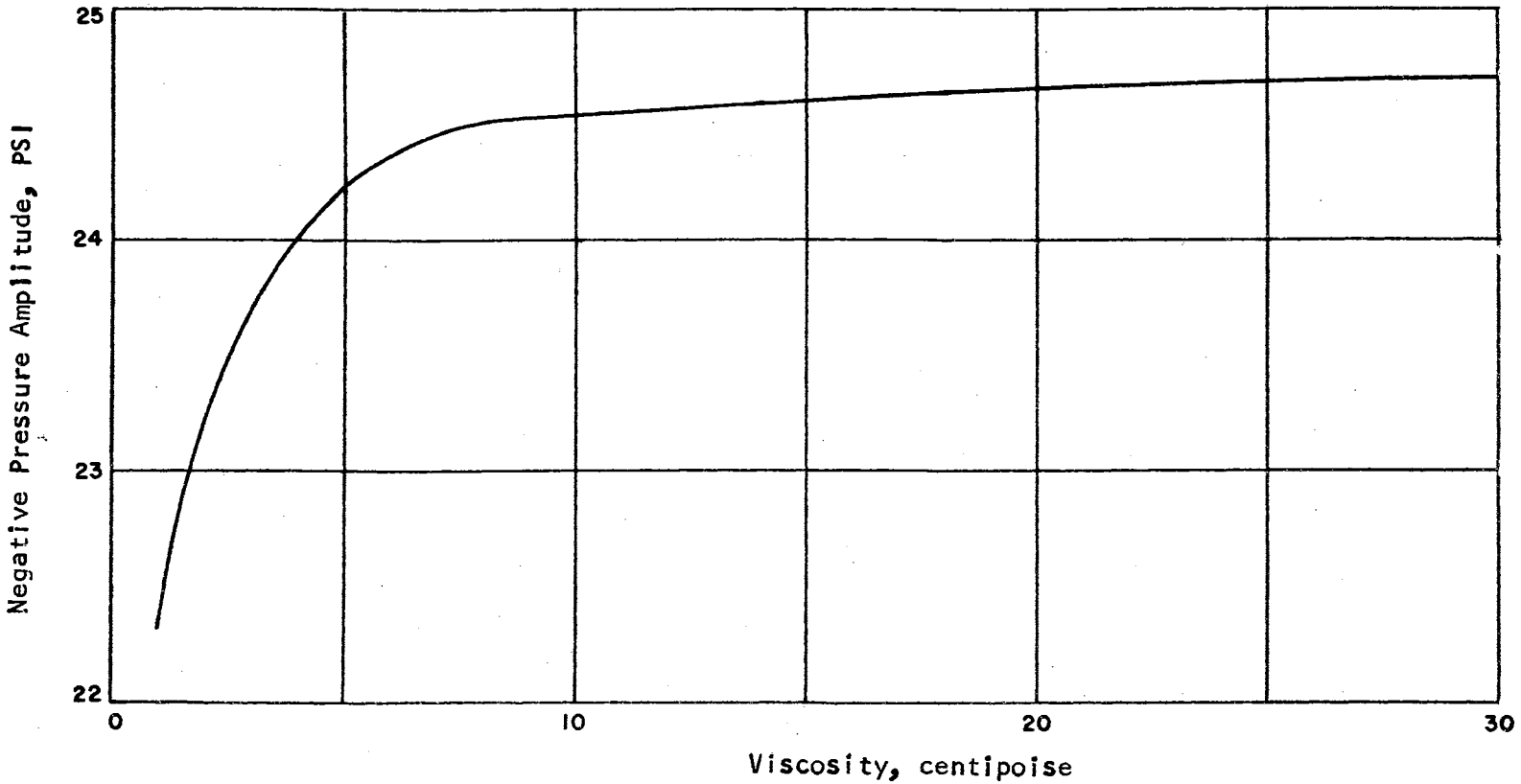

FIGURE 18. Negative Pressure Amplitude vs. Viscosity for $\omega = 400$, $a = 0.05$ and $z = 31$

would be adequate since the pressure equation agreed so well with the experimentally observed values of pressure.

Figure (19) shows how the azimuthal velocity amplitude varies with the azimuthal coordinate, z. From this figure, it is noticed that the fluid with the highest value for viscosity, diethylene glycol, has the largest variation in velocity between the top and the bottom of the fluid column while the fluid with the lowest value for viscosity, water, has the least variation in velocity. This implies that fluids with low values of viscosity are better able to follow the motion of the tube, or, in other words, fluids with low fluid viscosities will have the least variation between the velocity of the surface and the velocity of the bottom of the tube.

Figure (20) is a plot of the azimuthal velocity amplitude as a function of the frequency. From this figure, it can be seen that the azimuthal velocity amplitude is essentially a linear function of the frequency. ω.

Figure (21) is a sketch of the azimuthal velocity profile as a function of the radius for different instants of one period. The magnitudes of the velocities in this figure are with respect to the motion of the wall. That is, the velocity profile in Figure (21) is as it would appear to an observer moving with the same velocity as the wall.

Although the radial velocity amplitude is at least three orders of magnitude less than the azimuthal velocity amplitude, it was decided to present those results since they could become important under certain conditions. For example, if the radius, R, was increased

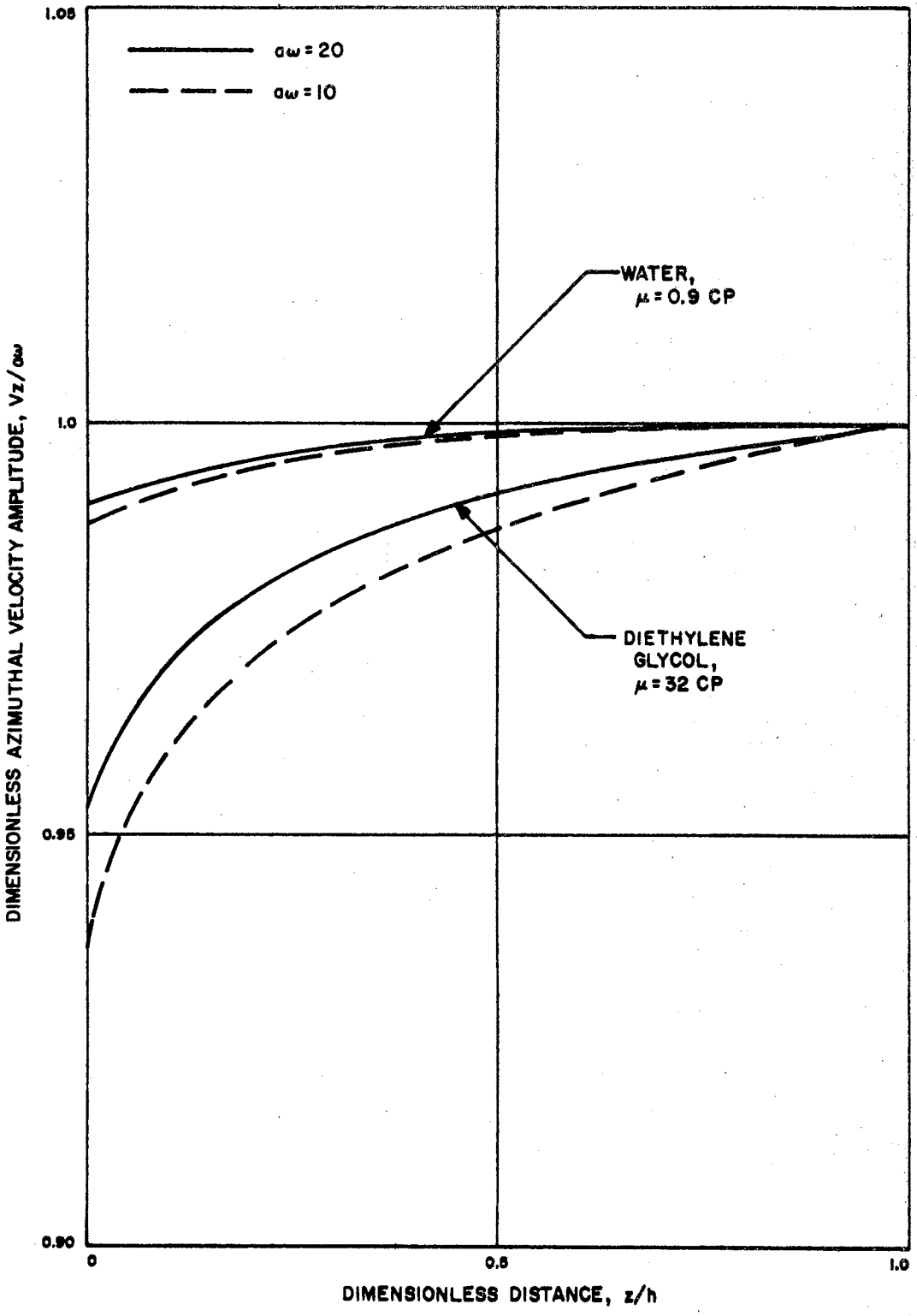

FIGURE 19. Dimensionless Azimuthal Velocity Amplitude vs. Height at r = 0.8

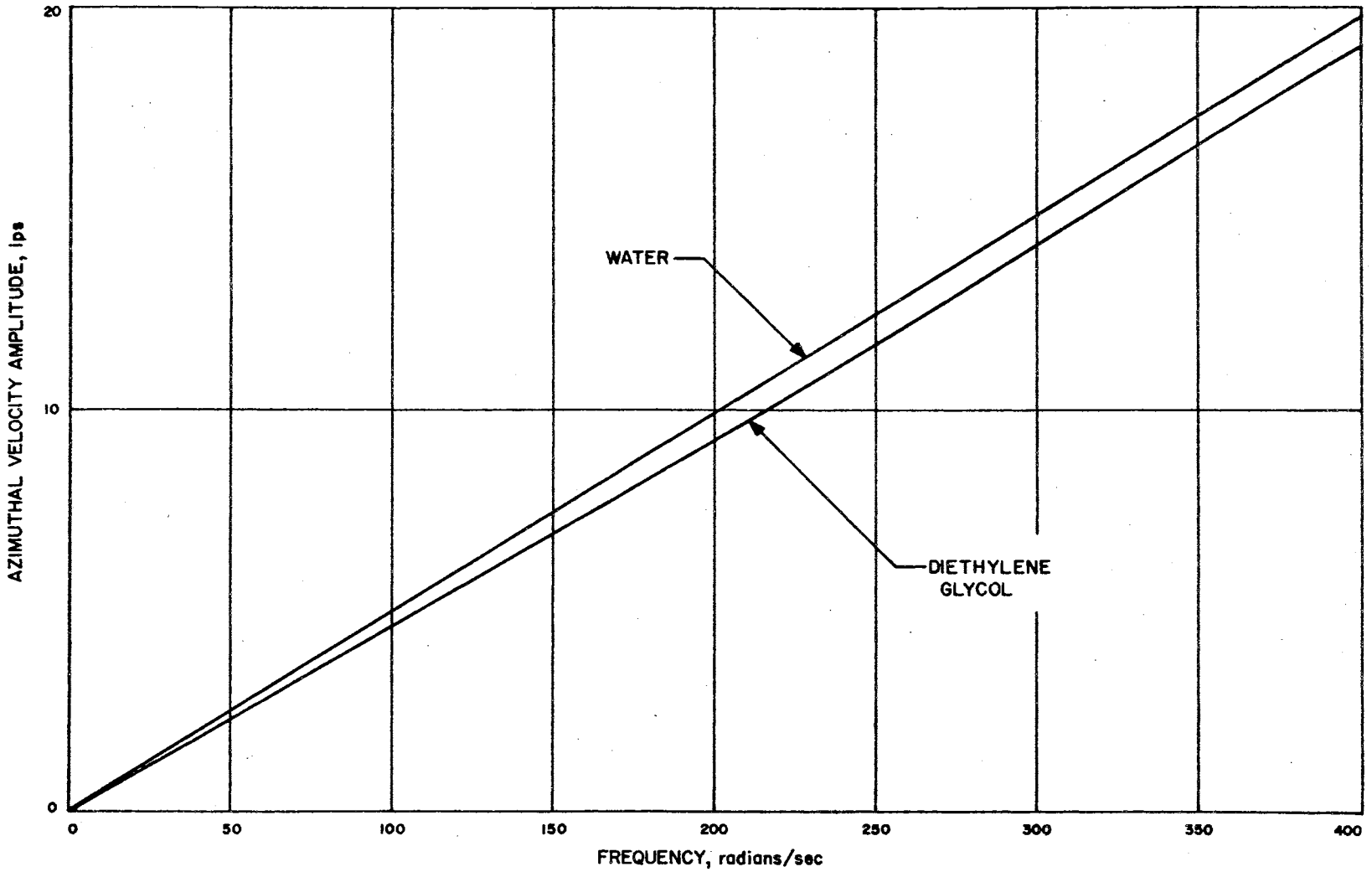

Figure 20. Azimuthal Velocity Amplitude vs. Frequency at z = 0 and r = 0.8

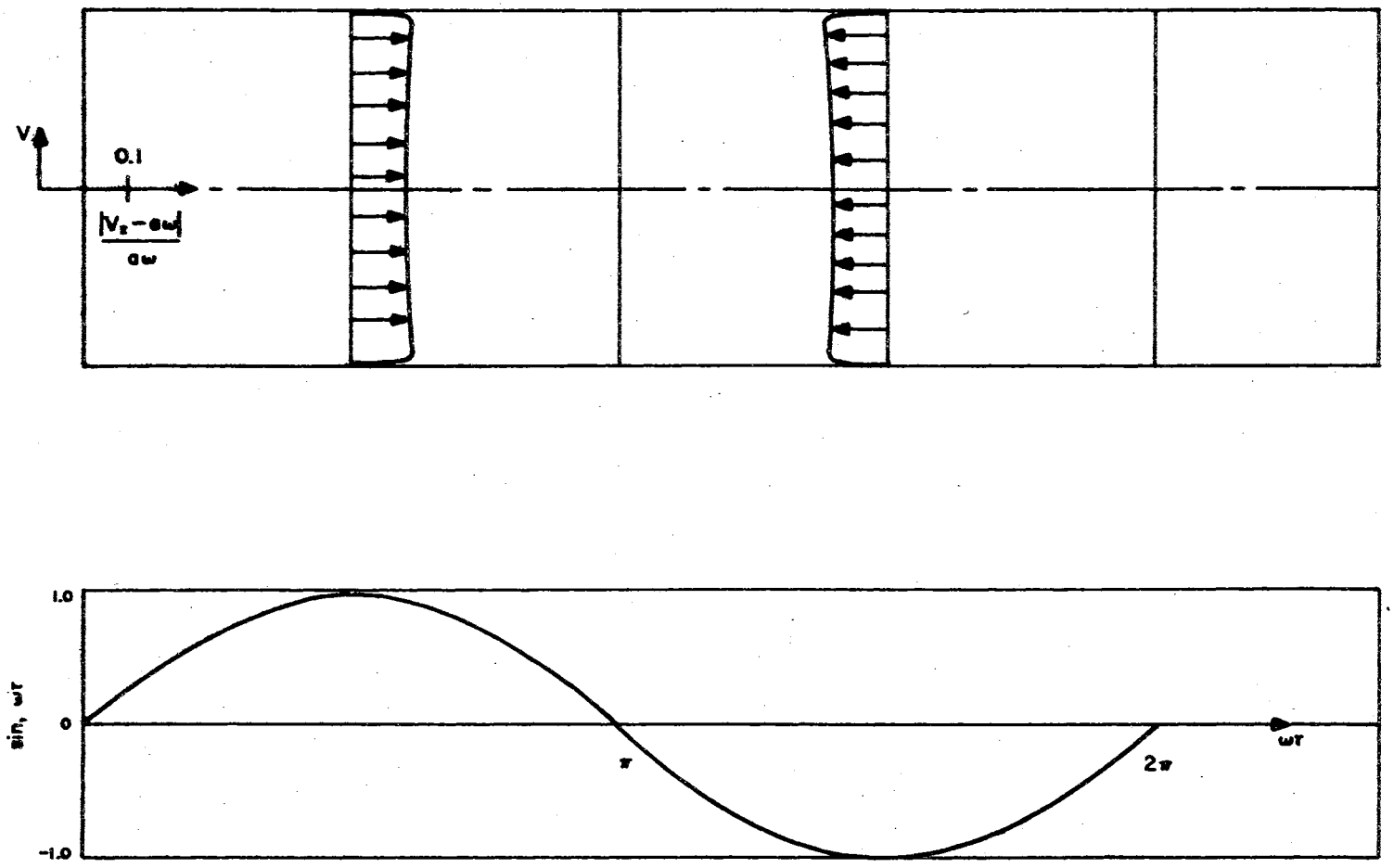

FIGURE 21. Azimuthal Velocity Profile at Different Instants of One Period for Diethylene Glycol at $z = 0$ and $\omega = 200$

by one order of magnitude and the fluid height, h, was decreased by one order of magnitude, the radial velocity amplitude would be approximately one order of magnitude less than the azimuthal velocity amplitude. It is clear that under these conditions the radial velocity would be an important parameter.

Figure (22) is a plot of the radial velocity amplitude as a function of the azimuthal coordinate, z. Besides showing the variation of the velocity amplitude with respect to z, it also shows the dependence on the fluid viscosity. That is, the fluid with the highest value of viscosity, diethylene glycol, will have the highest value of velocity amplitude and the fluid with the lowest value of viscosity, water, will have the lowest value for the velocity amplitude. All fluids with viscosities between the above-mentioned fluids will have values of radial velocity amplitude between the two curves in Figure (22). Figure (22) will be accurate up to a value of z, which is not affected by the bottom of the tube. The exact position where the radial velocity is unaffected by the bottom surface is undetermined. The reason for this uncertainty is due to the linear independence of the Bessel Functions in the radial and azimuthal velocity equations. This independence means that the only way for both the radial and the azimuthal velocity equations to equal zero in the second part of the solution in Chapter IV is for their respective coefficients to equal zero. This would mean that the cos ($\gamma_n h$) and the sin ($\gamma_n h$) would both equal zero which is impossible. So the only condition that could be satisfied at the tube bottom was for the azimuthal velocity to equal zero. But, this should not be taken to mean that it is physically impossible to satisfy both velocity conditions at the bottom of the

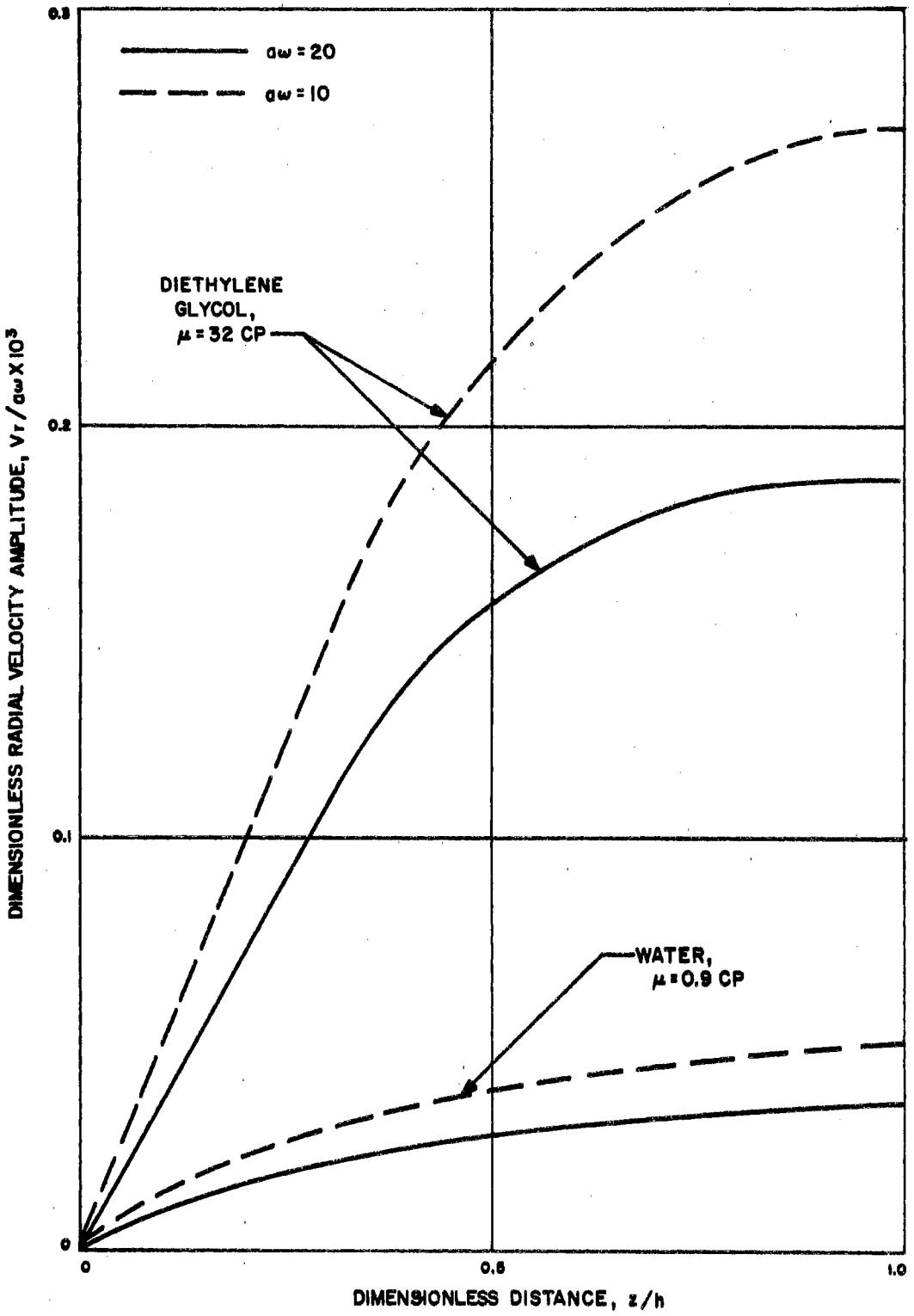

FIGURE 22. Dimensionless Radial Velocity Amplitude vs. Height at r = 0.8

tube. This could probably be realized by a consideration of nonlinear terms in the origina' differential. This would result in functions which are no longer linearly independent. The assumption of the existence of these functions does not imply that they can be found. It is more likely that only numerical solutions are practical.

Figure (23) shows how the radial velocity amplitude will vary with the frequency. Again, it should be noticed that the more viscous fluids will have larger values of radial velocity than the less viscous fluids.

Figure (24) is a plot of the radial velocity profile of diethylene glycol as a function of the radius, r, for different instants of one period. From the figure, it is observed that the radial velocity will increase in magnitude up to a value of r which is very close to the wall. It then decreases very rapidly to a value of zero at the wall. For diethylene glycol at $\omega = 400$, the maximum value for the radial velocity occurs at $r = 0.97$ inch. This maximum radial velocity will occur at different values of r for different fluids. This fact can be seen by inspecting Eq. (IV-67). From that equation, it is noticed that the second and the third term within the brackets contain an exponential term

$$\text{Exp}\left(\sim\sqrt{\frac{\omega}{2\nu}}\ (r-1)\right)$$

which makes the above two terms negligible for all values of r less than about 0.95 inches for the fluids considered in this study. For values of r greater than 0.95 inches, the exponential term will approach unity

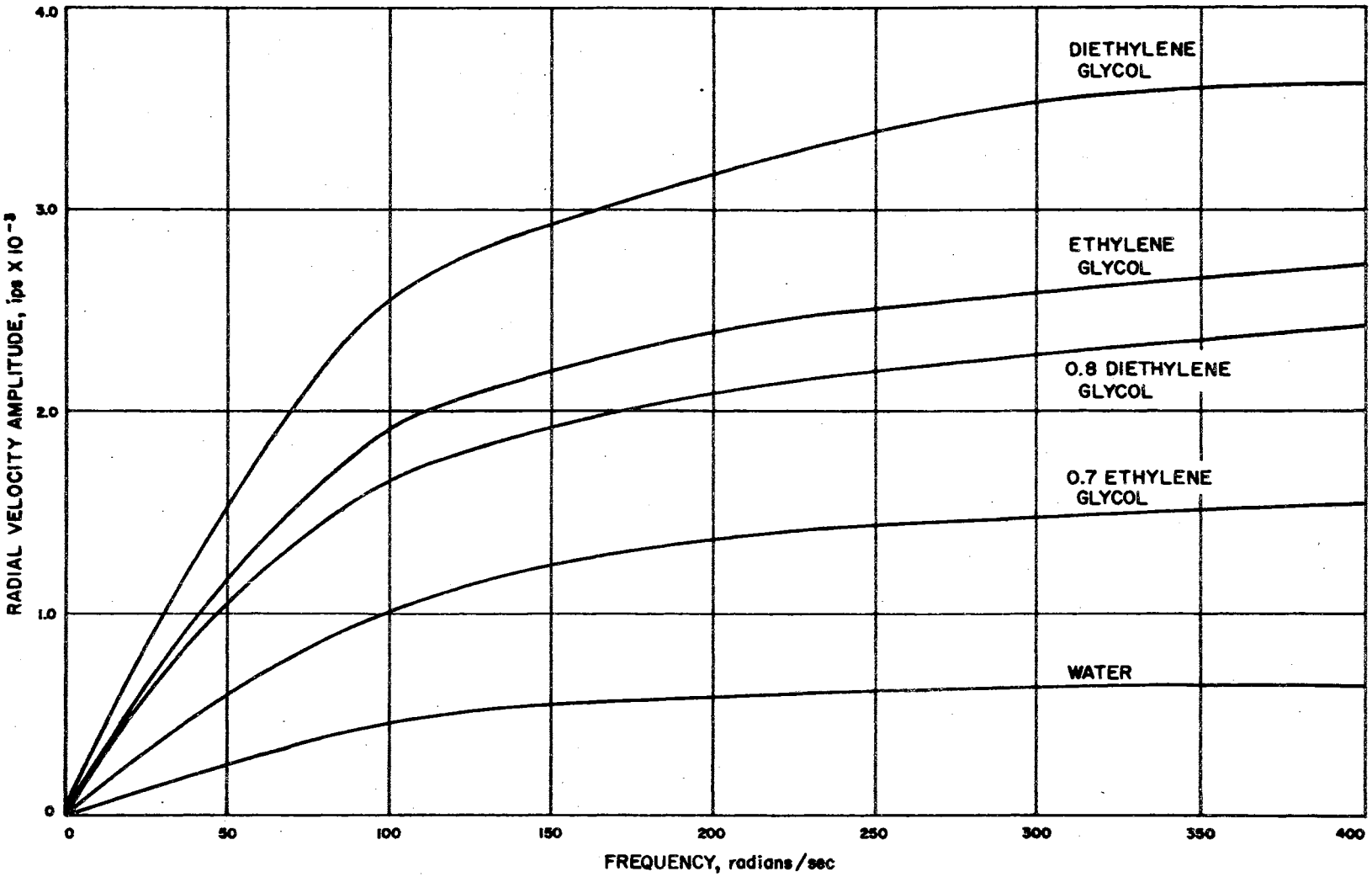

FIGURE 23. Radial Velocity Amplitude vs. Frequency for $z = 23$, $\omega = 400$ and $h = 31$

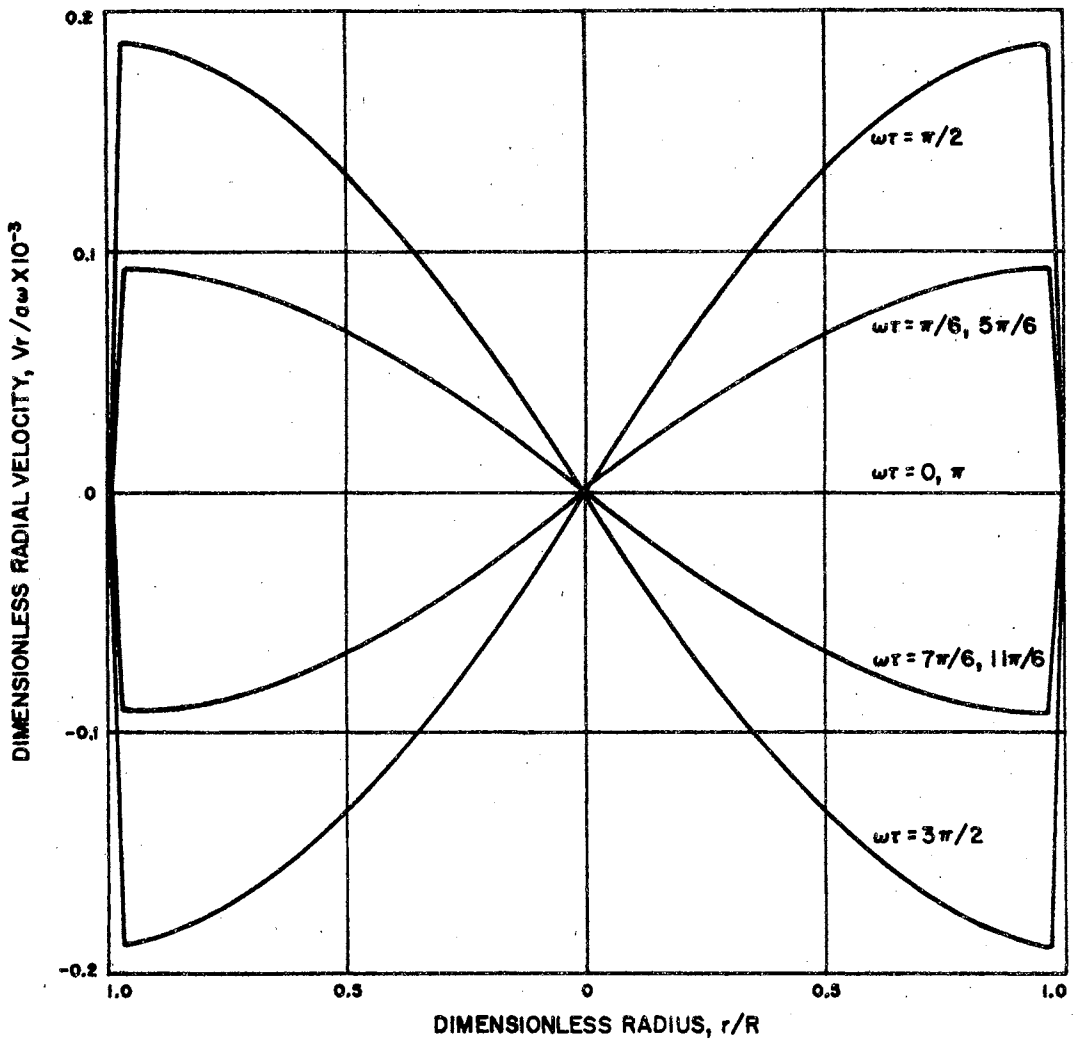

FIGURE 24. Radial Velocity Profile at Different Instants of One Period for Diethylene Glycol at z = 23, ω = 400, a = 0.05 and h = 31

thereby making the second and third terms of Eq. (IV-67) important. In fact, when r is equal to the radius of the tube the sum of the second and third terms of Eq. (IV-67) will be equal to the first term of that equation, thereby making the radial velocity zero at the wall. For values of r between 0.95 inch and 1 inch, the exact position of the maximum radial velocity will also be dependent on the frequency, ω, and the viscosity, ν. That is, the position of the maximum radial velocity can be moved closer to the wall by either increasing the value of ω or by decreasing the value of ν. Table III gives the approximate position of the maximum radial velocity for all the fluids considered at a frequency of 400 radians per second.

TABLE III

POSITION OF MAXIMUM RADIAL VELOCITY
AT ω = 400 RADIANS PER SECOND

Water	70% Eth. Gly.	80% Dieth. Gly.	Eth. Gly.	Dieth. Gly.
>0.99 inch	0.99 inch	0.98 inch	0.98 inch	0.97 inch

Dimensionless Analysis

Due to the complexity of the derived equations in Chapter IV, it was decided to use a dimensionless analysis treatment on the results obtained to see if a simplified relationship could be derived which would adequately describe the pressure conditions within the tube.

From the derivations of Chapter IV, it can be stated that the negative pressure amplitude will be a linear function of the azimuthal coordinate, z, and unknown functions of the input acceleration, $a\omega^2$, the fluid density, ρ, the fluid viscosity, μ, and the tube radius, R. Under

this assumption, the negative pressure amplitude equation will have the following form:

$$P = f\left(a\omega^2,\ \rho,\ \mu,\ R\right)\ z \quad .$$

For any form of the unknown function f, the following relationship must be satisfied:

$$\frac{P}{Z} = \left(\frac{L}{T^2}\right)^a \left(\frac{FT^2}{L^4}\right)^b \left(\frac{FT}{L^2}\right)^c \left(L\right)^d \quad .$$

For dimensional homogeneity, the exponents of F, L and T on both sides of the equation must be the same:

$$\begin{aligned} F: \quad 1 &= \quad b + c \ , \\ L: \quad -3 &= a - 4b - 2c + d, \end{aligned}$$

and

$$T: \quad 0 = -2a + 2b + c \ .$$

When the above simultaneous equations are solved

$$a = 1 + \frac{d}{3} \ ,$$

$$b = 1 + \frac{2d}{3} \ ,$$

$$c = \frac{-2d}{3} \ ,$$

$$d = d \ ,$$

and the solution is

$$P = \rho a\omega^2 z\ f\left((a\omega^2)^{1/3},\ \frac{\rho}{\mu}^{2/3},\ R\right) \ .$$

Since the answer obtained by dimensional analysis will always have an unknown function that must be determined experimentally, the equation

can be assumed to be of the following form:

$$\frac{P}{\rho a\omega^2 z} = c \left(\frac{a\omega^2}{\nu^2} R^3 \right)^{d/3} \qquad \text{(V1-1)}$$

Eq. (V1-1) states that at a height z and for a given input $a\omega^2$, P is the negative pressure amplitude of the fluid, assuming that the initial pressure of the fluid is zero. But at a height z, the fluid will have an initial pressure greater than the ullage pressure by the amount ρgh. This additional pressure is due to the weight of the fluid column above the position z. Now, if it is assumed that the ullage pressure is zero, Eq. (V1-1) can be rewritten in the following form:

$$P = \rho a\omega^2 z\, c \left(\frac{a\omega^2}{\nu^2} R^3 \right)^{d/3} - \rho gh \quad , \qquad \text{(V1-2)}$$

or in dimensionless form

$$\frac{P}{\rho a\omega^2 h} = \left\{ c \left(\frac{a\omega^2}{\nu^2} R^3 \right)^{d/3} - \frac{g}{a\omega^2} \right\} \frac{z}{h} \quad . \qquad \text{(V1-3)}$$

Before an attempt is made to correlate Eq. (V1-3) with the experimental results, it would be wise to consider the effect of the variables ω and μ on the negative pressure amplitude. From Figure (18) it appears that the constants in Eq. (V1-3) should be evaluated for fluids with viscosities less than 10 cp. and for fluids with viscosities greater than 10 cp. since the slope of the curve changes rather abruptly in that region.

Figure (25) is a plot of the dimensionless negative pressure amplitude, $P/\rho a\omega^2 h$, as a function of the frequency, ω. From this figure it is noticed that the slope of the curve changes rather abruptly in a region around 150 radians per second. Thus, it seems logical that the constants c and d/3 should be determined in each of the four regions listed below:

(a) $\omega < 150$, $\mu < 10$,

(b) $\omega < 150$, $\mu > 10$,

(c) $\omega > 150$, $\mu < 10$,

and

(d) $\omega > 150$, $\mu > 10$.

When the results of the present analysis are fitted to Eq. (V1-3) by the least squares method technique, the following values for d and c are obtained:

$\omega < 150$:	$\mu < 10$	$c = 0.9014$, $d = 0.0198$,
	$\mu > 10$	$c = 0.8306$, $d = 0.0396$,
$\omega > 150$:	$\mu < 10$	$c = 0.9022$, $d = 0.0198$,
	$\mu > 10$	$c = 0.957$, $d = 0.01398$.

Figure (26) compares the results obtained from Eq. (V1-3) with the results obtained from the equations of Chapter IV.

From the figure mentioned above, it is noticed that the dimensional analysis approach yields an equation which gives a good

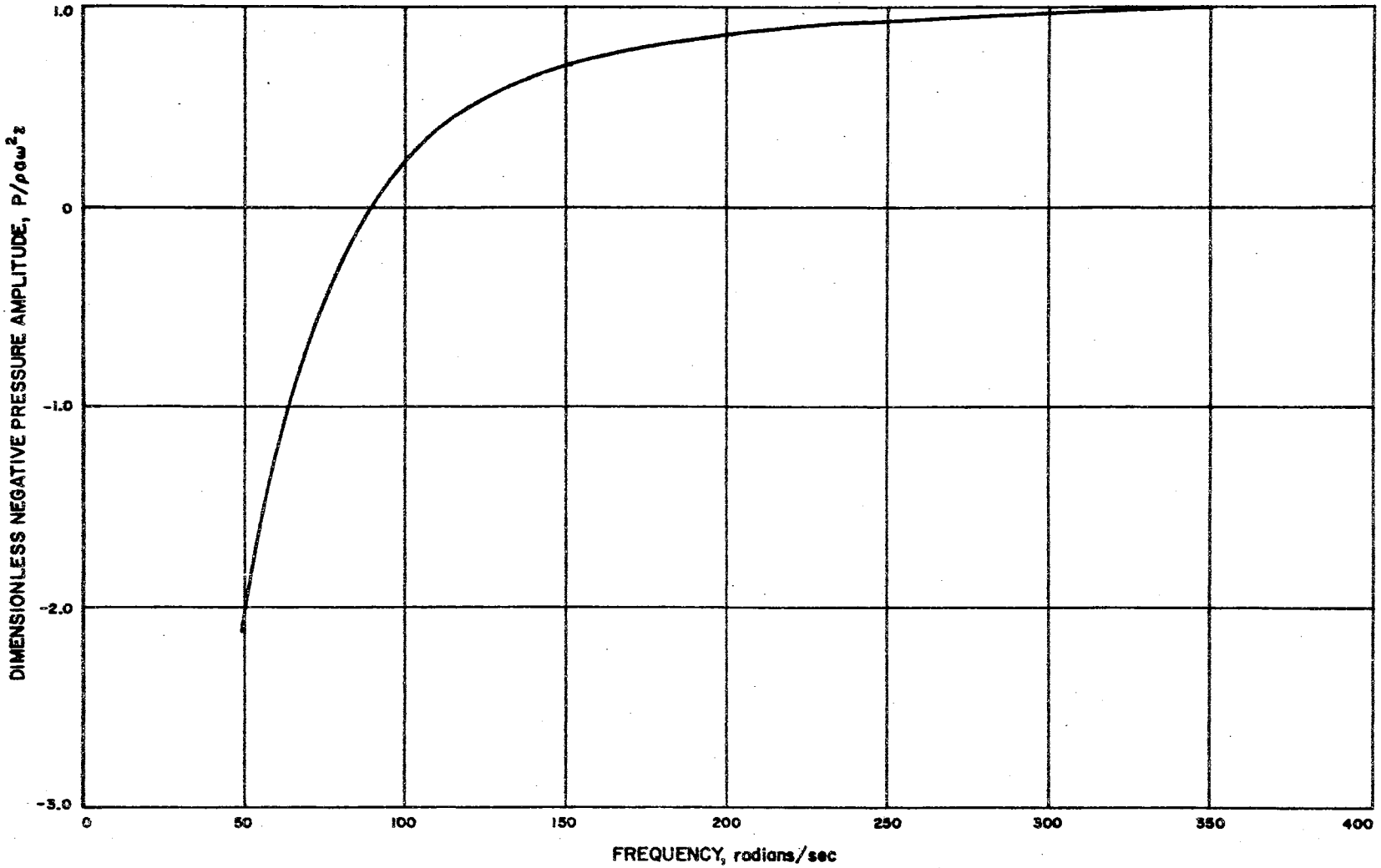

FIGURE 25. Dimensionless Negative Pressure Amplitude vs. Frequency for Water at z = 31

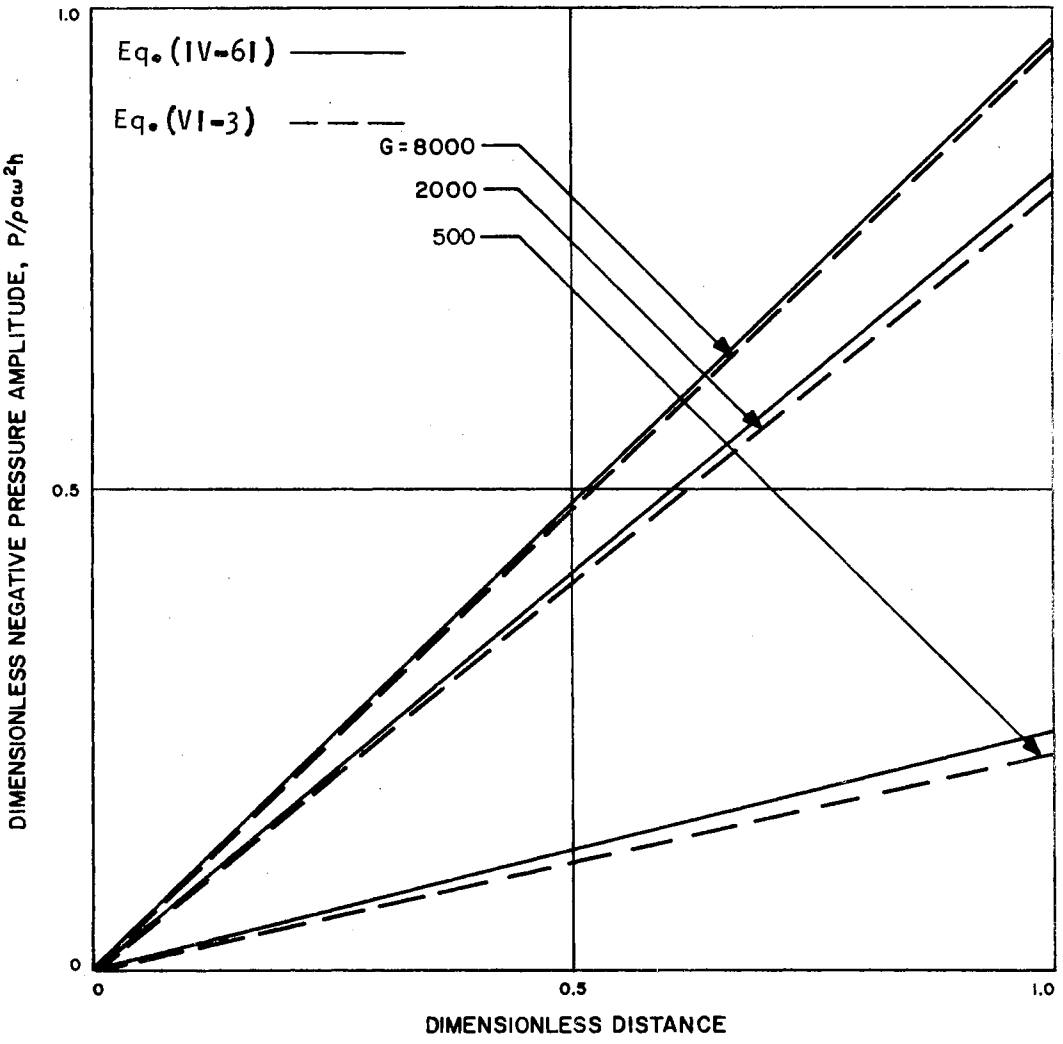

FIGURE 26. Comparison Between Theoretical Equation and Dimensionless Analysis Equation

approximation for the negative pressure amplitude values for the fluids under investigation. But before this equation can be applied to other situations, it should be compared with the results obtained from fluids with viscosities larger than 35 centipoise and from fluids in containers with radii both larger and smaller than one inch.

The plots presented in this chapter give a clear picture of the dependence of the pressure, azimuthal velocity and radial velocity on the spatial coordinates, the frequency and the fluid viscosity. Though the plots are drawn for the specific problem outlined at the end of Chapter IV, the equations of Chapter IV are general and can be applied to any problem which satisfies the given initial conditions and the governing equations.

When an approximate solution is desired, Eq. (VI-3) may give an adequate answer. But when greater accuracy is desired, the equations of Chapter IV should be used.

CHAPTER VII

CONCLUSIONS AND RECOMMENDATIONS

A general, straight-forward, analytical procedure has been presented which predicts the pressure field and the velocity field within a fluid-filled vibrating cylindrical tube. The procedures developed can be applied to problems that are defined by a cylindrical coordinate system with angular symmetry. Although the solution is developed for problems with small vibrational amplitude and frequency, the method used in obtaining this solution is straight-forward and can be applied to problems with large values for amplitude and frequency.

From the charts of the previous chapter, it is noticed that cavitation is most likely to occur at or near the bottom of the tube since the negative pressure is greatest there. It should also be noticed that the negative pressure amplitude will decrease for a decreasing value of viscosity. In fact, for fluids with small values of viscosity the negative pressure amplitude decreases much more rapidly as the viscosity is decreased than for fluids with large values of viscosity. The precise value where this transition occurs cannot be stated, since it occurs over a range of viscosity values, but it is felt that 10 centipoise is a representative number.

Since cavitation and its subsequent cavitation damage can be reduced by selecting a fluid with maximum difference between tensile strength and negative pressure for a given input condition, this

study demonstrates that this is equivalent to selecting a fluid of high tensile strength and low viscosity. For example, in the fluids investigated in this study, water had the highest value of surface tension and the lowest value of viscosity. Thus, of the five fluids considered, water would be the least likely to cavitate.

A graphical presentation of the azimuthal and radial velocity profiles has been given. These charts present a clear picture of the velocity variations with respect to the azimuthal coordinate, the radius and the frequency. The only discrepancy occurred in the radial velocity vs. z plot where a finite value for the radial velocity amplitude at the tube bottom is shown. Physically, the radial velocity amplitude should equal zero at the tube bottom. But due to the lack of linearly independent functions which would satisfy both the azimuthal velocity amplitude and the radial velocity amplitude at the tube bottom, only the azimuthal velocity amplitude was satisfied at that point. This has already been explained in the previous chapter.

A simplified pressure equation was obtained using the dimensional analysis technique. This equation agrees with the values obtained using the equations of Chapter IV but it should be compared with more experimental results so that more accurate values of the constant, c, and the exponent, d, can be obtained.

A computer program has been written which can be used on machines which will accept the IBM 1620 Fortran notation without Format. In addition to printing the results on the IBM printer, it will also punch the results on IBM cards so that the plot programs listed in Appendix B can be used if so desired.

To conclude this study, a discussion of possible future investigations follows.

A natural extension to the present study would be to include the effect of angular dependence. That is, non-circular cylindrical containers could be used in the testing. This angular dependence should present no great problem in that the techniques used in the present study can be used for this study. Another area that should be investigated is that of elastic walled cylinders. This problem has received some attention in that the wall was thought to act like a series of isolated oscillating hoops. The underlying assumption in this method is the fact that the motion is purely radial. In a real situation the wall may move in a radial, azimuthal and angular direction with the respective motions being dependent on each other. It would be very interesting to incorporate this movement of the wall as a boundary condition for the equations of motion to see what effect this movement has on the pressure and the velocity of the fluid.

A multiple-axis vibration test of a fluid-filled cylindrical tube would be interesting in that it could be determined if the different inputs would have the effect of adding to one another, subtracting from one another, or if they are completely independent of one another.

Another area of future study would be to obtain a solution that would satisfy the condition of zero velocity for both the radial and the azimuthal velocity at the tube bottom. As has been discussed previously, this would probably necessitate the use of a numerical solution.

BIBLIOGRAPHY

1. Abramson, H. N., "Dynamic Behavior of Liquid in Moving Container," Applied Mechanics Review, Vol. 16, No. 7, July, 1963 pp. 501-506.

2. Abramson, H. N., "Liquid Dynamic Behavior in Rocket Propellant Tanks," Proceedings of ONR/AIA Symposium on Structural Dynamics of High Speed FLight, 1961, pp. 287-318.

3. Bauer, H. F., Dynamics of Liquid Propellant Vehicles," Proceedings of ONR/AIA Symposium on Structural Dynamics of High Speed Flight, 1961, pp. 319-355.

4. Beams, J. W., "Tensile Strengths of Liquid Argon, Helium, Nitrogen, and Oxygen," Physics of Fluids, Vol. 2, No. 1, January-February, 1959, pp. 1-40.

5. Benson, S. W. and Gerjuoy, E., "The Tensile Strengths of Liquids," Journal of Chemical Physics, Vol. 17, No. 10, October, 1949, pp. 914-198.

6. Benson, S. W. and Golding, R. A., "A Reduced Equation of State for Gases and Liquids," Journal of Chemical Physics, Vol. 19, No. 11, November, 1951, pp. 1413-1415.

7. Berthelot, M., "Sur la Dilatation Forcee des Liquides," Ann. de Chimie, Vol. 30, 1850, pp. 232-237.

8. Binder, R. C., Advanced Fluid Mechanics, Vol. 1, Prentice Hall, Englewood Cliffs, New Jersey, 1958.

9. Briggs, L. J., "Limiting Negative Pressure of Water," Journal of Applied Physics, Vol. 21, July, 1950, pp. 721-722.

10. Briggs, L. J., "The Limiting Negative Pressure of Acetic Acid, Benzene, Aniline, Carbon Tetrachloride, and Chloroform," Journal of Chemical Physics, Vol. 19, No. 7, July, 1951, pp. 970-972.

11. "British Association Mathematical Tables," Vol. 6, Cambridge University Press, London, England.

12. Bull, T. H., "The Tensile Strengths of Liquids Under Dynamic Loading," Philosophical Magazine, Series 8, Vol. 1, No. 2, February, 1956, pp. 153-165.

13. Bull, T. H., "The Tensile Strengths of Viscous Liquids Under Dynamic Loading." British Journal of Applied Physics, Vol. 7, November, 1956, pp. 416-418.

14. Cooper, R. M, "Dynamics of Liquids in Moving Containers," ARS Journal, Vol. 30, August, 1960, pp. 725-729.

15. Fisher, J. C., "The Fracture of Liquids," Journal of Applied Physics, Vol. 19, November, 1948, pp. 1062-1067.

16. Fisher, J. C., "The Limiting Hydrostatic Tension of Water Near 0°C," Journal of Applied Physics, Vol. 21, October, 1960 p. 1068.

17. Frenkel, J., Kinetic Theory of Liquids, Dover Publications, New York, 1955.

18. Furth, R., "The Statistical Treatment of the Thermodynamics of Liquids by the Theory of Holes," Proceedings of Cambridge Philosophical Society, Vol. 37, 1941, pp. 252-275.

19. Graham, E. W., "The Forces Produced by Fuel Oscillation in a Rectangular Tank," Report SM-13748, Douglas Aircraft Company Inc., Santa Monica, California.

20. Graham, E. W., and Rodriquez, A. M., "The Characteristics of Fuel Motion Which Affect Airplane Dynamics," Journal of Applied Mechanics, Vol. 19, September, 1952, pp. 381-388.

21. Harvey, E. N., Barnes, D. K., McElroy, W. D., Whiteley, A. H., and Pease, D. C., "Removal of Gas Nuclei From Liquids and Surfaces," Journal of Cellular and Comparative Physiology, Vol. 67, January, 1945, pp. 956-957.

22. Harvey, E. N., McElroy, W. D., and Whiteley, A. H., "On Cavity Formation in Water," Journal of Applied Physics, Vol. 18, February, 1947, pp. 162-172.

23. Joffe, A. F., "Mechanical and Electrical Strength and Cohesion," Transactions of the Faraday Society, Vol. 24, 1928, pp. 65-72.

24. Knapp, R. T., "Cavitation and Nuclei," ASME Transactions, Vol. 80, August, 1958, pp. 1315-1324.

25. Kuper, C. G., and Trevena, D. H., "The Effect of Dissolved Gases on the Tensile Strength of Liquids," Proceedings of the Physical Society, Vol. 65A, 1952, pp. 46-54.

26. Lewis, G. M., "The Tensile Strength of Liquids in Berthelot Tubes," Proceedings of the Physical Society, Vol. 78, Part 1, July, 1961, pp. 133-144.

27. Lorell, J., "Forces Produced by Fuel Oscillations," Progress Report 20-149, Jet Propulsion Laboratory, California Institute of Technology, Pasadena, California.

28. Marsden, C. and Mann, S., Solvents Guide, Wiley, New York, 1963.

29. Misener, A. D., and Hebert, G. R., "Tensile Strength of Liquid Helium II," Nature, Vol. 177, No. 4516, May 19, 1956, pp/ 946-947.

30. Morse, P. M. and Feshback, H., Methods of Theoretical Physics, McGraw Hill, New York, 1953.

31. Schoenhals, R. J., and Overcamp, T. J., "Pressure Distribution and Bubble Formation Induced by Longitudinal Vibration of a Flexible Liquid-Filled Cylinder," NASA TM X-53353, September, 1965.

32. Schy, A. A., "A Theoretical Analysis of the Effects of Fuel Motion on Airplane Dynamics," NACA TN 2280, January, 1951.

33. Scott, A. F., Shoemaker, D. P., Tanner, K. N., and Wendel, J. G., "Study of the Berthelot Method for Determining the Tensile Strength of a Liquid," Journal of Chemical Physics, Vol. 16, No. 5, May, 1948, pp. 495-502.

34. "Standard Mathematical Tables," Twelfth Edition, Chemical Rubber Publishing Co., Cleveland, Ohio.

35. Temperley, H. N. V., and Chambers, LL. G., "The Behavior of Water Under Hydrostatic Tension: 1," Proceedings of the Physical Society, Vol. 58, 1946, pp. 420-436.

36. Temperley, H. N. V., "The Behavior of Water Under Hydrostatic Tension: II," Proceedings of the Physical Society, Vol. 58, 1946, pp. 436-443.

37. Temperley, H. N. V., "The Behavior of Water Under Hydrostatic Tension: III," Proceedings of the Physical Society, Vol. 59, 1947, pp. 199-208/

38. Vincent, R. S., "Measurement of Tension in Liquids by Means of a Metal Bellows,' Proceedings of the Physical Society, Vol. 53, 1941, pp. 126-140.

39. Vincent, R. S., "The Viscosity Tonometer - A New Method of Measuring Tension in Liquids," Proceedings of the Physical Society, Vol. 55, 1943, pp. 41-48.

40. Vincent, R. S., and Simmonds, G. H., "Examination of the Berthelot Method of Measuring Tension in Liquids," Proceedings of the Physical Society, Vol. 55, 1943, pp. 376-382.

41. Worthington, A. M., "An Experimental Determination of the Volume-Extensibility of Ethyl Alcholol," Philosophical Transactions, Vol. 183, 1892, pp. 355-371.

APPENDIX A

SUPPLEMENT TO CHAPTER 1V

The purpose of this Appendix is to supplement the derivations of Eq. (1V-56) from Eq. (1V-31), Eq. (1V-59) from Eq. (1V-52), Eq. (1V-64) from Eq. (1V-63), and Eq. (1V-67) from Eq. (1V-54) with the steps that are necessary for a smooth transition between the above mentioned equations.

Derviation of Eq. (1V-56)

The complex part of the first term on the right-hand side of Eq. (1V-31) is

$$A + iB = \frac{\sqrt{K}}{1} \frac{\sinh \frac{\sqrt{K}}{1} Z}{\cosh \frac{\sqrt{K}}{1} h} , \qquad (A-1)$$

where A and B are the real and the imaginary parts of the above equation, 1 equals

$$1 = -i \frac{c^2}{\omega_\nu} ,$$

and

$$K = \alpha_n^2 + i \frac{\omega}{\nu}$$

The principle root of $\sqrt{K}$ is

$$\sqrt{K} = \sqrt[4]{K\,\bar{K}}\ \mathrm{Exp}\left(i\,\frac{\theta}{2}\right) \quad , \qquad \text{(A-2)}$$

where

$$\theta = \tan^{-1}\ \frac{\omega/\nu}{\alpha_n^{\,2}} \quad ,$$

and $\bar{K}$ is the complex conjugate of K.

The principle root of 1 is

$$1 = \sqrt{\frac{\epsilon^2}{\omega/\nu}}\ \mathrm{Exp}\left(-i\,\frac{\pi}{4}\right) \quad . \qquad \text{(A-3)}$$

From Eq. (A-2) and Eq. (A-3) the term $\frac{\sqrt{K}}{1}$ can be written in the following form:

$$\frac{\sqrt{K}}{1} = \left(\frac{K\,\bar{K}}{1\,\bar{1}}\right)^{1/4}\ \mathrm{Exp}\left(i\ \left(\frac{\theta}{2}+\frac{\pi}{4}\right)\right) \quad . \qquad \text{(A-4)}$$

The real part of Eq. (A-4) is

$$R = \frac{\omega/\nu}{c}\left(\left(\frac{\sqrt{K\,\bar{K}}+\alpha_n^{\,2}}{4}\right)^{1/2} - \left(\frac{\sqrt{K\,\bar{K}}+\alpha_n^{\,2}}{4}\right)^{1/2}\right) \qquad \text{(A-5)}$$

and the imaginary part is

$$1 = \frac{\omega/\nu}{c}\left(\left(\frac{\sqrt{K\,\bar{K}}-\alpha_n^{\,2}}{4}\right)^{1/2} + \left(\frac{\sqrt{K\,\bar{K}}+\alpha_n^{\,2}}{4}\right)^{1/2}\right) \quad . \qquad \text{(A-6)}$$

Within the limitations of the defined problem, it can be stated that

$$\alpha_n^{\,2} << \frac{\omega}{\nu} \quad . \qquad \text{(A-7)}$$

Under the simplifying assumption of Eq. (A-7), Eq. (A-5) and Eq. (A-6) take the following form:

$$R = 0 \tag{A-8}$$

and

$$1 = \frac{\omega}{c} \quad . \tag{A-9}$$

Eq. (A-1) can now be written as

$$A + iB = i\frac{\omega}{c}\,\frac{\sinh i\frac{\omega}{c} Z}{\cosh i\frac{\omega}{c} h} \quad . \tag{A-10}$$

The real part of the above equation is

$$A = -\frac{\omega}{c}\,\frac{\sin \frac{\omega}{c} Z}{\cos \frac{\omega}{c} h} \tag{A-11}$$

and since $\frac{\omega}{c} \ll 1$ for all ω and c, Eq. (A-11) can be rewritten as

$$A = -\left(\frac{\omega}{c}\right)^2 Z \quad . \tag{A-12}$$

Eq. (A-12) is used to obtain Eq. (IV-56) from Eq. (IV-31).

To show the equivalence between the first two terms of Eq. (IV-31) all that is necessary is to show that the real and the imaginary parts of the second term are equal to the real and the imaginary parts of Eq. (A-10).

The complex part of the second term on the right-hand side of Eq. (IV-31) is

$$C + iD = \frac{\sqrt{K}}{1}\,\frac{\sinh \frac{\sqrt{K}}{1} Z}{\cosh \frac{\sqrt{K}}{1} h} \quad , \tag{A-13}$$

where C and D are the real and the imaginary parts of Eq. (A-13). The principle root of $\sqrt{K}$ is

$$\sqrt{K} = \sqrt[4]{K\,\bar{K}} \quad \text{Exp} \left(i \frac{\theta}{2}\right)$$

where

$$\theta = \tan^{-1} - \frac{\omega/\nu}{\alpha_n^2} \quad .$$

The principle root of 1 is

$$1 = \frac{c^2}{\omega/\nu} \text{ Exp} \left(i \frac{\pi}{4}\right) \quad . \tag{A-15}$$

From Eq. (A-14) and Eq. (A-15), an equation similar to Eq. (A-4) can be written:

$$\frac{\sqrt{K}}{1} = \left(\frac{K\,\bar{K}}{1\,\bar{1}}\right)^{1/4} \quad \text{Exp} \left(i \left(\frac{\theta}{2} - \frac{\pi}{4}\right)\right) . \tag{A-16}$$

The real part of the above equation is

$$R' = \frac{\omega/\nu}{c}\left(\left(\frac{K\,\bar{K} + \alpha_n^2}{4}\right)^{1/2} - \left(\frac{K\,\bar{K} - \alpha_n^2}{4}\right)^{1/2}\right) \tag{A-17}$$

and the imaginary part is

$$1' = -\frac{\omega/\nu}{c}\left(\left(\frac{K\,\bar{K} + \alpha_n^2}{4}\right)^{1/2} + \left(\frac{K\,\bar{K} - \alpha_n^2}{4}\right)^{1/2}\right) \tag{A-18}$$

If the simplifying assumption of Eq. (A-7) is again used, Eq. (A-17) and Eq. (A-18) can be written in the following form:

$$R' = 0 \tag{A-19}$$

and

$$1' = -\frac{\omega}{c} \quad . \tag{A-20}$$

The above two equations allow Eq. (A-13) to be written in the following form:

$$C + iD = -i\frac{\omega}{c}\,\frac{\sinh\left(-i\frac{\omega}{c}\,Z\right)}{\cosh\left(-i\frac{\omega}{c}\,h\right)} \quad , \tag{A-21}$$

The above equation can be rewritten as

$$C + iD = i\frac{\omega}{c}\,\frac{\sinh\left(i\frac{\omega}{c}\,Z\right)}{\cosh\left(i\frac{\omega}{c}\,h\right)} \quad , \tag{A-22}$$

which is identical with Eq. (A-10) and the equivalence between the two terms of Eq. (1V-31) is proved.

Derivation of Eq. (1V-59)

The complex part of the first term on the right-hand side of Eq. (1V-52) can be written as

$$E + iF = \frac{\beta_1\, l_1\, (\tau_1)}{DENOM} \tag{A-23}$$

where E and F are the real and the imaginary parts of the above equation and DENOM is defined in Chapter 1V. The term τ_1 is

$$\tau_1 = \sqrt{\gamma_n^2 + i\frac{\omega}{\nu}}$$

which can be approximated by

$$\tau_1 = \sqrt{i\frac{\omega}{\nu}} \tag{A-24}$$

since $\frac{\omega}{\nu}$ is much larger than γ_n^2 for all values of γ_n . Eq. (A-24) can be written in the following form:

$$\tau_1 = \sqrt{\frac{\omega}{2\nu}} \quad i\sqrt{\frac{\omega}{2\nu}} \tag{A-25}$$

where only the principle root is considered. The term β_1 can be approximated by

$$\beta_1 = \gamma_n \tag{A-26}$$

since

$$\frac{\omega^2 c^2}{c^4 + \omega^2 \nu^2} << \gamma_n^2$$

and

$$\frac{\omega^3 \nu}{c^4 + \omega^2 \nu^2} << \gamma_n^2$$

for all values of γ_n.

From Eq. (A-25), the modified Bessel Functions can be written in the following form:

$$l_1(\tau_1) = \text{bei}_1 \sqrt{\frac{\omega}{\nu}} - i\,\text{ber}_1 \sqrt{\frac{\omega}{\nu}} \tag{A-27}$$

and

$$l_o(\tau_1) = \text{ber} \sqrt{\frac{\omega}{\nu}} + i\,\text{bei} \sqrt{\frac{\omega}{\nu}} \,. \tag{A-28}$$

To simplify the arithmetic calculations, the following symbols will be used for the ber and the bei functions:

$$a = \text{ber}_1 \sqrt{\frac{\omega}{\nu}} \,,$$

$$b = \text{bei}_1 \sqrt{\frac{\omega}{\nu}} \,,$$

$$c = \text{ber} \sqrt{\frac{\omega}{\nu}} \,,$$

$$d = \text{bei} \sqrt{\frac{\omega}{\nu}} \,,$$

and

$$f = \sqrt{\frac{\omega}{2\nu}} \,. \tag{A-29}$$

From the notation of Eq. (A-29), Eq. (A-21) can be written in the following form:

$$E + iF = \frac{b - ia}{M - iN} \quad . \tag{A-30}$$

where

$$M = \gamma_n b\, l_1(\gamma_n) - fcl_1(\gamma_n) + fdl_1(\gamma_n) \quad ,$$

and

$$N = a\,\gamma_n\, l_o(\gamma_n) + fcl_1(\gamma_n) + fdl_1(\gamma_n) \quad .$$

The real part of the above equation is

$$E = \frac{bM + aN}{M^2 + N^2} \quad . \tag{A-31}$$

For large values of $\frac{\omega}{\nu}$, Eq. (A-29) can be written in the following form:

$$a = \frac{\mathrm{Exp}\ \sqrt{\frac{\omega}{2\nu}}}{\left(2\pi \sqrt{\frac{\omega}{\nu}}\right)^{1/2}} \cos\left(\sqrt{\frac{\omega}{2\nu}} + \frac{3\pi}{8}\right),$$

$$b = \frac{\mathrm{Exp}\ \sqrt{\frac{\omega}{2\nu}}}{\left(2\pi \sqrt{\frac{\omega}{\nu}}\right)^{1/2}} \sin\left(\sqrt{\frac{\omega}{2\nu}} + \frac{3\pi}{8}\right),$$

$$c = b \quad ,$$

and

$$d = -a \quad . \tag{A-32}$$

When the above approximations are substituted into Eq. (A-31), the following equation results:

$$E = -\frac{NUM}{DEN} \quad . \tag{A-33}$$

The second term on the right-hand side of Eq. (1V-52) can be written in the following form:

$$G + iH = \frac{\beta_2 \, l_1 \, \tau_2)}{DENOM} \qquad \text{(A-34)}$$

If the same procedure as was used before is used on Eq. (A-34), it is an easy task to show that the real part of Eq. (A-34) is the same as Eq. (A-33). Since G is equal to E, the two terms on the right-hand side of Eq. (1V-52) can be combined. The resulting equation is Eq. (1V-59).

Derivation of Eq. (1V-64)

The second term on the right-hand side of Eq. (1V-63) can be written as

$$J + iK = \frac{(f + i f) \, l_1 (\gamma_n) \, l_o (\tau_1 r)}{M - \ldots} \, , \qquad \text{(A-35)}$$

where the notation of Eq. (A-29) is used and where τ_1 equals

$$\tau_1 = \sqrt{\frac{\omega}{2\nu}} + i \sqrt{\frac{\omega}{2\nu}} \, .$$

The first term in Eq. (1V-63) is similar to Eq. (A-23) and is not included in this analysis.

Since τ r is a large number, greater than 100, for all values of r used, a good approximation for l_o (τ r) can be written:

$$l_o (\tau r) = \frac{\operatorname{Exp}\left(\sqrt{\frac{\omega}{2\nu}} \, r\right)}{\left(2\pi \sqrt{\frac{\omega}{\nu}} \, r\right)^{1/2}} \left(\sin\left(\sqrt{\frac{\omega}{2\nu}} \, r + \frac{3\pi}{8}\right) - i \cos\left(\sqrt{\frac{\omega}{2\nu}} \, r + \frac{3\pi}{8}\right)\right) . \qquad \text{(A-36)}$$

When Eq. (A-36) is substituted into Eq. (A-35), the following equation for J results:

$$J = \left(\frac{NUM1}{DEN} \sin\left(\sqrt{\frac{\omega}{2\nu}}\, r + \frac{3\pi}{8}\right) + \frac{NUM2}{DEN} \cos\left(\sqrt{\frac{\omega}{2\nu}}\, r + \frac{3\pi}{8}\right)\right) \frac{\mathrm{Exp}\left(\sqrt{\frac{\omega}{2\nu}}\,(r-1)\right)}{\sqrt{r}} \quad . \qquad \text{(A-37)}$$

The above equation is used to obtain Eq. (1V-64) .

If the term

$$\tau_2 = \sqrt{\frac{\omega}{2\nu}} - i\sqrt{\frac{\omega}{2\nu}}$$

is used in the above analysis, an equation similar to Eq. (A-37) will be obtained.

Derivation of Eq. (1V-67)

The first part of Eq. (1V-66) is similar to Eq. (A-23) and the second part can be written in the following form:

$$L + iM = \frac{I_1(\gamma_n)\, I_1(\tau r)}{M - iN} \qquad \text{(A-38)}$$

where the notation of Eq. (A-29) is used. The term τ_1 will be used in this analysis but it should be remembered that the final result will be the same for τ_2 .

The term for the modified Bessel Function is

$$I_1(\tau_1 r) = \frac{\mathrm{Exp}\left(\sqrt{\frac{\omega}{2\nu}}\, r\right)}{\left(2\pi\sqrt{\frac{\omega}{\nu}}\, r\right)} \left(\sin\left(\sqrt{\frac{\omega}{2\nu}}\, r + \frac{3\pi}{8}\right)\right.$$

$$- i \cos\left(\sqrt{\frac{\omega}{2\nu}}\, r + \frac{3\pi}{8}\right)\Bigg) \quad . \qquad \text{(A-39)}$$

When Eq. (A-39) is substituted into Eq. (A-38), the following equation for L results:

$$L = \sqrt{\frac{\nu}{2\omega}} \left(\frac{NUM1 + NUM2}{DEN} \sin\left(\sqrt{\frac{\omega}{2\nu}}\,(r-1)\right) \quad +(-) \right.$$

$$\left. \frac{NUM1 - NUM2}{DEN} \cos\left(\sqrt{\frac{\omega}{2\nu}}\,(r-1)\right) \right) \frac{\mathrm{Exp}\left(\sqrt{\frac{\omega}{2\nu}}\,(r-1)\right)}{\sqrt{r}} \quad . \qquad \text{(A-40)}$$

The above equation is used to obtain Eq. (1V-67) from Eq. (1V-66).

APPENDIX B

SOLUTION PROGRAM AND PLOT PROGRAMS FOR PRESSURE, AXIMUTHAL VELOCITY AND RADIAL VELOCITY EQUATIONS

In this appendix, a complete listing of the program for the solution of the pressure equation, the azimuthal and radial velocity equations is given in IBM 1620 Fortran notation without Format along with programs which present the output data in graphical form by using the IBM 1627 plotter. The listing is supplemented with physical definitions of the quantities called for as input data and those received as output data.

Program for the Solution of the Pressure and Velocity Equations

Before any reference is made to the program listing, the Fortran quantities defined below should be read.

(a) BO = Bessel function of zeroth order.

(b) B1 = Bessel function of first order.

(c) BMO = modified Bessel function of zeroth order.

(d) BM1 = modified Bessel function of first order.

(e) BMR = modified Bessel function of zeroth order whose argument is a function of the radius.

(f) BMR1 = modified Bessel function of first order whose argument is a function of the radius.

(g) SR = roots of equation (IV-23).

(h) W = circular frequency (rad./sec).

(i) Z = azimuthal coordinate (inches).

(j) R = radial coordinate (inches).

(k) PRES = maximum negative pressure experienced by the fluid (PSI).

(l) VR = maximum radial velocity experienced by the fluid (inches/second).

m VZ = maximum azimuthal velocity experienced by the fluid (inches/second).

(n) RHO = density of the fluid (lb_m/ft^3).

(o) H = height of the liquid column (inches).

(p) GNU = inverse of the fluid viscosity ($sec/inches^2$).

(q) G = acceleration due to gravity ($inches/sec^2$).

(r) A = amplitude of the tube (inches).

All of the above quantities are floating point numbers and must be defined with a decimal point.

The solution program in Fortran notation is given in the following three pages.

Plot Programs for the Output Data from the Pressure and the Velocity Equations

The following two definitions are needed before reading the listings of the plot programs.

PROGRAM LISTING

```
      DIMENSION B0(30,6),B1(150),BM0(11),BM1(11),BMR(11,6)
     1SR(150)
      DIMENSION W(8),Z(11),R(7),PRES(8,11,7),VR(8,11,7)
     1VZ(8,11,7)
      DIMENSION BMR1(11,6)
      READ 3,((B0(N,NR),N=1,30),NR=1,6)
      READ 3,(B1(N),N=1,150)
      READ 4,(BM0(M),M=1,11)
      READ 4,(BM1(M),M=1,11)
      READ 3,(SR(N),N=1,150)
      READ 3,((BMR(M,NR),M=1,11),NR=1,6)
      READ 3,((BMR1(M,NR),M=1,11),NR=1,6)
      READ 11,(W(K),K=1,8)
      READ 11,(Z(K1),K1=1,11)
      READ 11,(R(K2),K2=2,7)
  100 READ 1,A,RHO,H,GNU,G,AA,AB,AC,AD,AE,AF
      PUNCH 14,AA,AB,AC,AD,AE,AF
      PUNCH 15,A,RHO,H,GNU
      PRINT 19, AA,AB,AC,AD,AE,AF
      PRINT 20, A, RHO, H, GNU
      R(1) = 0.
      A1=SQRTF(GNU/2.)
      DO 80 K=1,8
      PRINT 7,W(K)
      AP=A*RHO*W(K)**2/333849.6
      DO 90 K1=1,11
      PRINT 8, Z(K1)
      PRINT 12
      P0=0.
      PAA=Z(K1)*(-2.)
      P2=RHO*Z(K1)*(G+A*W(K)**2)/667699.2
      DO 150 N=1,150
      P = PAA /(SR(N)*B1(N))
      P0=P0+P
  150 CONTINUE
      XM=0.
      P1=0.
      DO 160 M=1,11
      XM=XM+1.
      GN=((2.*(XM-1.)+1.)/2.)*3.14159/H
      S=(-1.**(M+1))*COSF(GN*Z(K1))/(H*SINF(GN*Z(K1)))
      T=A1*SQRTF(W(K))*BM1(M)-GN*BM0(M)
      U=SINF(GN*Z(K1))*(-2.)
      X=(GN*BM0(M))**2+GNU*W(K)*BM1(M)**2-2.*GN*A1*SQRTF(W(K))
     1*BM0(M)*BM1(M)
      P=(S*T*U)/X
      P1=P1+P
```

PROGRAM LISTING - continued

```
160 CONTINUE
    PRES(K,K1,1)=AP*(P0+P1)+P2
    VZ(K,K1,1) =     A*W(K)*(P0/Z(K1)+P1)
    VR(K,K1,1) = 0.
    PRINT 9,R(1),P0,P1,PRES(K,K1,1),P2
    NR=0
    DO 110 K2=2,7
    NR=NR+1
    PA=0.
    DO 50  N=1,30
    P=PAA*B0(N,NR)/(SR(N)*B1(N))
    PA=PA+P
 50 CONTINUE
    PA1=0.
    BMUD = 0.
    XM=0.
    DO 60  M=1,11
    XM=XM+1.
    GN=((2.*(XM-1.)+1.)/2.)*3.14159/H
    S=(-1.**(M+1))/(H*GN)
    T=A1*SQRTF(W(K))*BM1(M)-GN*BM0(M)
    UA=BMR(M,NR)*SINF(GN*Z(K1))*(-2.)
    X=(GN*BM0(M))**2+GNU*W(K)*BM1(M)**2-2.*GN*A1*SQRTF(W(K))
   1*BM0(M)*BM1(M)
    BMUD = GN * BMR1(M,NR)/BMR(M,NR)
    P=(S*T*UA)/X
    PA1=PA1+P
    P1=GN*COSF(GN*Z(K1))*P/SINF(GN*Z(K1))
    PA2=PA2+P1
    BARF=P*BMUD
    BARF1=BARF1+BARF
 60 CONTINUE
    VZ(K,K1,K2)=A*W(K)*(PA/Z(K1)+PA2)
    VR(K,K1,K2 )=A*W(K)*BARF1
    PRES(K,K1,K2)=AP*(PA+PA1)+P2
    PRINT 9,R(K2),PA,PA1,PRES(K,K1,K2),P2
110 CONTINUE
    PUNCH 13,PRES(K,K1,1),PRES(K,K1,2),PRES(K,K1,3),
   1PRES(K,K1,4),PRES(K,K1,5),PRES(K,K1,6),PRES(K,K1,7),K,K1
 90 CONTINUE
 80 CONTINUE
    PRINT 18
    PRINT 19, AA,AB,AC,AD,AE,AF
    PRINT 20, A, RHO, H, GNU
    DO 61 K=1,8
```

PROGRAM LISTING - continued

```
      PRINT 7,W(K)
      DO 62 K1=1,11
      PRINT 8, Z(K1)
      PRINT 21
      PUNCH 16, VZ(K,K1,1),VZ(K,K1,2),VZ(K,K1,3),VZ(K,K1,4),
     1VZ(K,K1,5),VZ(K,K1,6),VZ(K,K1,7),K,K1
      PUNCH 17, VR(K,K1,1),VR(K,K1,2),VR(K,K1,3),VR(K,K1,4),
     1VR(K,K1,5),VR(K,K1,6),VR(K,K1,7),K,K1
      DO 63 K2=1,7
      PRINT 22,R(K2),VR(K,K1,K2),VZ(K,K1,K2)
   63 CONTINUE
   62 CONTINUE
   61 CONTINUE
    1 FORMAT (5F10.0,6A3)
    3 FORMAT (6(3X,F10.0))
    4 FORMAT (7F10.0)
    7 FORMAT (14H  OMEGA EQUALS ,F7.2//)
    8 FORMAT (12H   Z EQUALS ,F7.2//)
    9 FORMAT (15X,F6.3,3( 9X,E14.8),10X,E14.8)
   11 FORMAT (6F10.0)
   12 FORMAT (15X,6HRADIUS,16X,2HP0,21X,2HP1,16X,13HMIN.
     1 PRESSURE,11X,13HMAX. PRESSURE//)
   13 FORMAT (7E10.4,4X,I2,2X,I2)
   14 FORMAT (14H   OUTPUT FOR ,6A3)
   15 FORMAT (7H   A = ,F6.4,8H  RHO = ,F8.4,6H  H = ,F5.1,8H
     1 GNU = ,F9.4)
   16 FORMAT (7E10.4,4H VZ ,I2,2X,I2)
   17 FORMAT (7E10.4,4H VR ,I2,2X,I2)
   18 FORMAT (51X,19H1MAXIMUM VELOCITIES//)
   19 FORMAT (14H1  OUTPUT FOR ,6A3)
   20 FORMAT (6H  A = ,F10.3,6X,7H RHO = ,F10.3,6X,5H H = ,
     1F10.3,6X,7H GNU = ,F10.3,//)
   21 FORMAT (15X,6HRADIUS,16X,6HRADIAL,23X,1HZ//)
   22 FORMAT (15X,F6.3,12X,E14.8,13X,E14.8)
      GO TO 100
      END
```

(a) CHAR = subroutine instructing the pen on the IBM 1627 plotter to write.

(b) PLOT = subroutine instructing the pen on the IBM 1627 plotter to move to a specified location.

These programs are included so that an investigator who desires only a pictorial representation of how the pressure and the velocity vary with respect to the spatial coordinates can utilize these plot programs and save much time over doing it himself.

In Fortran notation, the six-plot programs are given in the following twelve pages.

PLOT PROGRAM FOR RADIAL VELOCITY VS. r

```
      DIMENSION PRES(6),R(6),Z(6)
      READ 11,(R(K2),K2=1,6)
      READ 34,(Z(K1),K1=1,6)
   25 READ 5, AA,AB,AC,AD,AE,AF,AG
    5 FORMAT (14X,7A3)
    9 FORMAT (6E10.4)
   11 FORMAT (6F10.0 )
   34 FORMAT (6(F6.2,6X))
      DO 40 K1 = 1,6
      IC=101
      XMIN=0.
      XMAX=1.
      XL=5.0
      XD= .2
      YMIN= LOGF(.00001)
      YMAX= LOGF (1.)
      YL=10.
      YD= LOGF (10.)
      CALL PLOT (IC,XMIN,XMAX,XL,XD,YMIN,YMAX,YL,YD)
      CALL PLOT (99)
      CALL PLOT (90, .4   , LOGF (.0000071))
      CALL CHAR (0,0.1,0)
   17 FORMAT (10HR - INCHES)
      CALL PLOT (90,.175, LOGF (.000006))
      CALL CHAR (8,0.1,0,AA,AB,AC,AD,AE,AF,AG,Z(K1))
   16 FORMAT (7A3,5H  Z =,F6.2)
      DO 26 K=1,8
      READ 9, PRES(1),PRES(2),PRES(3),PRES(4),PRES(5),PRES(6)
      DO 27 K2=1,6
      CALL PLOT (0,R(K2),LOGF (PRES(K2)))
   27 CONTINUE
      CALL PLOT (99)
   26 CONTINUE
      CALL PLOT (90,-.1, LOGF (1.))
      CALL CHAR (0,0.1,0)
   21 FORMAT (5H    1.)
      CALL PLOT (90,-.1, LOGF (.1))
      CALL CHAR (0,0.1,0)
   42 FORMAT (5H    .1)
      CALL PLOT (90,-.12, LOGF (.0009))
      CALL CHARV(0,0.1,1)
   41 FORMAT     (21HRADIAL VELOCITY - IPS)
      CALL PLOT (90,-.1, LOGF (.01))
      CALL CHAR (0,0.1,0)
   43 FORMAT (5H   .01)
      CALL PLOT (90,-.1, LOGF (.001))
      CALL CHAR (0,0.1,0)
```

RADIAL VELOCITY VS. r - continued

```
44 FORMAT (5H .001)
   CALL PLOT (90,-.1, LOGF (.0001))
   CALL CHAR (0,0.1,0)
45 FORMAT (5H.0001)
   CALL PLOT (90,-.12,LOGF (.00001))
   CALL CHAR (0,0.1,0)
46 FORMAT (6H.00001)
   CALL PLOT (90,-.01 ,LOGF (.0000083))
   CALL CHAR (0,0.1,0)
18 FORMAT (2H0.)
   CALL PLOT (90,.175, LOGF (.0000083))
   CALL CHAR (0,0.1,0)
31 FORMAT (2H.2)
   CALL PLOT (90,.375, LOGF (.0000083))
   CALL CHAR (0,0.1,0)
19 FORMAT (2H.4)
   CALL PLOT (90,.575, LOGF (.0000083))
   CALL CHAR (0,0.1,0)
32 FORMAT (2H.6)
   CALL PLOT (90,.775, LOGF (.0000083))
   CALL CHAR (0,0.1,0)
33 FORMAT (2H.8)
   CALL PLOT (90,.995, LOGF (.0000083))
   CALL CHAR (0,0.1,0)
35 FORMAT (3H1.0)
   DO 70 N = 1,2
   CALL PLOT(7)
70 CONTINUE
40 CONTINUE
   GO TO 25
   END
```

PLOT PROGRAM FOR AZIMUTHAL VELOCITY VS. Z

```
      DIMENSION PRES(6),      Z(6)
      READ 34,(Z(K1),K1=1,6)
   25 READ 5, AA,AB,AC,AD,AE,AF,AG
    5 FORMAT (14X,7A3)
    9 FORMAT (50X,E10.4)
   34 FORMAT (6(F6.2,6X))
      IC=101
      XMIN=11.
      XMAX=31.
      XL=5.0
      XD=4.
      YMIN=2.
      YMAX=22.
      YL=10.
      YD=2.
      CALL PLOT (IC,XMIN,XMAX,XL,XD,YMIN,YMAX,YL,YD)
      CALL PLOT (99)
      CALL PLOT (90, 19. ,1.395)
      CALL CHAR (0,0.1,0)
   17 FORMAT (10HZ - INCHES)
      CALL PLOT (90,14.5,1.12)
      CALL CHAR (7,0.1,0,AA,AB,AC,AD,AE,AF,AG)
   16 FORMAT (7A3,10H  R = 0.95)
      DO 26 K=1,8
      READ 9, PRES(1),PRES(2),PRES(3),PRES(4),PRES(5),PRES(6)
      DO 27 K1=1,6
      PRES(K1) = -PRES(K1)
      CALL PLOT (0,Z(K1),PRES(K1))
   27 CONTINUE
      CALL PLOT (99)
   26 CONTINUE
      CALL PLOT (90, 9.,21.975)
      CALL CHAR (0,0.1,0)
   21 FORMAT (4H 22.)
      CALL PLOT (90, 9.,17.975)
      CALL CHAR (0,0.1,0)
   22 FORMAT (4H 18.)
      CALL PLOT (90, 9.,9.975)
      CALL CHAR (0,0.1,0)
   30 FORMAT (4H 10.)
      CALL PLOT (90, 8.6, 9.8)
      CALL CHARV(0,0.1,1)
   41 FORMAT (24HAZIMUTHAL VELOCITY - IPS)
      CALL PLOT (90, 9.,13.975)
      CALL CHAR (0,0.1,0)
   23 FORMAT (4H 14.)
      CALL PLOT (90, 9.,5.975)
```

AZIMUTHAL VELOCITY VS. Z - continued

```
      CALL CHAR (0,0.1,0)
   24 FORMAT (4H  6.)
      CALL PLOT (90, 9.,1.975)
      CALL CHAR (0,0.1,0)
   28 FORMAT (4H  2.)
      CALL PLOT (90,10.80,1.66)
      CALL CHAR (0,0.1,0)
   18 FORMAT (3H11.)
      CALL PLOT (90,14.8,1.66)
      CALL CHAR (0,0.1,0)
   31 FORMAT (3H15.)
      CALL PLOT (90,18.8,1.66)
      CALL CHAR (0,0.1,0)
   19 FORMAT (3H19.)
      CALL PLOT (90,22.8,1.66)
      CALL CHAR (0,0.1,0)
   32 FORMAT (3H23.)
      CALL PLOT (90,26.8,1.66)
      CALL CHAR (0,0.1,0)
   33 FORMAT (3H27.)
      CALL PLOT (90,30.8,1.66)
      CALL CHAR (0,0.1,0)
   35 FORMAT (3H31.)
      CALL PLOT(7)
      PAUSE
      GO TO 25
      END
```

PLOT PROGRAM FOR AZIMUTHAL VELOCITY VS. r

```
      DIMENSION PRES(6),R(6),Z(6)
      READ 11,(R(K2),K2=1,6)
      READ 34,(Z(K1),K1=1,6)
   25 READ 5, AA,AB,AC,AD,AE,AF,AG
    5 FORMAT (14X,7A3)
    9 FORMAT (6E10.4)
   11 FORMAT (6F10.0      )
   11 FORMAT (6F10.0      )  )
   34 FORMAT (6(F6.2,6X))
      DO 40 K1 = 1,6
      PRINT 55, Z(K1)
   55 FORMAT (6X,F6.2)
      IC=101
      XMIN=0.
      XMAX=1.
      XL=5.0
      XD=.1
      YMIN=2.
      YMAX=22.
      YL=10.
      YD=2.
      CALL PLOT (IC,XMIN,XMAX,XL,XD,YMIN,YMAX,YL,YD)
      CALL PLOT (99)
      CALL PLOT (90,-.010,1.66)
      CALL CHAR (0,0.1,0)
   18 FORMAT (2H0.)
      CALL PLOT (90, .35 ,1.395)
      CALL CHAR (0,0.1,0)
   17 FORMAT (15HRADIUS - INCHES)
      CALL PLOT (90,.15,1.125)
      CALL CHAR (8,0.1,0,AA,AB,AC,AD,AE,AF,AG,Z(K1))
   16 FORMAT (7A3,5H  Z =,F6.2)
      CALL PLOT (90,.475,1.66)
      CALL CHAR (0,0.1,0)
   31 FORMAT (3H0.5)
      CALL PLOT (90,.975,1.66)
      CALL CHAR (0,0.1,0)
   19 FORMAT (3H1.0)
      DO 26 K=1,8
      READ 9, PRES(1),PRES(2),PRES(3),PRES(4),PRES(5),PRES(6)
      DO 27 K2=1,6
      PRES(K2) = -PRES(K2)
      CALL PLOT (0,R(K2),PRES(K2))
   27 CONTINUE
      CALL PLOT (99)
   26 CONTINUE
      CALL PLOT (90,-.1,21.975)
```

AZIMUTHAL VELOCITY VS. r - continued

```
      CALL CHAR (0,0.1,0)
   21 FORMAT (4H 22.)
      CALL PLOT (90,-.1,17.975)
      CALL CHAR (0,0.1,0)
   22 FORMAT (4H 18.)
      CALL PLOT (90,-.1,13.975)
      CALL CHAR (0,0.1,0)
   23 FORMAT (4H 14.)
      CALL PLOT (90,-.12, 9.8)
      CALL CHARV(0,0.1,1)
   41 FORMAT (24HAZIMUTHAL VELOCITY - IPS)
      CALL PLOT (90,-.1,9.975)
      CALL CHAR (0,0.1,0)
   30 FORMAT (4H 10.)
      CALL PLOT (90,-.1,5.975)
      CALL CHAR (0,0.1,0)
   24 FORMAT (4H  6.)
      CALL PLOT (90,-.1,1.975)
      CALL CHAR (0,0.1,0)
   28 FORMAT (4H  2.)
      CALL PLOT(7)
      PAUSE
   40 CONTINUE
      GO TO 25
      END
```

PLOT PROGRAM FOR PRESSURE VS. Z

```
      DIMENSION PRES(6),      Z(6)
      READ 34,(Z(K1),K1=1,6)
   25 READ 5, AA,AB,AC,AD,AE,AF,AG
    5 FORMAT (14X,7A3)
    9 FORMAT (50X,E10.4)
   34 FORMAT (6(F6.2,6X))
      IC=101
      XMIN= 11.
      XMAX= 31.
      XL=5.
      XD= 4.
      YMIN=-1.5
      YMAX=28.5
      YL=10.
      YD=3.
      CALL PLOT (IC,XMIN,XMAX,XL,XD,YMIN,YMAX,YL,YD)
      CALL PLOT (99)
      CALL PLOT (90, 9.2, 25.35)
      CALL CHAR (0,0.1,0)
   29 FORMAT (4H25.5)
      CALL PLOT (90, 9.2, 19.35)
      CALL CHAR (0,0.1,0)
   28 FORMAT (4H19.5)
      CALL PLOT (90, 8.6, 10.2)
      CALL CHARV (0, 0.1, 1)
   75 FORMAT (23HNEGATIVE PRESSURE - PSI)
      CALL PLOT (90, 9.2, 13.35)
      CALL CHAR (0,0.1,0)
   24 FORMAT (4H13.5)
      CALL PLOT (90, 9.2, 7.35)
      CALL CHAR (0,0.1,0)
   30 FORMAT (4H 7.5)
      CALL PLOT (90, 9.2, 1.35)
      CALL CHAR (0,0.1,0)
   21 FORMAT (4H 1.5)
      CALL PLOT (90, 9.2,- .35)
      CALL CHAR (0,0.1,0)
   22 FORMAT (4H  0.)
      CALL PLOT (90, 9.2,-1.65)
      CALL CHAR (0,0.1,0)
   23 FORMAT (4H-1.5)
      DO 26 K=1,8
      READ 9, PRES(1),PRES(2),PRES(3),PRES(4),PRES(5),PRES(6)
      DO 27 K1=1,6
      CALL PLOT (0,Z(K1),-PRES(K1))
   27 CONTINUE
      CALL PLOT (99)
```

PRESSURE VS. Z - continued

```
26 CONTINUE
   CALL PLOT (90,19.   , -2.385)
   CALL CHAR (0,0.1,0)
17 FORMAT (10HZ - INCHES)
   CALL PLOT (90,14.5, -2.82)
   CALL CHAR (7,0.1,0,AA,AB,AC,AD,AE,AF,AG)
16 FORMAT (7A3,8HR = 0.95)
   CALL PLOT (90,10.6 ,-1.996)
   CALL CHAR (0,0.1,0)
18 FORMAT (3H11.)
   CALL PLOT (90,14.6 ,-1.996)
   CALL CHAR (0,0.1,0)
31 FORMAT (3H15.)
   CALL PLOT (90,18.6, -1.996)
   CALL CHAR (0,0.1,0)
5( FORMAT (3H19.)
   CALL PLOT (90,22.6, -1.996)
   CALL CHAR (0,0.1,0)
52 FORMAT (3H23.)
   CALL PLOT (90,26.6, -1.996)
   CALL CHAR (0,0.1,0)
54 FORMAT (3H27.)
   CALL PLOT (90,30.6, -1.996)
   CALL CHAR (0,0.1,0)
55 FORMAT (3H31.)
   DO 70 N = 1,2
   CALL PLOT(7)
70 CONTINUE
   GO TO 25
   END
```

PLOT PROGRAM FOR PRESSURE VS. r

```
      DIMENSION PRES(6),R(6),Z(6)
      READ 11,(R(K2),K2=1,6)
      READ 34,(Z(K1),K1=1,6)
   25 READ 5, AA,AB,AC,AD,AE,AF,AG
    5 FORMAT (14X,7A3)
    9 FORMAT (6E10.4)
   11 FORMAT (6F10.0      )
   34 FORMAT (6(F6.2,6X))
      DO 40 K1 = 1,6
      IC=101
      XMIN= 0.
      XMAX=1.
      XL=5.
      XD=.2
      YMIN=-1.5
      YMAX=28.5
      YL=10.
      YD=3.
      CALL PLOT (IC,XMIN,XMAX,XL,XD,YMIN,YMAX,YL,YD)
      CALL PLOT (99)
      CALL PLOT (90,-.09,-1.65)
      CALL CHAR (0,0.1,0)
   23 FORMAT (4H-1.5)
      CALL PLOT (90,-.09,- .35)
      CALL CHAR (0,0.1,0)
   22 FORMAT (4H  0.)
      CALL PLOT (90,-.09, 1.35)
      CALL CHAR (0,0.1,0)
   21 FORMAT (4H 1.5)
      CALL PLOT (90,-.09, 7.35)
      CALL CHAR (0,0.1,0)
   30 FORMAT (4H 7.5)
      CALL PLOT (90,-.12, 10.2)
      CALL CHARV (0, 0.1, 1)
   75 FORMAT (23HNEGATIVE PRESSURE - PSI)
      CALL PLOT (90,-.09, 13.35)
      CALL CHAR (0,0.1,0)
   24 FORMAT (4H13.5)
      CALL PLOT (90,-.09, 19.35)
      CALL CHAR (0,0.1,0)
   28 FORMAT (4H19.5)
      CALL PLOT (90,-.09, 25.35)
      CALL CHAR (0,0.1,0)
   29 FORMAT (4H25.5)
      DO 26 K=1,8
      READ 9, PRES(1),PRES(2),PRES(3),PRES(4),PRES(5),PRES(6)
      DO 27 K2=1,6
```

PRESSURE VS. r - continued

```
      CALL PLOT (0,R(K2),-PRES(K2))
   27 CONTINUE
      CALL PLOT (99)
   26 CONTINUE
      CALL PLOT (90, .4   , -2.385)
      CALL CHAR (0,0.1,0)
   17 FORMAT (10HR - INCHES)
      CALL PLOT (90,.175, -2.82)
      CALL CHAR (8,0.1,0,AA,AB,AC,AD,AE,AF,AG,Z(K1))
   16 FORMAT (7A3,5H  Z =,F6.2)
      CALL PLOT (90,-.010,-1.996)
      CALL CHAR (0,0.1,0)
   18 FORMAT (2H0.)
      CALL PLOT (90,.175, -1.996)
      CALL CHAR (0,0.1,0)
   31 FORMAT (3H.2 )
      CALL PLOT (90,.375, -1.996)
      CALL CHAR (0,0.1,0)
   50 FORMAT (3H.4 )
      CALL PLOT (90,.575, -1.996)
      CALL CHAR (0,0.1,0)
   52 FORMAT (3H.6 )
      CALL PLOT (90,.775, -1.996)
      CALL CHAR (0,0.1,0)
   54 FORMAT (3H.8 )
      CALL PLOT (90,.975, -1.996)
      CALL CHAR (0,0.1,0)
   55 FORMAT (3H1.0)
      DO 70 N = 1,2
      CALL PLOT(7)
   70 CONTINUE
   40 CONTINUE
      GO TO 25
      END
```

PLOT PROGRAM FOR RADIAL VELOCITY VS. Z

```
      DIMENSION PRES(6),R(6),Z(6)
      READ 34,(Z(K1),K1,1,6)
   25 READ 5,AA
   25 READ 5, AA,AB,AC,AD,AE,AF,AG
    5 FORMAT (14X,7A3)
    9 FORMAT (6(10.4)
   34 FORMAT (6(F6.2,6X))
      IC=101
      XMIN= 11.
      XMAX= 31.
      XL=5.0
      XD= 2.
      YMIN= LOGF(.00001)
      YMAX= LOGF (1.)
      YL=10.
      YD= LOGF (10.)
      CALL PLOT (IC,XMIN,XMAX,XL,XD,YMIN,YMAX,YL,YD)
      CALL PLOT (99)
      CALL PLOT (90, 19. , LOGF (.0000071))
      CALL CHAR (0,0.1,0)
   17 FORMAT (10HZ - INCHES)
      CALL PLOT (90,14.5, LOGF (.000006))
      CALL CHAR (7,0.1,0,AA,AB,AC,AD,AE,AF,AG)
   16 FORMAT (7A3,10H  R=0.95)
      DO 26 K=1,8
      READ 9, PRES(1),PRES(2),PRES(3),PRES(4),PRES(5),PRES(6)
      DO 27 K1=1,6
      CALL PLOT (0,Z(K1),LOGF (PRES(K1)))
   27 CONTINUE
      CALL PLOT (99)
   26 CONTINUE
      CALL PLOT (90,9.0, LOGF (1.))
      CALL CHAR (0,0.1,0)
   21 FORMAT (5H    1.)
      CALL PLOT (90,9.0, LOGF (.1))
      CALL CHAR (0,0.1,0)
   42 FORMAT (5H    .1)
      CALL PLOT (90,8.6 , LOGF (.0009))
      CALL CHARV(0,0.1,1)
   41 FORMAT     (21HRADIAL VELOCITY - IPS)
      CALL PLOT (90,9.0, LOGF (.01))
      CALL CHAR (0,0.1,0)
   43 FORMAT (5H   .01)
      CALL PLOT (90,9.0, LOGF (.001))
```

RADIAL VELOCITY VS. Z - continued

```
      CALL CHAR (0,0.1,0)
   44 FORMAT (5H .001)
      CALL PLOT (90,9.0, LOGF (.0001))
      CALL CHAR (0,0.1,0)
   45 FORMAT (5H.0001)
      CALL PLOT (90,8.6 ,LOGF (.00001))
      CALL CHAR (0,0.1,0)
   46 FORMAT (6H.00001)
      CALL PLOT (90,10.8 ,LOGF (.0000083))
      CALL CHAR (0,0.1,0)
   18 FORMAT (2H11)
      CALL PLOT (90,14.5, LOGF (.0000083))
      CALL CHAR (0,0.1,0)
   31 FORMAT (2H15)
      CALL PLOT (90,18.5, LOGF (.0000083))
      CALL CHAR (0,0.1,0)
   19 FORMAT (2H19)
      CALL PLOT (90,22.5, LOGF (.0000083))
      CALL CHAR (0,0.1,0)
   32 FORMAT (2H23)
      CALL PLOT (90,26.5, LOGF (.0000083))
      CALL CHAR (0,0.1,0)
   33 FORMAT (2H27)
      CALL PLOT (90,30.5, LOGF (.0000083))
      CALL CHAR (0,0.1,0)
   35 FORMAT (2H31)
      DO 70 N = 1,2
      CALL PLOT(7)
   70 CONTINUE
      GO TO 25
      END
```

VITA

George Patrick Mulholland

Candidate for the Degree of

Doctor of Philosophy

Thesis: THE EFFECT OF MECHANICAL VIBRATIONS ON THE NEGATIVE PRESSURE OF PURE LIQUIDS

Major Field: Mechanical Engineering

Biographical:

Personal Data: Born in Philadelphia, Pennsylvania, July 12, 1938, the son of George P. and Bridgett T. Mulholland.

Education: Received the Bachelor of Science degree in Mechanical Engineering from New Mexico State University, University Park, New Mexico, in January, 1961; received the Master of Science degree in Mechanical Engineering from New Mexico State University, University Park, New Mexico, in June, 1962; completed requirements for the Doctor of Philosophy degree in May, 1967.

Professional experience: Graduate assistant in the Mechanical Engineering Department of New Mexico State University, University Park, New Mexico, for the spring semester of the 1960-61 academic year and the 1961-62 academic year; temporary engineering employee of Rocketdyne Division of North American Aviation, Canoga Park, California, during summer of 1962; temporary engineering employee of Los Alamos Scientific Laboratory, Los Alamos, New Mexico, for summer of 1963; graduate assistant in the Mechanical Engineering Department of Oklahoma State University, Stillwater, Oklahoma, for the academic years of 1962-63, 1963-64, and 1964-65; Senior Research Engineer at the Jet Propulsion Laboratory, Pasadena, California during 1965-66; presently employed as an Assistant Professor in the Department of Mechanical Engineering of New Mexico State University, Las Cruces, New Mexico.

Professional Organizations: The author is a member of the following honorary organizations: Pi Mu Epsilon, Sigma Tau, and Pi Tau Sigma.